Structure-function relationship of von Willebrand factor.

Collagen-binding and platelet adhesion at physiological shear rate conditions using an *in vitro* flow-chamber model.

Inaugural-Dissertation
to obtain the academic degree
Doctor rerum naturalium (Dr. rer. nat.)

submitted to the Department of Biology, Chemistry and Pharmacy
of Freie Universität Berlin

by
Birte Fuchs
from Schwerin

Berlin, February 2009

Prof. Dr. Rüdiger Horstkorte
Institute of Biochemistry and Molecular Biology
Charité – Universitätsmedizin Berlin
Campus Benjamin Franklin

In cooperation with Dr. Christoph Kannicht
Octapharma R&D
Molecular Biochemistry Department Berlin

2005-2009

1st Reviewer: Prof. Dr. Carsten Niemitz
2nd Reviewer: Prof. Dr. Rüdiger Horstkorte

Date of defence: April 30th 2009

The soul, which is spirit, can not dwell in dust; it is carried along to dwell in the blood.

Saint Aurelius Augustine

Acknowledgement

This thesis is the result of three and a half year of work, which would have not been possible without the company and support by many people. I would like to thank all of them for their guidance and enthusiasm.

First of all I wish to express my sincerest gratitude to my supervisor Dr. Christoph Kannicht for the opportunity to accomplish my PhD thesis at Octapharma R&D Berlin, but first and foremost for his support, helpful discussions, his encouragement and confidence in me.

I am deeply grateful to Prof. Dr. Rüdiger Horstkorte for his guidance and invaluable support in preparing this thesis, as well as his disposition to review.

Special thanks go to Prof. Dr. Carsten Niemitz for accompanying my thesis as well as for review, helping me to substantially improve this work.

I am very much obliged to all the members of Octapharma R&D Berlin for their helpfulness and support; their comradeship, the marvellous working atmosphere, and for their invaluable assistance.

Appreciation goes also to my colleagues from Octapharma R&D Vienna and especially to my colleagues in Lachen for their support, trust and motivation.

I am deeply indebted to Prof. Dr. Ulrich Budde and his collegues for giving me the opportunity to learn in their laboratory, their friendliness and helpful discussions.

I thank Dr. Kjell S. Sakariassen for his benefit and scientific dialogues regarding the flow-chamber system.

I express my gratitude to A. Schulz from the department of Chemistry and Biochemistry/Organic Chemistry, FU Berlin, for her kind assistance realising the AFM measurements.

Sincere thanks to my friends for valuable conversations, proofreading and – most precious – their encouragement during all these years; for listening and distraction in times of need.

I am grateful to all the people who accompanied me over the last years, for cheerful times, for ‘rainy days’, for moral and mental support and experiences beyond comparison.

Last but not least I wish to express my deepest gratitude to my family for their unlimited confidence, love and understanding. It’s great to know that there is always a place to come to.

Index of contents

1 Introduction

Haemostasis is a pivotal process and requires the combined action of blood platelets, vascular- and plasmatic factors. It is divided into two steps: (i) the primary haemostasis, associated with cellular mechanisms (thrombocytes), and (ii) the secondary haemostasis, mediated by a complex system of extrinsic and intrinsic signalling cascades involving coagulation factors. In flowing blood, platelet adhesion to sites of vascular injury is mediated by the von Willebrand Factor (VWF), being the critical determinant of thrombus formation at high arterial shear rate conditions. The VWF is named after the Finnish physician Erik A. von Willebrand, who examined a family with bleeding histories affecting both sexes on the Åland islands during 1925. Von Willebrand concluded that the disease was a previously unknown form of haemophilia and termed it 'pseudo-haemophilia' – now called Von Willebrand Disease (VWD) – with a prolonged bleeding time as its most prominent symptom [von Willebrand, 1931; von Willebrand & Jürgens, 1933]. VWF was foremost purified in the early 1970s, and its complete amino acid sequence was first published in 1986 [Titani *et al.*, 1986]. Research over the last decades provided considerable progress in the understanding of VWF assembly, function, and the molecular basis of VWD.

1.1 Biosynthesis of VWF

VWF is a large glycoprotein which circulates in plasma as a series of heterogeneous multimers, mediating platelet tethering, translocation and finally adhesion to areas of injured endothelium under physiological high arterial blood flow conditions above a critical threshold of 500 - 1,000 s^{-1} shear rate [Savage *et al.*, 1996; Ruggeri 2004]. Furthermore, VWF protects coagulation factor VIII (FVIII) from rapid proteolytic inactivation [Matsushita *et al.*, 1994].

The protein is encoded distally on the short arm of chromosome 12 and synthesised by endothelial cells and megacaryocytes, generating a primary translation product of 2,813 amino acids (AA), including a signal peptide of 22 residues, a large pro-peptide of 741 and the mature subunit of 2,050 residues (pre-pro-VWF). The gene of 178 - 180 kb with 52 exons encodes the VWF monomer with a molecular weight (MW) of 250 - 270 kDa, composed of areas of internal homology determined as A, B, C and D-domains, providing binding sites to a variety of proteins. Pro-VWF molecules dimerise through disulfide bonds

near their carboxyl termini (“tail to tail”) within the endoplasmic reticulum (ER), and subsequently VWF dimers are transported to the Golgi apparatus to form large multimers, sizing up to 20,000 kDa via *N*-terminal disulfide bridges (“head to head”). In the Golgi apparatus, also proteolytic removal of the pro-peptide and glycosylation takes place [extensively reviewed by Sadler, 1998]. Plasma VWF is derived by endothelial cells: about 95 % of endothelial VWF molecules are constitutively secreted to a plasma concentration of 10 µg/mL (50 nM or rather 1 IU/mL), whereas the remainder is stored in cytoplasmatic granules (Weibel-Palade bodies) or in the α-granules of platelets [Wagner *et al.*, 1991]. Ultra-large VWF of storage granules can be secreted via a regulated pathway upon stimulation [Ruggeri & Ware, 1993]. A schematic diagram of the VWF processing is shown in Fig. 1.

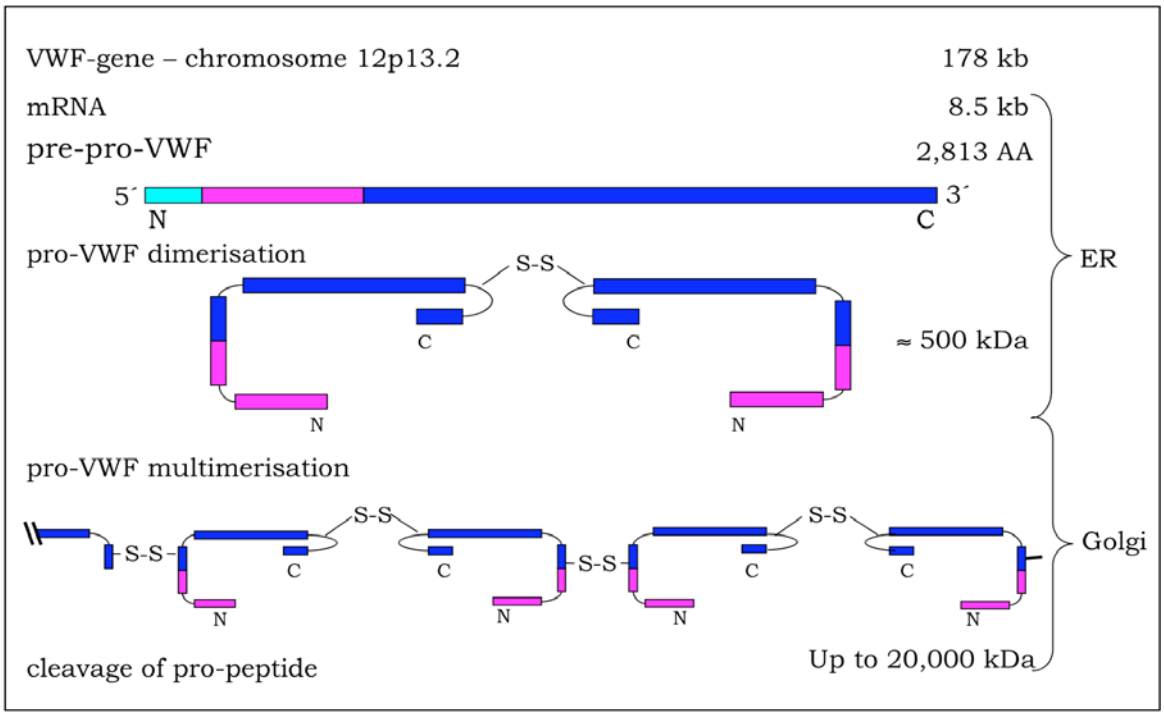

Fig. 1: Schematic diagram of VWF processing. The primary translation product comprises 2,813 amino acids (AA), including a signal peptide, a large pro-peptide and the mature subunit (pre-pro-VWF). Intersubunit disulfide bonds are formed near the carboxyl-termini of pro-VWF dimers in the endoplasmatic reticulum (ER). Additional intersubunit disulfide bonds are formed near the amino-terminus of the mature subunits to assemble multimers in the Golgi apparatus. The pro-peptide is cleaved off, but stays non-covalently associated with the VWF multimers and is secreted concomitantly. The graph is adapted from Colman *et al.*, “Hemostasis and Thrombosis – Basic principles & clinical practice.” Page 253.

Upon secretion, large VWF multimers are broken down into smaller species by the processing metalloprotease ADAMTS-13 (a disintegrin and metalloprotease with thrombospondin type 1 motifs), which cleaves the peptidyl bond between Y1,605 and M1,606 within the A2 domain of VWF, generating circulating plasma VWF of various multimer sizes [Dong, 2005]. This cleavage also produces VWF subunit fragments of 176 kDa and 140 kDa, responsible for the 'satellite bands' that flank the major band on VWF multimer gels [Dent *et al.*, 1991; Furlan *et al.*, 1993].

1.2 Posttranslational modifications of VWF

Within endothelial cells, VWF undergoes complex posttranslational modifications before secretion [Kaufman, 1998], preserving the multimeric structure and, therefore, the function of VWF. The protein is rich in cysteines and the mature subunit is extensively glycosylated with 12 *N*-linked and 10 *O*-linked oligosaccharides, accounting for about 19 % of the mass of a VWF monomer [Vlot *et al.*, 1998], which are believed to contribute to the structural and functional integrity of the protein [Millar & Brown, 2006]. Additionally, one or both of the oligosaccharides at Asn384 and Asn468 of the mature subunit are sulphated [Carew *et al.*, 1990], and all cysteine residues appear to be paired in disulfide bonds in the secreted protein [Marti *et al.*, 1987].

The *N*-linked oligosaccharide chains of VWF purified from plasma have been shown to express covalently linked ABH blood group antigenic determinants [Matsui *et al.*, 1992; Matsui *et al.*, 1993; Matsui *et al.*, 1999], additionally present only on two other plasma glycoproteins: FVIII and α_2-macroglobulin [Sodetz *et al.*, 1979; Matsui *et al.*, 1993]. Interestingly, ABH determinants are not present on platelet derived VWF [Brown *et al.*, 2002]. Plasma VWF antigen levels (VWF:Ag) show a widely distribution in normal population, whereas the ABH blood group phenotype is an important determinant: blood group H individuals exhibit VWF plasma levels 25 - 30 % lower than non-H individuals [reviewed by O'Donnel & Laffan, 2001; Jenkins & O'Donnel, 2006], which might be attributed to a decreased survival of VWF [reviewed by Lenting *et al.*, 2007].

VWF is also subjected to *O*-linked glycosylation, but whether and how differences in *O*-glycosylation contribute to the intracellular sorting and/or secretion of VWF is not jet fully

understood. The majority of *O*-linked carbohydrates are composed of the sialylated tumor-associated T-antigen [Samor *et al.*, 1989], and studies on VWF with de-sialylated *O*-linked T-antigen revealed an association with VWF plasma levels and the presence of these glycan structures on VWF, suggesting that an increased extent of sialylated *O*-linked T-antigen contributes to a reduced VWF survival [van Schooten *et al.*, 2007].

Recombinant VWF lacking *O*-linked carbohydrates showed a diminished capacity to promote platelet agglutination in the presence of ristotecin [Carew *et al.*, 1992], evidently because *O*-linked glycans are mainly clustered around the platelet-binding domain of VWF [Denis *et al.*, 2008]. Besides, *N*-linked oligosaccharides are crucial for VWF polymerisation [Wagner *et al.*, 1986], and sialylation of both *N*- and *O*-linked glycan branches seems to be important to prevent premature clearance via receptors that recognise non-sialylated terminal galactose residues [Morell *et al.*, 1971], supported by studies done in mice lacking sialyltransferase [Ellies *et al.*, 2002].

1.3 Structure and function of VWF

VWF performs its haemostatic function through binding to FVIII, to platelet surface glycoproteins, and to constituents of connective tissue. In primary haemostasis, VWF initiates platelet aggregation via binding to exposed structures of injured vessel walls at physiological high arterial shear rates [Sadler, 1998; Ruggeri, 2002]. In secondary haemostasis, VWF supports platelet aggregation because of its binding to FVIII, therefore protecting the coagulation factor from rapid proteolytic inactivation. Furthermore, VWF is thought to assist during platelet aggregation by bridging adjacent platelets at high shear rates. The function of VWF is strongly shear rate dependent, whereas fluid dynamic conditions as well as mechanical forces are crucial for the conformational transition of VWF to develop its interaction with endothelial matrix proteins as well as platelets in case of vessel injury.

1.3.1 Subunit organisation and multimer structure

The homooligomeric protein mature subunits of VWF are built from four types of conserved structural domains assembled into D'-D3-A1-A2-A3-D4-B1-B2-B3-C1-C2-C3-CK, providing binding sites to a variety of proteins, e.g. FVIII, platelet glycoprotein (GP)Ib, glucosaminoglycans, heparin and collagen types I-VI [reviewed by Sadler, 1998; Ruggeri, 2007]. For detailed description of VWF binding sites refer to Fig. 2.

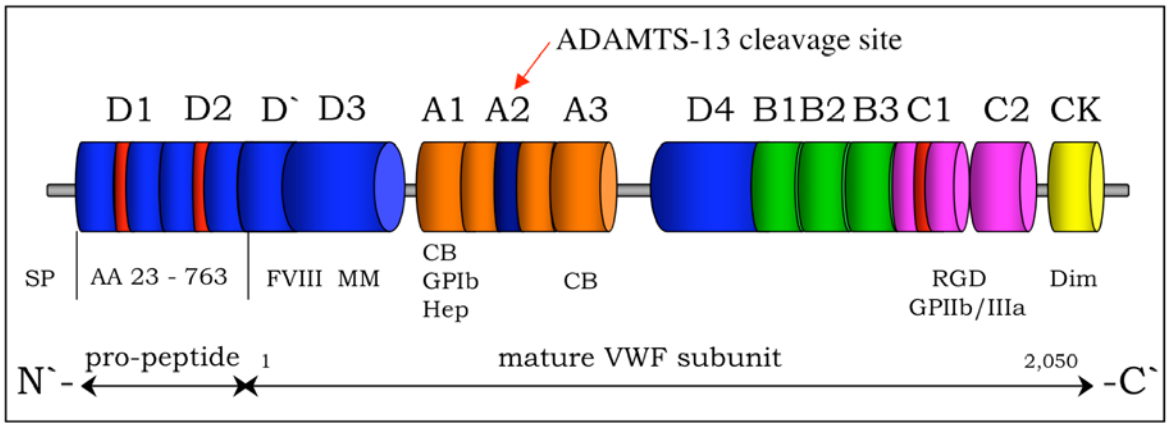

Fig. 2: Subunit structure of VWF. Areals of internal homology are determined as A, B, C and D-domains, whereas A-repeats exhibit sequence analogy with complement factor B, type VI collagen, chicken cartilage matrix protein and the integrin-α chains. Binding to coagulation factor VIII (FVIII) is allocated to the D'/D3 domains of VWF. The A1 domain comprises the binding site for non-fibrillar collagen type VI (CB) as well as the binding sites for heparin (Hep) and platelet glycoprotein Ib (GPIb), whereas the binding site for fibrillar type I and III collagens is located in the A3 domain (CB). C-repeats show analogy with segments of pro-collagen and thrombospondin, and contribute to platelet adhesion via interaction between activated platelet glycoprotein IIb/IIIa (GPIIb/IIIa) and the VWF Arg-Gly-Asp sequence (RGD). The ADAMTS-13 cleavage site between Tyr1,605 – Met1,606 is located within the A2 domain. The C-terminal dimerisation site is localised in the cysteine knot (CK) domain, whereas the multimerisation site (MM) lies in the D3 domain. The pro-peptide comprises amino acids 23 – 763, and the mature VWF subunit consists of 2,050 amino acids. SP: signal peptide.

Subsequent to the assembly of high molecular weight (HMW) VWF multimers via disulfide bridging, secreted VWF undergoes further processing: plasma VWF exhibits a unique multimeric structure caused by proteolytic cleavage of secreted HMW forms of VWF by ADAMTS-13 within the A2 domain of the protein, resulting in a complex banded pattern of VWF oligomers in multimer analysis (Fig. 3). The smallest detectable unit with a molecular mass of around 500 kDa represents the VWF dimer, whereas the polymers are built by

an even number of VWF subunits. Because of the asymmetric cleavage of the native subunit into fragments of 140 and 176 kDa, respectively, the intermediate VWF multimer bands are flanked by satellite bands, resulting in a complex quintuplet structure in high resolution agarose gels [Budde *et al.*, 2006 (2)]. The clearly distinguishable faster and slower migrating bands encompassing a VWF multimer on agarose gels are thought to lack one *N*-terminal fragment and possess an additional *N*-terminal fragment, respectively [Fischer *et al.*, 1998 (2)]. This structural model is supported by the altered heparin affinity of the VWF triplet bands, whereas faster migrating triplet bands lacking one *N*-terminal fragment exhibit a reduced affinity to heparin [Fischer *et al.*, 1999]. Even though VWF satellite bands are known to have an altered heparin affinity – eventually the *N*-terminal fragment also includes the FVIII- and platelet binding domains as well as one interaction site to collagen – the impact of triplet structure on VWF function has not been investigated so far.

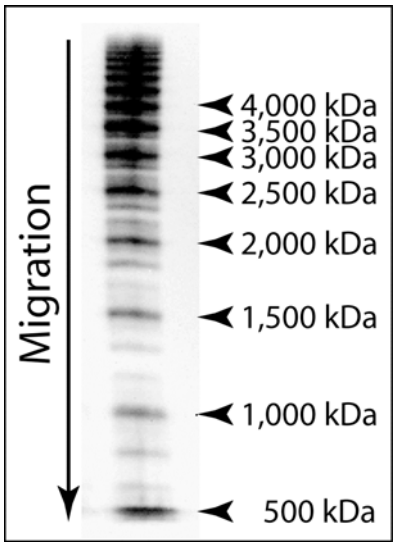

Fig. 3: Characteristic multimeric pattern of plasma VWF. Commercially available standard human plasma was subjected to 1.6 % agarose gel electrophoresis. The first band is representative for the VWF dimer of around 500 kDa, whereas larger bands are composed of additional numbers of dimers (bottom to top). Flanking subbands are visible surrounding the individual VWF multimers.

1.3.2 Stabilisation of coagulation factor VIII (FVIII)

FVIII is an essential cofactor in blood coagulation [Spiegel *et al.*, 2004], synthesised in liver cells. Upon release, the inactive FVIII precursor protein binds to VWF, and circulates in plasma non-covalently attached to the *N*-terminal moiety of VWF via its light chain [Fang *et al.*, 2007]. VWF protects FVIII from proteolytic inactivation through activated protein C and factor Xa [Vlot *et al.*, 1998], and promotes release of FVIII into the circulation. Consequently, patients lacking the VWF also exhibit reduced FVIII plasma levels caused by rapid clearance, and therefore patients with von Willebrand disease type 3 (cf. 1.4) are additionally suffering from secondary FVIII deficiency. Furthermore, VWF is associated with a reduced immunogenicity of FVIII, preventing the endocytosis of FVIII by human dendritic cells [Dasgupta *et al.*, 2007]. These findings also support the idea of lower immunogenicity of plasma-derived VWF/FVIII concentrates compared to recombinant FVIII products [reviewed by Lacroix-Desmazes *et al.*, 2008].

1.3.3 VWF-mediated platelet adhesion

In vivo thrombus formation requires platelet adhesion to exposed structures of the extracellular matrix (ECM) upon lesions in the blood vessel wall. This interaction is mediated by VWF, whereas the interplay between VWF and injured layers of the ECM as well as between VWF and platelets is crucial for haemostasis at high arterial wall shear rates above a threshold of 500 to 1,000 s^{-1} [Weiss *et al.*, 1978; Savage *et al.*, 1998].

Interestingly, ultralarge VWF multimers secreted upon stimulation of subendothelial Weibel-Palade bodies or α-granules of platelets are able to spontaneously aggregate with platelets without requiring collagen, shear, or chemical stimulation [Arya *et al.*, 2002]. In healthy individuals, these multimers are rapidly cleaved into smaller forms by ADAMTS-13 and do not accumulate in circulation [Dong *et al.*, 2002]. Lack of ADAMTS-13 or impaired function of this enzyme leads to the life-threatening disease thrombotic thrombocytopenic purpura (TTP), characterised by haemolytic anaemia caused by consumption of coagulation factors with microthrombi and end organ damage [reviewed by Sadler, 2008].

Initiation of arterial thrombus formation

The hypothetic model to explain VWF-mediated platelet adhesion is based on two presumptions: (i) in flowing blood, VWF appears as a ‘ball of yarn’ configuration and does not interact with the platelet glycoprotein receptor GPIb-IX-V under physiological conditions, because the GPIb binding domain is concealed. The affinity towards GPIb-IX-V is regulated by conformational changes in VWF, which are induced by immobilisation and shear. This ‘activation’ of VWF results in the exposure of binding sites within the VWF A1 domain responsible for interaction with platelet GPIbα [Slayter *et al.*, 1985; Kang *et al.*, 2007]. This is supported by studies showing a conversion of VWF from its loosely coiled structure into elongated filaments upon exposition to high shear stress [Siedlecki *et al.*, 1996], suggesting that shear modulates between ‘low affinity’ and ‘high affinity state’ of VWF. Furthermore, binding of the VWF A1 domain to platelet GPIb in the absence of flow requires the addition of chemical modulators, such as the snake venom protein botrocetin, or the bacterial antibiotic glycopepide ristocetin [Howard & Ferkin, 1971; Read *et al.*, 1989].

In addition, it is presumed that (ii) a transient interaction with platelet GPIb and immobilised VWF with a fast off-rate proceeds, whereas but shear induces a permanent interaction between the second VWF receptor on platelet surface, glycoprotein IIb/IIIa (GPIIb/IIIa) and VWF. Only this second interaction is capable to arrest platelets [Goto *et al.*, 1995]. This hypothesis is supported by perfusion studies on collagen-coated surfaces, showing reversible interaction of platelets with collagen-bound VWF under flow [Moroi *et al.*, 1997].

Taken together, the widely accepted concept of VWF-mediated platelet adhesion at physiological high fluid shear stress involves VWF binding to subendothel – e.g. collagen – resulting in platelet translocation along the surface in the direction of flow via reversible VWF-GPIb bonds. This slow motion allows the establishment of additional interactions, i.e. between VWF and GPIIb/IIIa, resulting in platelet activation via transducing signals and aggregation to the surface in a biphasic adhesion process [reviewed by Sadler *et al.*, 1998; Ruggeri, 2007]. The mechanism of platelet tethering, translocation and adhesion is depicted in Fig. 4, which was taken from Ruggeri [2002].

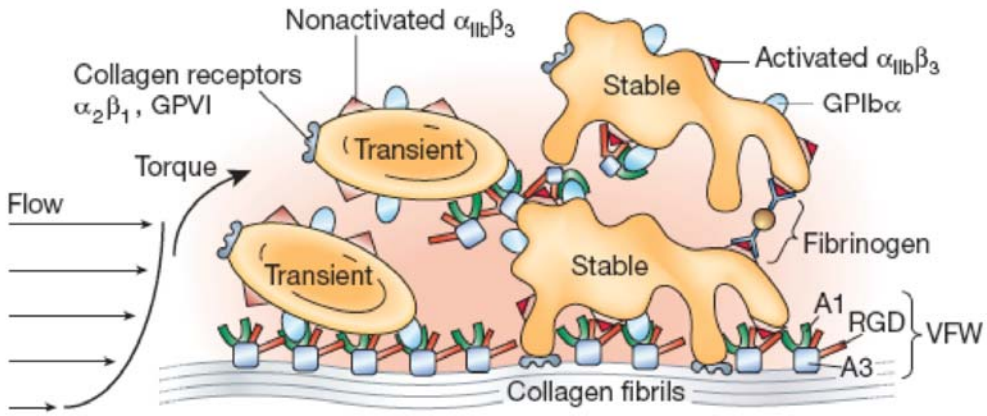

Fig. 4: Biphasic model of VWF-mediated platelet adhesion according to Ruggeri [2002]. VWF becomes immobilized on ECM, transient bonds between VWF and platelet GPIb result in translocation of platelets along the surface in the direction of flow. Secondary interactions between platelet surface receptors and extracellular collagen result in stable platelet adhesion, and finally adhesion through binding of activated platelets to various plasma proteins.

VWF-binding to connective tissue

Immobilisation of VWF occurs at exposed structures of the ECM at sites of vascular injury. Besides other ECM components, such as fibronectin, laminin, nidogen, proteoglycans and fibulin, collagens type I, III-VI, VIII and XII-XIV have been located in the vasculature [Kehrel, 1995]. Amongst them, types I, III and VI are considered to be the most active collagens in terms of haemostasis [Saelman *et al.*, 1993; Sixma *et al.*, 1995]. Binding sites of VWF to collagens I, III and VI have been assigned to the A1 and A3 domain [Roth *et al.*, 1986; Pareti *et al.*, 1987; Hoylaerts, 1997], whereas in the absence of the A3 domain the A1 domain is able to sustain stable platelet adhesion to collagen type I and III under flow conditions [Bonnefoy *et al.*, 2006]. Surface plasmon resonance-based studies as well as perfusion studies revealed that VWF preferentially binds to collagen type III [Li *et al.*, 2002; Moroi *et al.*, 1997]. But the characteristics of collagens used in perfusion studies strongly vary with regard to fibrillar structure, composition, and purity, presumably influencing the physical properties and therefore alter the interaction with VWF [Savage *et al.*, 1999; discussed by Lisman *et al.*, 2007; Moroi & Jung, 2007]. Besides interaction with collagens, VWF exhibits adhesive properties to a variety of other proteins present in the ECM: a binding site to heparin

and sulfatides within the A1 domain might be important for the interaction with proteoglycans and sulphated glycosphingolipids, and its interaction with fibrin is known to contribute to platelet adhesion on atherosclerotic vessels [reviewed by Ruggeri, 2007].

An additional interesting attribute of VWF is its ability for self-association, enabling soluble plasma VWF to reversibly interact with surface-bound or endogenous subendothelial VWF to form a sufficiently adhesive surface to mediate platelet adhesion at high shear rates occurring in circulation [Savage *et al.*, 2002; Barg *et al.*, 2007].

1.4 Von Willebrand Disease (VWD)

VWD is the most common inherited bleeding disorder characterised by a quantitative and/or qualitative VWF deficiency, with a prevalence of up to 1.3 % depending on the subtype and wide heterogeneity of symptoms [Kessler, 2007]. VWD is classified into three major categories: type 1, type 2 and type 3, whereas type 1 and 3 are associated with quantitative VWF deficiencies, and type 2 patients exhibit qualitative – and partially additionally quantitative – VWF abnormalities. Type 1 VWD is connected with moderately reduced VWF, whereas type 3 patients show virtually complete absence of VWF. Because of the enormous heterogeneity of the functional and structural defects, type 2 VWD is further separated into four subcategories: 2A, 2B, 2M and 2N [Sadler, 1994]. Subtyping of VWD type 2 comprises variants with decreased platelet adhesion accompanied by a selective decrease of the HMW VWF multimers (2A), with aberrant VWF exhibiting an increased affinity to platelet GPIb resulting in increased proteolysis of the protein by ADAMTS-13 (2B), VWF showing defective platelet adhesion but a physiological VWF multimer pattern (2M) as well as VWF variants revealing a markedly decreased affinity for coagulation FVIII accompanied by an increased FVIII clearance (2N) [reviewed in Sadler *et al.*, 2006]. Table 1 summarises the classification of VWD based on the homepage of the Scientific and Standardization Committee on von Willebrand factor of the International Society of Thrombosis and Haemostasis (ISTH SSC VWF)

Table 1: Classification of VWD adapted from the ISTH SSC VWF information homepage.

VWD classification	Description
Type 1	Partial quantitative deficiency of VWF Inheritance: Typically autosomal dominant Characteristics: Parallel reductions in VWF antigen (VWF:Ag) and FVIII, normal multimer distribution
Type 2A	Qualitative VWF defect Inheritance: Generally autosomal dominant, caused by missense mutations within the VWF A2 repeat, group 1 (defect in intracellular transport) or group 2 (increase in proteolysis in plasma after secretion) Characteristics: Absence of the largest multimers, low levels of VWF ristocetin cofactor activity (VWF:RCo) relative to VWF:Ag
Type 2B	Qualitative VWF defect Inheritance: Autosomal dominant Characteristics: (Usually) reduced high molecular weight multimers, enhanced ristocetin-induced platelet agglutination (RIPA) although VWF:RCo may be normal
Type 2M	Qualitative VWF defect Inheritance: Autosomal dominant Characteristics: Specific defects in platelet/VWF interaction, normal range of multimers
Type 2N	Qualitative VWF defect Inheritance: Autosomal recessive Characteristics: Defective VWF binding to FVIII and consequently low levels of circulating FVIII
Type 3	Clinically severe quantitative disorder Inheritance: Usually autosomal recessive (or occasionally a manifestation of homozygous or compound heterozygous inheritance of type 1 VWD) Characteristics: Markedly reduced or absent platelet and plasma VWF (less than 0.05 IU/mL), FVIII activity also reduced

1.5 Assessment of VWF function and VWD diagnosis

Although flow exerts a critical influence on VWF function, commonly used assays for determination of VWF activity and VWD diagnosis, like Ristocetin cofactor activity (VWF:RCo) or collagen binding activity (VWF:CB), are performed at relatively low shear rates or static conditions [Fischer *et al.*, 1998 (1)]. Routine laboratory assessment of VWF function does not involve the application of flow devices, because analysis is cumbersome, time-consuming and requires professional skilled personnel. Therefore, assays were designed for the diagnosis of VWD with sensitivity to detect especially the HMW VWF multimers missing in some VWD type 2 subtypes. Particularly the differential diagnosis of type 2 VWD requires the combined implementation of assays reflecting the ability of VWF to bind to collagen and to platelet GPIb. VWF functions are assumed to be reflected by VWF:CB, VWF:RCo, or ristocetin induced platelet agglutination (RIPA) in combination with the determination of VWF antigen level (VWF:Ag) and FVIII coagulant activity (FVIII:C). Only the joint application of at least three different VWF assays allows certain diagnosis and classification of VWD. Additionally, blood coagulation parameters as well as bleeding history of the family eventually indicate presence of VWD, and for final classification VWF multimer analysis (VWF MMA) and screening of the VWF gene for special mutations associated with VWD subtypes are recommended for classification [Schneppenheim, 2005; Budde *et al.*, 2006 (2)].

1.5.1 Static assays to determine VWF activity and VWD diagnosis

Collagen binding activity – VWF:CB

VWF:CB is used as a functional assay for VWF collagen binding. Assays to determine VWF:CB are especially used for the discrimination between VWD type 1 and 2, measuring the ability of plasma-derived VWF to bind to collagen using ELISA techniques [Brown & Bosak, 1986]. The power of VWF:CB to discriminate between functional and dysfunctional VWF is considerably better than of VWF:RCo because of less inter-assay and inter-laboratory variability [Michiels *et al.*, 2006]. However, the source and type of collagen used in these studies have an impact on the sensitivity against high molecular forms of VWF [Favaloro, 2000]. VWF:CB using human pepsin digested type III collagen exhibits an equal

affinity for low, intermediate, and high molecular weight VWF multimers, whereas use of fibrillar collagen type I predominantly binds HMW VWF multimers, allowing better discrimination between VWD type 1 and 2 [Neugebauer *et al.*, 2002].

Ristocetin cofactor activity – VWF:RCo

Another assay to determine the function of circulating VWF multimers is VWF:RCo. The ability of VWF to aggregate (formalin fixed) platelets in the presence of the antibiotic ristocetin is measured using variable methods, and often used to determine the ability of VWF to mediate platelet adhesion under flow, albeit the shear rates applied by different instruments do not mimic physiological high arterial blood flow conditions. VWF:RCo is a quantitative assay and allows detection of qualitative VWF abnormalities, because the interaction of VWF with the platelet membrane receptor GPIb in the presence of ristocetin is dependent on the multimerisation degree of VWF. However, VWF:RCo is not ideally suited to determine low VWF concentrations of less than 0.1 IU/mL, and inter-assay as well as inter-laboratory deviation is very high [Michiels *et al.*, 2006]. A variant of this assay is represented by RIPA, measuring the ristocetin-induced aggregation of platelet-rich plasma under agitation using an aggregometer [Weiss, 1975].

Determination of VWF antigen level – VWF:Ag

The assessment of VWF:Ag is generally used in diagnosis of VWD, because the antigen level is reduced in the majority of patients. ELISA-based assays are commercially available, but – as well as other assays for the assessment of VWF function – exhibit relatively high inter- and intra-laboratory variances. Since these assays quantitatively measure the VWF:Ag level, no evidence on the functionality of the present VWF or its multimeric composition can be given. But the ratio between VWF:Ag and VWF:RCo or VWF:CB is highly relevant for the discrimination between VWF type 1 and 2: most patiens with VWF type 2 – except type 2N – exhibit a decreased ratio below 0.6 of VWF:Ag/VWF:RCo and VWF:Ag to VWF:CB [Michiels *et al.*, 2006]. In contrast, plasma of type 1 VWD patients show a ratio of about 1 for both assays, possessing equally decreased values of all VWF parameters below 0.6 IU/mL because of a quantitative VWF deficiency.

FVIII coagulant activity – FVIII:C

The FVIII:C is determined by incubation of endogenous VWF/FVIII isolated from patient plasma with fixed amounts of a recombinant FVIII:C, and bound VWF is measured using a chromogenic test or labelled monoclonal antibodies against FVIII:C [Michiels *et al.*, 2006]. Subsequently, the immobilised VWF is measured and plotted against the bound FVIII:C [Budde *et al.*, 2002]. The knowledge of FVIII:C is essential for the identification of patients suffering from VWD type 2N, because they exhibit an impaired binding of VWF to FVIII, resulting in a decreased half-life of the coagulation factor. Furthermore, the FVIII:C level is a reliable indicator for the severity of the haemorrhagic risk.

Multimer analysis of VWF – VWF MMA

The multimeric pattern of VWF on agarose gels is very helpful in VWD diagnostics, indicating loss of high molecular weight forms of VWF as well as an aberrant VWF triplet structure. In combination with analyses of the VWF gene, this method allows a reliable classification of VWD subtypes in type 2 VWD. Densitometric evaluation of chemiluminescence signals allows quantification of VWF multimers, however, it is difficult to produce gels with ideal distributed signals [Budde *et al.*, 1993; Budde, 2008]. VWF cannot enter the pores of a polyacrylamide gel because of its size, so agarose gels are used to determine the multimeric distribution of VWF. The use of low resolution gels of 0.7 - 1.2 % is recommended for the separation of the largest VWF multimers, but medium resolution gels of 1.4 - 2.0 % agarose are sufficient for VWD diagnosis and give a better resolution of the VWF triplet structure. The contribution of VWF MMA to diagnosis and classification of VWD is extensively reviewed by Budde *et al.* [2006 (2)]. An example of a VWF multimer medium resolution gel is given in Fig. 3. Although the method has become less cumbersome, the analysis still lasts three days and requires professional skilled personnel, and is therefore only performed in specialised laboratories.

1.5.2 Genetic approach to classify VWD

Advancing knowledge of various genetic defects of VWD subtypes in some cases allows differentiated classification of VWD phenotypes: mutation cluster exist in some regions of the VWF gene, associated with VWD type 2A or 2B, enabling systematic analysis of defined gene regions [Schneppenheim & Budde, 2005; Peake & Goodeve, 2007]. However, many patients suffering from type 1 VWD do not exhibit mutations within the VWF gene, suggesting more complex correlations also involving defects in other genes participating in VWF biosynthesis [Lillicrap, 2007].

1.5.3 VWF function under flow

Since VWF is essential for platelet adhesion to dissected subendothel only at physiological high arterial blood flow conditions, its function is strongly dependent on hydrodynamic and rheological parameters present in human circulation. However, the definition of the velocity and hydrodynamic profile in blood vessels is very difficult, because it varies with regard to plasma viscosity, contingent of red blood cells, cell deformability, flow rate and the properties of the blood vessel itself. All these characteristics strongly affect *in vivo* haemostasis and thrombus formation. Plasma viscosity and the portion of red blood cells influence the local shear stress, and red cells are crucial for pushing the smaller platelets to the vessel wall layer enabling contact with the subendothelium [reviewed by Zwaginga *et al.*, 2006]. Therefore, it is important to consider these aspects employing assays for the investigation of VWF under flow.

Flow devices in haematology

Two types of flow-chambers exist for studying platelet interaction with the vessel wall: parallel plate and annular perfusion chambers. In the 1970th, Baumgartner began to investigate the role of platelets in terms of thrombotic events using annular flow devices, perfusing subendothelium with whole blood to study platelet adhesion. These ‘Baumgartner chambers’ became rapidly accepted; allowing the investigation of haemostatic events under well defined experimental conditions [e.g. Baumgartner, 1973; Baumgartner *et al.*, 1976]. Parallel plate perfusion chambers were developed by Sakariassen and colleagues a few years

later, facilitating blood perfusion studies to various components of the vessel wall under different shear rate conditions [Sakariassen *et al.*, 1983]. The parallel plate perfusion chambers were further developed over the last decades for *in vitro* and *ex vivo* studies on haemostasis as well as drug efficacy or VWD, aiming to minimise the sample volume and standardise the experimental procedure [e.g. Moroi *et al.*, 1997; Remijn JA, 2001; Gutierrez *et al.*, 2008; historical review by Sakariassen *et al.*, 2004]. Albeit flow devices provide a promising tool to determine VWF activity under flow and might be helpful in classification of VWD [Zwaginga *et al.*, 2007], there are still no standardised flow assays available, and handling of existing devices remains challenging and cumbersome.

Surface Plasmon Resonance (SPR)

The technique of SPR is based on the excitation of surface plasmons by light, whereas surface plasmons are electromagnetic waves propagating parallel to a metal interface on the boundary between metal (e.g. gold) and an external medium (e.g. liquid). A sensor chip, composed of a glass carrier with a thin layer of gold, is coupled with a dextran matrix and a ligand is immobilised onto the surface. An optical SPR detector is placed on the glass-side of the chip measuring the ‘mass’ adsorbing to the immobilised ligand via changes in the local refractive index upon adsorption of biomolecules, and thus allows the detection of unlabelled samples in real time [Jönsson *et al.*, 1991]. The method was initially used to study antibody-antigen interactions, whereas the technique facilitates conclusions about the binding kinetics: association and dissociation are measured in arbitrary units, displayed in a sensorgram, and mathematical correlation is used to obtain binding constants [Karlsson *et al.*, 1991]. A schematic diagram of the SPR principle is depicted in Fig. 5.

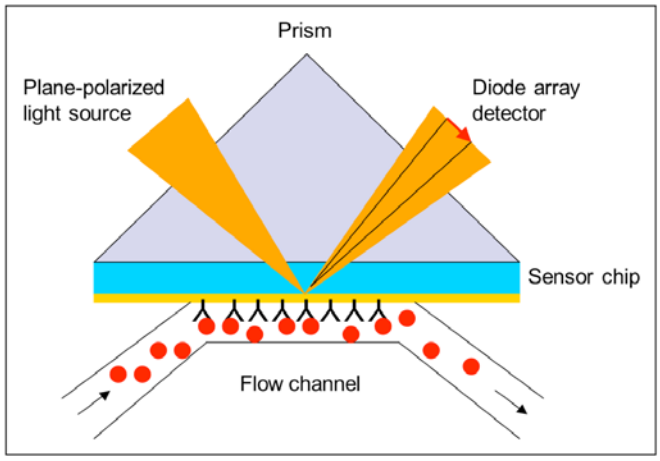

Fig. 5: Schematic diagram of the SPR principle. A ligand is coupled to a dextran matrix on the sensor chip and the analyte is perfused through the flow channel. A light beam excites surface plasmons in their resonance frequency at a given wavelength and angle. Binding is measured as a function of time through changes in the local refractive index, depicted as resonance units in the sensorgram. Changes less than 1 pg/mm will be noticed.

Recently, SPR-based technology was used to determine the binding kinetics of VWF to different types of collagen [Saenko *et al.*, 2002], sulphated carbohydrates [Suda *et al.*, 2006; Wakao *et al.*, 2008], laminin [Inoue *et al.*, 2008], and to investigate platelet adhesion using a modified SPR-based flow-chamber device [Hansson *et al.*, 2007]. However, data analysis is complicated due to the complexity of the VWF protein and the variety of binding sites provided by its multimeric structure. Additionally, mathematical models are capable to simulate either 1:1 (Langmuir) binding kinetics or bivalent analyte model [Karlsson, 1994], and do not take into account the heterogeneity and potential multi-ligand structure of such a complex protein.

2 Objective

The multimeric glycoprotein Von Willebrand Factor (VWF) is essential for primary haemostasis in flowing blood. Although VWF function was studied extensively during the last thirty years, VWF activity assays are generally performed at relatively low shear rates or under static conditions. However, *in vivo* VWF has to bind to exposed components of the extracelluar matrix, and continuatively mediate stable platelet adhesion under physiological flow conditions.

This thesis presents investigations of the VWF function under high arterial shear rates. Aim of the research project was the establishment of an *in vitro* flow-chamber model to examine the ability of VWF to mediate platelet adhesion under physiological conditions, which is extensively characterised. Experiments were performed in commercially available flow-devices applying low to high shear rates occurring in the human circulatory system. VWF-mediated platelet adhesion was monitored using time-lapse microscopy.

The established flow-chamber model was implemented to compare the ability of different commercially available VWF-containing concentrates to mediate stable platelet adhesion at high arterial shear rates. Furthermore, VWF was fractionated according to its multimeric composition using Fast Protein Liquid Chromatography technique (FPLC) with a size exclusion column to obtain low, intermediate and high molecular weight VWF multimers. These fractions were investigated with regard to their ability to mediate platelet adhesion at 1,700 s^{-1} shear rate on collagen type III. The results were compared to VWF affinity to collagen type III using Surface Plasmon Resonance (SPR) in order to determine the correlation between VWF multimer size and function.

3 Materials and methods

3.1 Materials

3.1.1 Chemicals and other materials

Chemical products were obtained from Sigma-Aldrich Chemie (Steinheim, Germany) and Roth (Karlsruhe, Germany) in high-purity quality. Disposables were purchased from Falcon (Heidelberg, Germany), Eppendorf (Hamburg, Germany) and Nunc (Wiesbaden, Germany). Chromatography columns were from GE Healthcare Biosciences (Uppsala, Sweden). Ultrapure water (HPLC-water) was obtained from J.T. Baker (Deventer, Netherlands). Special reagents, chemicals and material from other manufacturers are specified below.

Product	**Manufacturer**
Agarose high gelling temperature – SAEKEM HGT (P) agarose	Cambrex BioScience, Rockland, US
Agarose low gelling temperature – Agarose Type VII LGT	Sigma-Aldrich Chemie, Steinheim, Germany
Albumin from bovine serum	Sigma-Aldrich Chemie, Steinheim, Germany
Biacore Sensor Chip CM5	GE Healthcare Bio-Sciences, Uppsala, Sweden
BioRad filter paper model 583 GelDryer	BioRad, Hercules, US
Cell tracker green CMFDA (5-chlormethyl-fluorescein diacetate dye)	Molecular Probes, Eugene, USA
Centrifugal filter devices, 100.000 MWCO	Millipore, Schwalbach, Germany
Disposable 5 mL polypropylene columns	Pierce, Rockford, US
EC-Plan-NEOFLUAR objective, 40x/1.3 oil	Carl Zeiss MicroImaging, Jena, Germany
Equine tendon fibrillar collagen I – Kollagen-reagenz Horm®	NYCOMED Austria, Linz, Austria
Filter set 10 and 49 for Axio ObserverZ.1	Carl Zeiss MicroImaging, Jena, Germany
Flow-chambers, µ-slide VI flow	ibidi, Munich, Germany
Gel bond film, agarose gel support medium	Lonza, Rockland, US
Glass microfibre filters, GF/A	Whatman, Middlesex, UK

Glass plates, float glass 4 mm, 28 x 17 cm	Glas-design, Berlin, Germany
Leukocyte-depleted thrombocyte concentrate	Haema, Blood and Plasma Donation Centre Berlin, Germany
NCL-W silicon cantilever	NanoandMore, Wetzlar, Germany
Pasteurised, homogenised, UHT (Ultra-High Temperature processed) milk, 1.5 % fat	REWE-Handelsgruppe, Köln, Germany
Pepsin-digested collagen type III from human placental villi	Southern Biotechnology, Birmingham, US
Plan-APOCHROMAT objective, 63x/1.4 oil	Carl Zeiss MicroImaging, Jena, Germany
Protran nitrocellulose transfer membrane	Whatman, Dassel, Germany
Red blood cells, concentrate	Haema, Blood and Plasma Donation Centre Berlin, Germany
Roti-Blue 5x concentrate	ROTH, Karlsruhe, Germany
SDS-PAGE gels – ProGel 4 % Tris/Glycin gels, 10 x 10 cm	Anamed, Groß-Bieberau, Germany
Sephadex G-25	GE Healthcare Bio-Sciences, Uppsala, Sweden
Sepharose 2B	GE Healthcare Bio-Sciences, Uppsala, Sweden
Sepharose CL-2B	GE Healthcare Bio-Sciences, Uppsala, Sweden
SuperSignal West Pico chemiluminescent substrate	Pierce, Rockford, USA
Thrombin from human plasma, lyophilised powder	Sigma-Aldrich Chemie, Steinheim, Germany
UDP-α-D-Galactose, disodium salt	Calbiochem/Merck, Darmstadt, Germany

3.1.2 Test kits

Biacore amine coupling kit	GE Healthcare Bio-Sciences, Uppsala, Sweden
BioRad protein assay (dye reagent, 5x concentrate)	Bio-Rad Laboratories, Hercules, US
IMUBIND® VWF ELISA Kit	American Diagnostica, Stamford, US
Sigma FAST™ OPD tablet set (*o*-phenylene-diamine dihydrochloride)	Sigma-Aldrich Chemie, Steinheim, Germany
Technozym® VWF:Ag ELISA	Technoclone, Vienna, Austria

3.1.3 Antibodies

Clone	**Specificity**	**Conjugate/Label**	**Producer**
Monoclonal antibody (mAb) 82D6A3	Against VWF A3 domain	None	Prof. H. Deckmyn, Belgium
Monoclonal mouse IgG, SM1150F	Anti-CD62P (P-selectin)	FITC	Acris Antibodies, Hiddenhausen, Germany
Monoclonal mouse IgG, SM2291P (clone RFF-VIII R/1) MAH<VWF-GPIb>	Against GPIb binding domain of human VWF	None	Acris Antibodies, Hiddenhausen, Germany
Polyclonal goat IgG, A11001 GAM<IgG>	Anti-mouse IgG	Alexa Fluor® 488	Invitrogen, Karlsruhe, Germany
Polyclonal goat IgG, A11046 GAR<IgG>	Anti-rabbit IgG	Alexa Fluor® 350	Invitrogen, Karlsruhe, Germany
Polyclonal rabbit IgG, A0082 RAH<VWF>	Anti-human VWF	None	DakoCytomation, Glostrup, Denmark
Polyclonal rabbit IgG, P0226	Anti-human VWF	Horseradish peroxidase (HRP)	Biozol Diagnostica, Eching, Germany
Polyclonal swine IgG	Anti-rabbit IgG	FITC	DakoCytomation, Glostrup, Denmark

3.1.4 Calibrators and molecular weight standards

1st international standard von Willebrand factor, concentrate, NIBSC code 00/514	NIBSC, Hertfordshire, UK
Control Plasma Normal, lot 1P41000	Haemochrom Diagnostica, Essen, Germany
HiMark Pre-stained high molecular weight protein standard	Invitrogen, Karlsruhe, Germany

3.1.5 Plasma-derived VWF-containing concentrates

Concentrate	**Lot No.**	**Manufacturer**
Alphanate®	AS06019A AS07021A	Grifols Biologicals, Los Angeles, US
Fanhdi®	IBVA5HMHL1 (250 IE) IBVB5JLJM1 (500 IE)	Instituto Grifols, Barcelona, Spain
Haemate® P 500 Haemate® HS 500	24966911C 01866911A	CSL Behring, Marburg, Germany
Wilate® 900 IE	A715A189 A721A189 A721B189	Octapharma Pharmazeutika, Vienna, Austria
Wilfactin 100 IU/mL	07L05692 07L06238	LFB, Les Ulis, France

3.1.6 Equipment

Instrument	**Manufacturer**
Axio ObserverZ.1 inverted stage fluorescence microscope with AxioCam HR	Carl Zeiss MicroImaging, Jena, Germany
Biacore 2000	Biacore, Uppsala, Sweden
Biologic HR chromatography system	Bio-Rad Laboratories, Hercules; US
EI9001-XCell II Mini Cell system for SDS-PAGE	Novex, San Diego, USA
Electrophoresis unit Multiphor II equipped with EPH-Electrodes, electrophoresis power supply EPS 3501 XL, and thermostatic circulator MultiTemp III 230 VAC	GE Healthcare Bio-Sciences, Uppsala, Sweden
FACScan flow cytometer	Becton Dickinson, Franklin Lakes, US
FluoArc control gear	Carl Zeiss MicroImaging, Jena, Germany
FLUOstar OPTIMA microplate reader	BMG LABTECH, Jena, Germany
Fujifilm LAS-1000 chemiluminescence imaging system	Fujifilm Europe, Düsseldorf, Germany
Haereus centrifuge FRESCO17	Fisher Scientific, Schwerte, Germany
Hoefer TE Transphor electrophoresis unit	GE Healthcare Bio-Sciences, Uppsala, Sweden
Ibidi pump system	ibidi, Munich, Germany
Laser Spectroscatter 201	RiNa, Berlin, Germany
Nanoscope Multimode IIIa	Digital Instruments, Santa Barbara, US
PowerPac 200 power supply	BioRad, Hercules, US
PrimoR Benchtop centrifuge	Heraeus, Hanau, Germany
Smartline pump 1000	Knauer, Berlin, Germany
Spectrometer type Specord 40	Analytik Jena, Jena, Germany
Thermomixer comfort	Eppendorf, Hamburg, Germany
Titramix 100	Heidolph Instruments, Schwabach, Germany

3.1.7 Buffers and solutions

Buffer or solution	**Final concentration, components**
Acetate buffer	10 mM NaAc, pH 4.0
Agarose gel electrophoresis running buffer	250 mM Tris 1.925 M Glycine 0.5 % (w/v) Sodium dodecyl sulfate (SDS)
Agarose gel electrophoresis sample buffer	10 mM Tris-HCl, pH 8.0 10 mM Na_2EDTA 15 % (v/v) Glycerin 2 % (w/v) SDS
Agarose gel electrophoresis separation gel buffer	375 mM Tris-HCl, pH 8.8
Agarose gel electrophoresis stacking gel buffer	125 mM Tris-HCl, pH 6.8
Biacore running buffer (HBS-EP)	3.4 mM EDTA 10 mM HEPES 150 mM NaCl 0.005 % Tween 20, pH 7.4
Biacore surface regeneration solution A	1 mM EDTA 1 M NaCl 0.1 M Tri-sodium citrate dihydrate, pH 5.0
Biacore surface regeneration solution B	10 mM Taurodeoxycholic acid 100 mM Tris
Biacore surface regeneration solution C	0.1 M H_3PO_4
Blotting buffer	200 mM Na_2HPO_4 50 mM NaH_2PO_4 0.2 % (w/v) SDS, pH 7.4
Coomassie destaining solution	5 % (v/v) Ethanol
Coomassie staining solution	20 % (v/v) Ethanol 20 % (v/v) Roti-Blue, 5 x concentrate
ELISA blocking buffer	0.1 % (w/v) BSA 0.1 % (v/v) Tween 20 in PBS
ELISA coating buffer	7.5 mM Na_2CO_3 17 mM $NaHCO_3$, pH 9.6
ELISA stop solution	1 M HCl
ELISA washing solution	0.1 % (v/v) Tween 20 in PBS

Fixation solution	4 % (w/v) Paraformaldehyde (PFA) in PBS
Flow-chamber perfusion buffer	20 mM Tris-HCl, pH 7.4
Phosphate-buffered saline (PBS)	136 mM NaCl 2.7 mM KCl 15 mM Na_2HPO_4 x 2 H_2O 1.8 mM KH_2PO_4, pH 7.4
Platelet buffer	145 mM NaCl 10 mM HCO_3^--free N-2 hydroxyethylpiperazine-N'-2-ethanesulfonic acid (HEPES) 10 mM Glucose 0.2 mM Na_2HPO_4 5 mM KCl 2 mM $MgCl_2$ 0.3 % (w/v) Bovine serum albumin (BSA), pH 7.4
Polyacrylamide gel electrophoresis running buffer	25 mM Tris-HCl 150 mM Glycine 0.1 % (w/v) SDS, pH 8.8
Polyacrylamide gel electrophoresis sample buffer	10 % (v/v) Glycerin 60 mM Tris 0.003 % (v/v) Bromphenol blue 2.5 % (w/v) SDS 0.1 % (w/v) Dithiothreitol (DTT)
Polyacrylamide gel electrophoresis blotting buffer	25 mM Tris 114 mM Glycine 10 % (v/v) Ethanol
SEC buffer	20 mM Tris-HCl, pH 7.4 0.02 % (v/v) Tween 20

3.1.8 Software

Adobe Photoshop and Illustrator, CS3	Adobe, San Jose, USA
AutMess software module	Carl Zeiss MicroImaging, Jena, Germany
AxioVision 4.6	Carl Zeiss MicroImaging, Jena, Germany
Biaevaluation Software	GE Healthcare Bio-Sciences, Uppsala, Sweden
Image Gauge V3.3	Fujifilm Europe, Düsseldorf, Germany
Prism 4.01 for Windows	GraphPad Software, San Diego, US

3.2 Methods

3.2.1 Qualitative and quantitative characterisation of the VWF preparations

Utilised VWF-containing concentrates

For the establishment of the flow-chamber model, VWF provided by a commercially available plasma derived VWF/FVIII concentrate (Wilate®, lot A715A189) was implemented [Stadler *et al.*, 2006]. The separation of VWF into samples containing different multimeric structure via SEC was done using an exploratory sample of pdVWF. Flow-chamber concentrate comparison was performed with two different batches each of five commercially available VWF-containing concentrates: Wilate®, Humate®, Alphanate®, Fanhdi® and Wilfactin (for specification please refer to 3.1.5).

Protein concentration

Protein concentration was determined by the Bradford assay [Bradford, 1976] in a microtitre plate format using an eight-point dilution of BSA standard for calibration. The shift in the coomassie brilliant blue G-250 absorbance from 465 to 595 nm upon protein binding in acidic solution was detected in a FLUOstar OPTIMA microplate reader at 595 nm wavelength.

Determination of VWF antigen concentration

VWF:Ag concentrations were determined using the IMUBIND® VWF ELISA Kit or the Technozym® VWF:Ag ELISA according to the manufacturer's instructions. Because of cost-benefit ratios of the commercially available VWF:Ag test kits, exhibiting a standard deviation of around 20 %, an in-house sandwich ELISA for the determination of VWF:Ag concentration was established. A 96 well microtitre plate was coated with a polyclonal rabbit anti-human VWF antibody diluted 1:500 in coating buffer, and incubated at +4 °C over night (o/n). After blocking with ELISA blocking buffer (+37 °C, 1 h), triplicate samples containing VWF antigen and a six-point standard calibration curve in duplicate, diluted in blocking buffer, were applied and allowed to bind at +37 °C for 2 h. For detection, plates were incubated with a HRP-conjugated polyclonal rabbit anti-human VWF antibody, diluted 1:2,000 in

blocking buffer, for 2 h at +37 °C. Every incubation step was followed by three washing steps applying ELISA washing solution. Sigma Fast OPD tablet set was used as substrate, and after 15 min incubation on a shaker at room temperature (RT), colour development was stopped with 1 M HCl. All tempered incubation steps were done on a thermomixer comfort with MTP block at 400 rpm. Absorbance reading was performed using a FLUOstar OPTIMA microplate reader at 492 nm wavelength. The 1st international standard 00/514 was used for calibration.

SDS-PAGE and Western blotting

To determine the purity of the VWF/FVIII concentrate used for the establishment of the flow-chamber model, a polyacrylamide gel electrophoresis under reducing conditions was carried out using Pre-cast tris-glycine 4 % polyacrylamide gels. The electrophoresis was performed in an EI9001-XCell II Mini Cell electrophoresis unit at 100 V for 10 min, and subsequently at 200 V for about 1 h at RT using a sample volume of 20 µL. Gels were stained with coomassie brilliant blue o/n at RT for determination of protein content. Destaining was carried out using 5 % ethanol solution for 2 x 20 min at RT.

To assign the VWF bands, proteins were blotted onto a nitrocellulose membrane for 1.5 h at 200 V (about 1 mA/cm^2) on an ice bath. Membranes were subsequently blocked in 50 mL of 1.5 % UHT milk, and Western blot was carried out using a HRP-conjugated polyclonal rabbit anti-human VWF antibody, diluted 1:2,000 in 1.5 % UHT milk o/n at 4 °C. After two washing steps of 20 min each with 1.5 % UHT milk, the chemiluminescence signal was visualised using SuperSignal West Pico chemiluminescent substrate in a Fujifilm LAS-1000.

Dynamic Light Scattering (DLS)

DLS technique can be implemented to determine the size distribution of small particles in solution. Irradiation with monochromatic, coherent laser beam passing a colloidal dispersion results in scatters of light. In case of very small particles compared to the wavelength of the light, a uniform light scattering in all directions is obtained (Rayleigh scattering). The hydrodynamic radius of particles, polydispersities, or the presence of aggregates in protein samples can be observed because of time-dependent fluctuations in the scattered intensity due to the Brownian motion of small molecules in solution, whereas the distance

between scatters in solution is constantly changing with time and depends on the particle size, viscosity (refractive index of the solvent), and temperature of the solution.

The VWF/FVIII sample used for the flow-chamber development was reconstituted in water for injection containing 0.01 % Tween 20, passed through a 0.2 µm particle filter, and 100 µL were subjected to DLS. The experiment was performed in triplicate using a Laser Spectroscatter 201 with a measurement period of 2 min.

VWF multimer analysis (VWF MMA)

The multimeric distribution of the various VWF samples was evaluated using a horizontal discontinuous agarose gel electrophoresis technique developed by Budde *et al.* [1990; 2006 (2)]. Low resolution gels were composed of 1.2 % (w/v), and high resolution gels for illustration of the triplet structure were composed of 1.6 % LGT agarose, respectively. The stacking gel contained 0.8 % (w/v) HGT agarose. First, the separation gel was poured between glass plates using polyvinyl chloride spacer of 3 mm thickness. After gelling, gels were left for 2 h at +4 °C. The top of the separating gels was horizontally cut according to a template, glass plates were fixed together again and stacking gel was poured on top. After polymerisation, gels were kept for at least 1 h at +4 °C. Samples were prepared using a final concentration of 0.05 IU/mL VWF:Ag diluted with sample buffer for agarose gel electrophoresis. Standard human plasma was applied in a final dilution of 1:20. Frozen samples were thawed at +37 °C for 30 min at 400 rpm to exclude loss of VWF:Ag because of cryoprecipitation [Refaai *et al.*, 2006]. After addition of sample buffer, samples were incubated at +60 °C for 30 min and 400 rpm using a thermomixer. Filter papers were attached to top and bottom of the gel submerging in the buffer reservoirs to allow current conduction. A sample volume of 20 µL was applied per slot, and initially electrophoresis was carried out for 1 h at 65 V (25 mA/gel) and +15 °C until the dye front fully entered the gel. Slots were closed using stacking gel, and gels were covered with glass plates to avoid evaporation and dehydration. Electrophoresis was performed o/n at 55 V (15-18 mA/gel) for 16 - 18 h at +15 °C until the dye front reached the beginning of the filter paper. Finally, electrophoresis was executed at 120 V (45 mA/gel) for about 1 h until the dye front reached the bottom of the gel for better separation of the VWF subbands.

Subsequent to electrophoresis, proteins were electroblotted on a nitrocellulose membrane at 1.5 A for 4 h at a temperature below +20 °C using a tank blot Hoefer TE Transphor Electrophoresis unit. After blotting, membranes were blocked in 200 mL of 1.5 % UHT milk for 30 min at RT on a shaker, followed by incubation of membranes with a HRP-conjugated polyclonal rabbit anti-human VWF antibody, diluted 1:2,000 in 100 mL of 1.5 % UHT milk, for 1.5 h at RT on a shaker and stored at +4 °C o/n. Afterwards membranes were washed two times with 200 mL of 1.5 % UHT milk for 20 min each at RT on a shaker, extensively rinsed with water and the chemiluminescence signal was visualised as described above (cf. 3.2.1).

For determination of the VWF multimers bound to collagen under flow, the remaining liquid after perfusion of 1 IU/mL VWF:Ag at different shear rates for 4 min over a collagen-coated flow-chamber and extensively rinsing with buffer, was removed. Sample buffer for multimer analysis was added to the channels (50 µL), and slides were incubated at +60 °C for 30 min and 400 rpm on a thermomixer with a MTP block. The channel volume was quantitatively aspirated, transferred into EPC's, samples were diluted to about 0.05 IU/mL VWF:Ag and stored at -20 °C until multimer analysis. Repeated dissolution gave no more VWF signal when subjected to gel electrophoresis and Western blotting (data not shown).

3.2.2 Platelet isolation and labelling

Freshly prepared concentrates of leukocyte-depleted thrombocytes collected by aphaeresis were provided by Haema. The platelet concentrates were incubated with 200 µM UDP-α-D-Galactose and 10 µM CellTracker Green 5-chloromethylfluorescein diacetate dye (CMFDA) for 30 minutes at +37 °C and 300 rpm in the dark on a thermomixer. Platelets were washed and separated from plasma using a Sepharose 2B column according to Vollmar *et al.* [2003] with slight modifications. Briefly, 7 mL Sepharose 2B were washed with 50 mL of 0.9 % NaCl in a disposable filter, poured into a disposable polypropylene column and equilibrated with 5 column volumes of platelet buffer. Platelets were collected in clouded drops and diluted to 2.5 x 10^8 platelets/mL with platelet buffer for perfusion experiments.

3.2.3 Platelet counting

The platelet count was determined by a photometric method [Walkowiak *et al.*, 1997] using a spectrometer type Specord 40. The absorbance of the platelet preparations using a 1:10 dilution in platelet buffer was read at a wavelength of 800 nm against platelet buffer reference, and platelet concentration was calculated using the following equation:

$$N\left[10^8/mL\right] = \left\{\left[\frac{6.23}{\left(2.016 - k * \lambda * \frac{A}{800}\right)}\right] - 3.09\right\} * Dilution\ Factor$$

N = platelet count

λ = wavelength

k = cuvette layer thickness

A = absorbance at 800 nm

3.2.4 Determination of platelet activation

Platelet activation was measured by the expression of P-selectin on the platelet surface using a FACScan flow cytometer as described previously [Leytin *et al.*, 2000; Leytin *et al.*, 2002]. Platelets were diluted to 1 x 10^6 platelets/mL using platelet buffer, whereas preparations of 100 µL volume were used for Fluorescence Activated Cell Sorting (FACS) analysis. One platelet preparation was activated by the addition of human thrombin at a final concentration of 1 IU/mL and incubated at +37 °C, 300 rpm on a thermomixer for 10 min. A FITC-conjugated monoclonal anti-CD62P antibody against the activation marker P-selectin on the platelet surface was used to determine the degree of platelet activation during the isolation procedure using a concentration of 1 µg/mL. Samples were incubated for 30 min at +25 °C and 300 rpm in the dark. A volume of 300 µL platelet buffer was added and samples were centrifuged at 380 x g for 5 min. The supernatant was discarded and platelets were resuspended in 300 µL platelet buffer, followed by repeated conduction of the centrifugation procedure. Platelet pellets were dissolved in 300 µL platelet buffer and subjected to FACS analysis. The platelet population was identified on the basis of forward and side scatter, whereas gating on events identified as platelets was performed to exclude measurement of air

bubbles in the applied buffer, gauging fifteen thousand gated events for each sample. A control sample without addition of the antibody was used as a marker for autofluorescence.

3.2.5 Fractionation of VWF via SEC

Fractionation of pdVWF by multimer size was performed conducting Fast Protein Liquid Chromatography (FPLC) with a Size Exclusion Chromatography (SEC) column. The sepharose CL-2B column was tested and optimal separation conditions were established using an exploratory sample of pdVWF. Prior to fractionation, the column was equilibrated with three column volumes of SEC buffer. The separation was performed at a flow rate of 0.5 ml/min. A sample volume of 3 ml containing 115 IU/ml VWF:Ag pdVWF was applied onto the column. VWF started to elute after 60 mL running volume, and was collected into 26 fractions á 5 ml. The protein- and VWF:Ag concentration as well as the degree of multimerisation was determined using 1.2 % agarose gels. SEC was performed four times in order to obtain enough material to perform functionality studies, such as surface plasmon resonance-based collagen binding and flow-chamber experiments. Fractions were pooled according to VWF multimer size, creating three fractions of different multimeric composition: the High Molecular Weight (HMW) fraction contained predominantly 5 - 8mers, the Intermediate Molecular Weight (IMW) fraction was composed of mainly 4 - 6mers, and the Low Molecular Weight (LMW) fraction mostly contained VWF multimers 2 - 3, whereas the 1mer is usually attributed to a VWF dimer with a molecular weight of around 500 kDa according to the first band in VWF MMA. Fractions were stored at -80 °C until use.

3.2.6 Atomic Force Microscopy (AFM)

Flow-chambers were coated with either 100 µL/flow-channel 0.1 mg/mL human pepsin-digested collagen type III or equine tendon fibrillar collagen type I, dissolved in 50 mM acetic acid at +4 °C o/n, saturated with 1 % HSA in PBS for 1 h at RT and rinsed excessively with ultrapure water. Prior to microscopy, the channel bottom was excised, dried at RT and glued to a metal disc for microscopic analysis. The AFM measurements have been performed using a Nanoscope Multimode IIIa, operated in the tapping mode using silicone probes at resonance frequencies of 150 - 190 KHz under ambient conditions. The cantilever

was forced to oscillate near its resonance frequency. The force constant of the silicon cantilever with a size of 225 µm was at 48 N/m with a curvature radius of >10 nm.

3.2.7 Immunofluorescence of VWF

Flow-chambers were coated as described above and perfused with VWF at a concentration of 1 IU/mL VWF:Ag for 4 min at 1,700 s^{-1} shear rate. Subsequently, flow-chambers were rinsed with 15 channel volumes of flow-chamber perfusion buffer at the same shear rate. For immunofluorescence of collagen-bound VWF, two different antibodies were used: first, the flow-chambers were incubated with a primary monoclonal mouse antibody to human VWF, directed against the VWF-GPIb binding domain (MAH<VWF-GPIb>), utilised at 7 ng/mL, for 1 h at RT on a shaker. After excessive rinsing with PBS, flow-chambers were incubated with a polyclonal rabbit anti-human VWF antibody (RAH<VWF>) at 15 ng/mL again for 1 h at RT. After washing with PBS, the flow-chambers were incubated with a 1:1 mixture of secondary antibodies Alexa Fluor® 488 goat anti-mouse IgG (GAM<IgG>), and Alexa Fluor® 350 goat anti-rabbit IgG (GAR<IgG>), both utilised at 3 ng/mL, for 1 h at RT. Microscopic analysis was carried out using the Axio ObserverZ.1 fluorescence microscope at original magnification x 630.

3.2.8 Inhibition experiments

The specificity of the VWF-collagen binding was determined using the monoclonal (mAb) 82D6A3 directed against the A3-domain of VWF, which was kindly provided by H. Deckmyn (Belgium), according to Vanhoorelbeke *et al.* [2003]. VWF samples at 1 IU/mL VWF:Ag were preincubated with 2.5 µg/mL mAb 82D6A3 for 30 min prior to perfusion over the flow-chamber at 1,700 s^{-1} shear rate for 4 min, followed by either immunofluorescence using a polyclonal rabbit anti-human VWF antibody, or platelet perfusion over the generated surface for determination of platelet adhesion in real time using time lapse microscopy (see below). For immunofluorescence, a FITC-conjugated polyclonal swine anti-rabbit IgG was used as secondary antibody, utilised in accordance to the application of secondary antibodies described above.

3.2.9 Flow-chamber experiments

Commercially available flow-chambers were used for all perfusion studies, providing six perfusion channels on one µ-slide with a channel volume of 30 µL, and dimensions of 17 x 3.8 x 0.4 mm (length x width x height). To minimise the mechanical stress on suspended red blood cells and platelelets as well as to maintain unidirectional flow, the ibidi pump system was used. The utilised perfusion set required a sample volume of 10 mL, whereas the dead volume within the tubings was 0.3 mL, and the samples were recirculated unidirectional over the flow-chamber surface according to the perfusion time and applied flow rate necessary to obtain the various shear rates.

Flow-chambers were coated as described in section 3.2.6. Red blood cells were washed with 0.9 % NaCl at +4 °C and 1,500 x *g* until the supernatant was clear, and utilised at 33.$\overline{3}$ % haematocrit. Perfusion studies were performed using the ibidi pump system combined with a FPLC-pump at physiological low to high shear rates of 400, 1,700 and/ or 4,000 s^{-1} [Tangelder *et al.*, 1988; Stroev *et al.*, 2007], whereas the appropriate air pressure was adjusted according to each sample prior to perfusion studies dependent on its viscosity. Pump and tubings were blocked with 3 % BSA/PBS and washed with flow-chamber perfusion buffer before starting the experiment. VWF concentrations of 1 IU/mL VWF:Ag were applied for 4 min, and subsequently flow-chambers were rinsed with at least 15 channel volumes of flow-chamber perfusion buffer at the appropriate shear rate.

3.2.10 Determination of platelet surface coverage

Flow-chambers were prepared as described in chapter 3.2.6, followed by perfusion of CMFDA-labelled platelets, reconstituted with washed red blood cells in platelet buffer just prior to perfusion for surface coverage experiments. Time lapse microscopy was performed using an inverted-stage microscope equipped with an AxioCam and AxioVision 4.6 software, as well as an epifluorescent illumination attachment. The light strength was lowered to 40 % using the FluoArc control gear. Images were taken at intervals of 30 seconds for 31 cycles at randomly chosen positions within the centre of a flow-chamber channel during perfusion with an exposure time of 900 ms at original magnification x 400. For evaluation of the area

covered by adhered platelets, the obtained photo images, each reflecting an area of 0.1 mm^2, were analysed with the AutMess software module and plotted as a function of time.

For endpoint determination of the area covered by adhered platelets, flow-chambers were prepared as described, and subsequent to perfusion of 1 IU/mL VWF at 1,700 s^{-1} shear rate, fluorescence labelled platelets were perfused over the chambers for 5 min at the same shear rate. Platelets were immediately fixed applying 1 mL of 4 % PFA/PBS using a syringe, and rinsed with flow-chamber perfusion buffer before image acquisition. Images were taken at randomly chosen areas over the median centre of the flow-chamber channel, whereas 24 images were obtained per experiment. All experiments were performed using two different platelet preparations and performed in duplicate. The area covered by adhered platelets was determined using the AutMess software module, and statistical analyses were performed with GraphPad software as described under 3.2.12.

3.2.11 SPR-based collagen binding studies

Real-time collagen binding assay was performed in a Biacore 2000 system. Human pepsin-digested collagen type III was covalently coupled to the surface of a CM5 sensor chip using the amine coupling kit. The surface was activated by injecting 35 µl of the Biacore amine coupling kit in a 1:1 mixture at a flow rate of 5 µl/min. Subsequently, the ligand (collagen type III) was injected at a flow rate of 2 µl/min, whereas collagen was dialysed against acetate buffer prior to injection and diluted to 100 µg/ml. This step was manually stopped when a desired level of response units (RU) was reached. Finally, free *N*-hydroxy-succinimide ester binding sites on the surface were saturated with 35 µl of 1 M ethanolamine at a flow rate of 5 µl/min. In the reference flow cell, the activation with the Biacore amine coupling kit was followed directly by inactivation with ethanolamine. Using the Biacore 2000 instrument, 1,000 RU correspond to 1 ng/mm^2 surface density.

SPR of the VWF/FVIII concentrate used to establish the flow-chamber model

For determination of the binding kinetics of VWF to collagen type III, increasing concentrations of 3.5, 7.03, 14.06, 28.13 and 56.25 µg/mL VWF were injected to a collagen-coated CM5 chip at a flow rate of 20 µL/min – corresponding to a shear rate of 1,650 s^{-1} – for

3 min, followed by perfusion of 600 µl Biacore running buffer (HBS-EP) over the collagen surface. In between, the chip surface was regenerated using 30 % (v/v) ethylene glycol, pH 11.75 until the baseline level was reached. Binding profiles were evaluated using Biaevaluation software, and data were analysed by global fitting using the Langmuir 1:1 molecular interaction (A + B = AB) as well as the mathematical model for bivalent analyte. Non-specific binding was eliminated by subtraction of the reference flow cell. Best fits were chosen and the kinetic data (association rate constant [k_a], dissociation rate constant [k_d]) as well as affinity data (dissociation equilibrium constant [K_D]) were calculated by computer-based analysis. Calculation was based on the molecular weight of the VWF monomer with 270 kDa.

SPR of fractionated VWF

The three fractions obtained from SEC (HMW, IMW, LMW VWF multimers) were concentrated to about 200 µg/ml VWF:Ag using centrifugal filter device units with a 100 kDa molecular weight cut-off (MWCO). Dilution series in HBS-EP buffer yielding eight concentration levels of each sample – 0.09, 0.27, 0.8, 2.4, 7.4, 22, 66, and 200 µg/ml VWF – were applied to the collagen-coated chip. A Mix-sample containing all VWF multimers composed of the samples obtained via SEC served as control. VWF-collagen kinetics were archieved applying increasing concentrations of VWF samples with different portion of VWF multimers at 20 µL/min for 3 min (association phase), followed by perfusion of 600 µL of HBS-EP buffer over the chip surface (dissociation phase) to obtain real time binding data. Between injection of the different VWF concentrations, the chip surface was regenerated through injection of 10 µl Biacore surface regeneration solution A, B and C at a flow rate of 10 µl/min one after another. Binding experiments were performed at 25 °C using HBS-EP running buffer, and kinetics were calculated as described above.

3.2.12 Statistical analyses

Data was analysed using GraphPad Prism 4.01 for Windows. Comparison was performed using the student's t-test. Data are expressed as mean ± standard error of mean (SEM). A p-value of $p < 0.05$ was considered to indicate statistical significance.

4 Results

4.1 Establishment of an *in vitro* flow-chamber system

4.1.1 Characterisation of the VWF preparation

A commercially available VWF/FVIII preparation (Wilate®) was used for all experiments [Stadler *et al.*, 2006]. Wilate® was characterised using DLS, SDS-PAGE under reducing conditions followed by Western blot analysis determining the presence of VWF with an anti-human VWF antibody as well as with regard to its ability to bind to collagen under flow using SPR-based binding studies.

DLS measurements exhibited a pure preparation with the predominant presence of only one particle with a hydrodynamic radius (R) of about 36 nm after filtration through a 0.2 µm particle filter (Fig. 6).

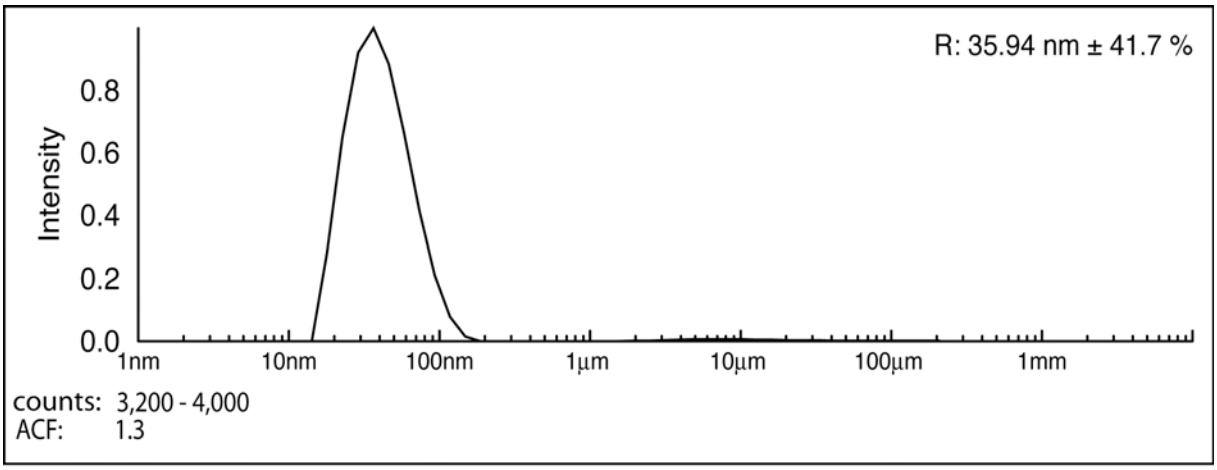

Fig. 6: Dynamic light scattering profile of the VWF preparation. The distribution profile of VWF molecules in solution determined a pure preparation with predominant presence of only one particle exhibiting a hydrodynamic radius (R) of around 36 nm.

The sample was additionally subjected to SDS-PAGE under reducing conditions, resulting in a main coomassie-stained protein band with a size of around 200 kDa (Fig. 7A). Three other bands with sizes of about 450, 230 and 150 kDa were detected in the sample but were very faint, indicating that the VWF preparation contained only trace amounts of other proteins. To prove the presence of VWF in the sample, Western blot analysis was carried out by transferring the proteins to a nitrocellulose membrane after SDS-PAGE using 4 %

polyacrylamide gels under reducing conditions (Fig. 7B). VWF was detected using a HRP-coupled anti-VWF antibody. The chemiluminescence signal revealed the presence of VWF in the main protein band around 200 kDa and below, exhibiting a smeary pattern. The coomassie-stained band at 450 kDa was also detected by the antibody, indicating the presence of marginal portions of the VWF dimer after denaturation.

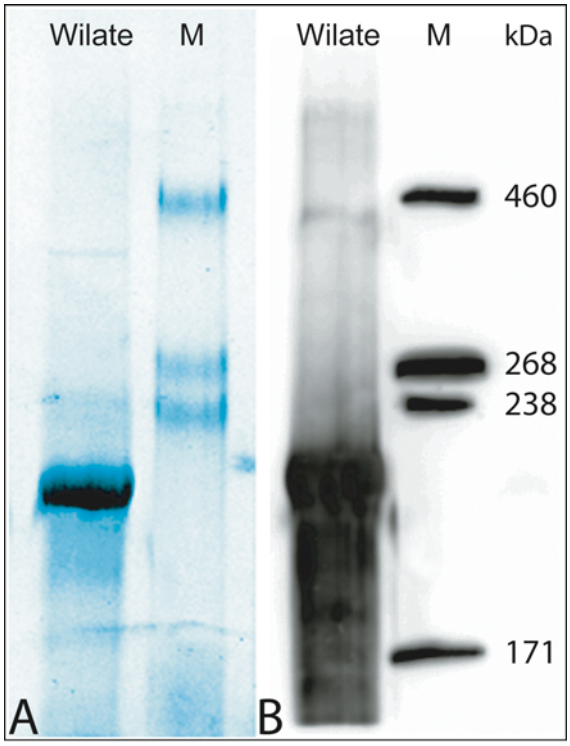

Fig. 7: Coomassie-stained SDS-PAGE gel of Wilate® (A) and Western blot analysis of the same sample (B). Using a 4 % polyacrylamide gel and SDS-PAGE, one main protein band with a size of around 200 kDa was detected after coomassie staining. Three other faint bands with sizes of about 450, 230 and 150 kDa were also present in the sample. After SDS-PAGE, proteins were transferred to a nitrocellulose membrane and probed using a HRP-coupled polyclonal anti-VWF antibody. The detected chemiluminescence signal visualised the main protein content at around 200 kDa with a smeary pattern below. A faint band at 450 kDa was also detected. M; molecular weight marker.

The ability of the VWF sample to bind to collagen under flow was investigated with SPR using the Biacore 2000 system. Real time collagen binding was evaluated on a CM5 sensor chip with covalently immobilised collagen type III. Sample dilution series of 204, 102, 51 and 25.5 nM VWF were injected at 20 µL/min corresponding to a shear rate of 1,650 s^{-1} at 25 °C, exemplarily shown in Fig. 8. The shear rate was selected in accordance to the flow-chamber experiments, which were performed at 1,700 s^{-1} shear rate, corresponding to a mean physiological shear rate in human circulation. Binding kinetics were obtained by global fitting using two different mathematical models: the 1:1 (Langmuir) molecular interaction (Fig. 8A) and the model for bivalent analyte (Fig. 8B). Non-specific binding was eliminated by subtraction of the reference flow cell. Calculation of the kinetic data was based on the molecular

weight of the VWF monomer of 270 kDa. The kinetic data obtained for both mathematical models is summarised in Table 2.

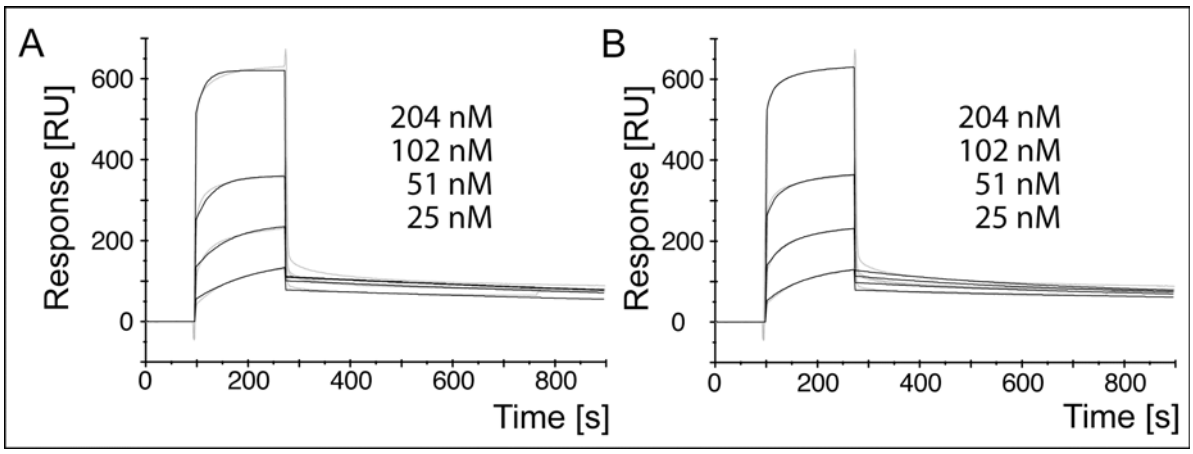

Fig. 8: SPR binding profile of Wilate® to human pepsin digested collagen type III. SPR sensorgrams of increasing concentrations of 25, 51, 102 and 204 nM VWF (bottom to top) using Wilate® at a flow rate of 20 µL/min are shown (light grey curves). Injection time of VWF was 3 min, indicated on the x-axis, whereas the binding level is depicted as response units (RU) on the y-axis. Black curves are representative for the mathematical model used to obtain kinetic data. A: 1:1 (Langmuir) binding model. B: bivalent analyte model. Positive slopes indicate association of VWF to collagen, whereas negative slopes refer to dissociation between analyte and immobilised ligand after buffer perfusion.

Table 2: Kinetic data of Wilate®-collagen binding. SPR sensorgrams were analysed using the mathematical model for 1:1 (Langmuir) binding as well as the model for bivalent analyte. k_a: association rate constant; k_d: dissociation rate constant; K_D: equilibrium dissociation rate constant, χ^2: cumulated differences between measured binding and the mathematical model.

1:1 (Langmuir) binding			
k_a [1/Ms]	k_d [1/s]	K_D [M]	χ^2
2.88 E+05	5.60 E-04	1.95 E-09	26.806

Bivalent analyte						
k_a1 [1/Ms]	k_d1 [1/s]	K_D1 [M]	k_a2 [1/Ms]	k_d2 [1/s]	K_D2 [M]	χ^2
1.33 E+05	1.61 E-03	1.21 E-08	2.29 E+02	5.70 E-02	2.49 E-04	12.741

The cumulated differences between the measured binding and the mathematical model, expressed as the chi-square distribution (χ^2), was 26.8 for the 1:1 molecular interaction and 12.7 for the model of bivalent analyte, indicating a better correlation for the simulation based on the bivalent analyte model. For the illustrated binding profile, 860 RU collagen type III have been immobilised on the chip surface, and the maximal binding capacity (R_{max}) for the illustrated binding profile was 163.23 RU (data not shown). Association rate constants (k_a) ranged from 2.88×10^5 1/Ms for the Langmuir model and 1.33×10^5 1/Ms for the first interaction and 2.29×10^2 1/Ms for the second interaction using the mathematical model of the bivalent analyte. Dissociation rate constants (k_d) ranged from 5.60×10^{-4} 1/s for the 1:1 molecular interaction and 1.61×10^{-3} 1/s (k_d1) and 5.70×10^{-2} 1/s (k_d2) for the bivalent analyte model, respectively. Generally, very low equilibrium dissociation rate constants (K_D) were observed, ranging from 1.95 nM using the Langmuir binding model and 12.1 nM for the first interaction applying the bivalent interaction model. However, the K_D-value obtained for the second interaction using the mathematical simulation of the bivalent analyte model was remarkably higher due to lower k_a- and higher k_d-values, indicating a considerably lower binding affinity compared to the first interaction (Table 2).

4.1.2 Analysis of platelet activation

Leukocyte-depleted thrombocyte concentrates collected by aphaeresis were characterised with regard to their activation level using FACS-analysis. FITC-labelled anti-CD62P (P-selectin) antibodies were used to determine the degree of platelet activation during the isolation procedure; wheras the expression of P-selectin on the platelet surface is used as an activation marker for platelets [Leytin *et al.*, 2000; Leytin *et al.*, 2002]. The platelet population was identified on the basis of forward and side scatter, whereas gating on events identified as platelets was performed to exclude measurement of air bubbles in the applied buffer (Fig. 9A). Fifteen thousand gated events were measured for each sample. For each experiment, the control sample without labelling was used as a marker for autofluorescence to distinguish activated platelets exposing the platelet activation marker P-selectin (Fig. 9B; M1). As a positive control, platelets were activated using 1 IU/mL human thrombin, resulting in a fluorescence shift of around 80 % of the entire platelet population to a higher relative fluorescence (Fig. 9C; M2). Obtained platelet concentrates exhibited an activation level of

12 % (Fig. 9D; M2), whereas the activation level increased to about 19 % during the platelet isolation procedure (Fig. 9E; M2). Compared to the activation level of platelets in human plasma of 8 - 12 % [Reverter *et al.*, 1994], thrombocyte preparations used for the flow-chamber experiments exhibited a slightly higher activation level due to stress induced by transportation, labelling and isolation procedures. Therefore, a control flow-channel without application of VWF was included in every flow experiment to determine the background level of platelet adhesion without substitution of VWF. This assured the quality of the applied platelet preparation with regard to its activation level, since platelets are able to liberate VWF out of their α-granules upon activation, which contributes to platelet adhesion in the absence of external VWF.

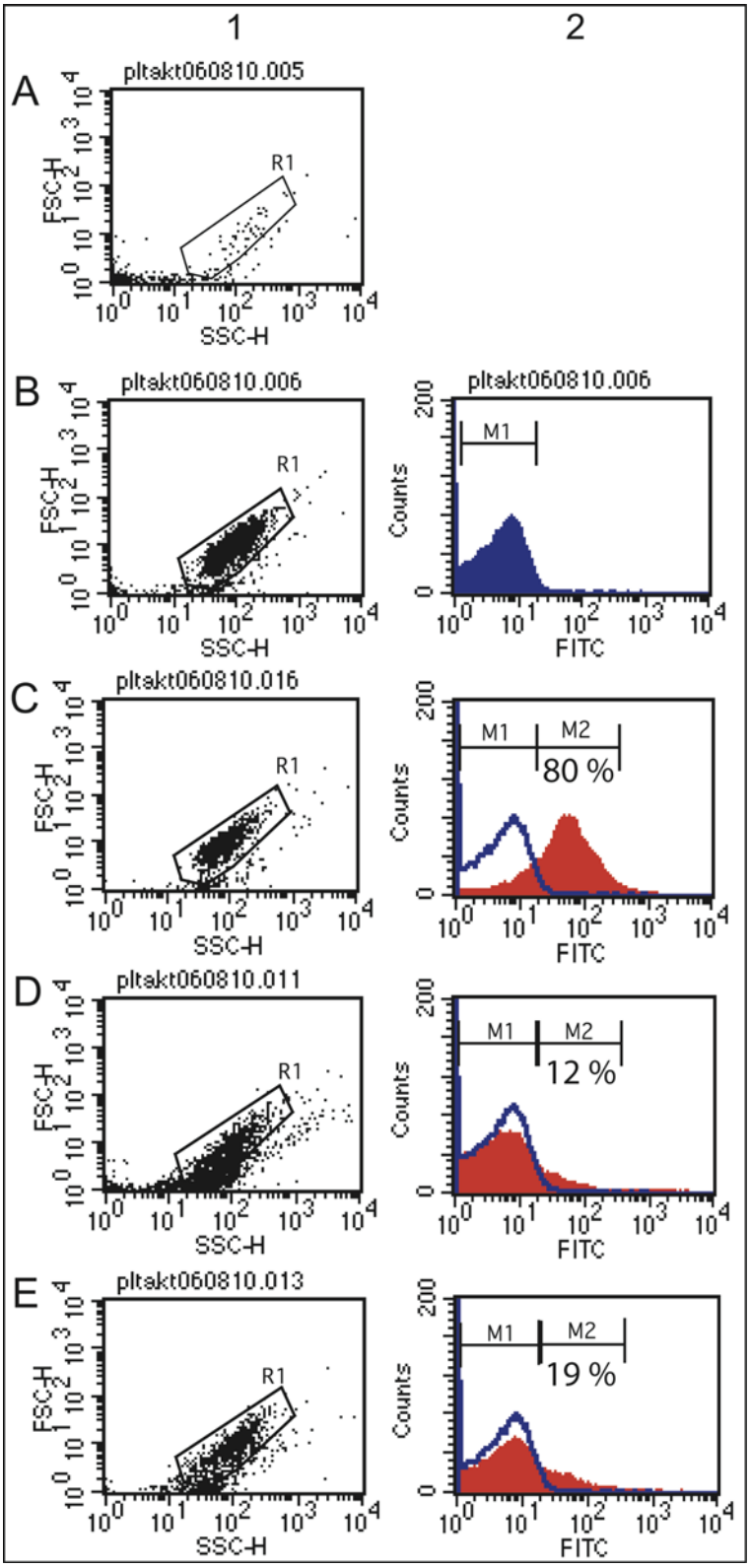

Fig. 9: Determination of the platelet activation level. FACS analysis: FITC-labelled anti-CD62P (P-selectin) antibodies were used to determine the degree of platelet activation during isolation procedure. The platelet population was identified on the basis of forward (FSC, y-axis) and side scatter (SSC, x-axis), whereas gating on events identified as platelets was performed to exclude measurement of air bubbles in the applied buffer (A; R1). A control sample without labelling was used as a marker for autofluorescence to distinguish activated platelets exposing the platelet activation marker P-selectin (B; M1). As a positive control, platelets were activated using thrombin resulting in a fluorescence shift of around 80 % of the entire platelet population to a higher relative fluorescence (C; M2). Obtained platelet concentrates exhibited an activation level of 12 % (D; M2), whereas during the platelet isolation procedure the activation level increased to about 19 % (E; M2). Panel 1: Dot plot, SSC vs. FSC. Panel 2: Intensity of fluorescence expressed as histogram plots.

4.1.3 Characterisation of the flow-chamber surface

Determination of the collagen coating concentration

For determination of the adequate coating concentration, µ-slides VI were layered with increasing concentrations of human pepsin digested collagen type III. After perfusion of 1 IU/mL VWF for 4 min using a mean physiological shear rate of 1,700 s^{-1}, the amount of VWF bound to collagen type III under flow was determined by an antigen ELISA (Fig. 10). Coating concentrations of 1, 5, 10, 20, 50, 100 and 500 µg/mL collagen type III are indicated on the x-axis of the graph. For negative control, flow-chambers were coated with 1 % BSA (w/v), and additionally VWF was perfused over the plastic slide to determine the background signal. The amount of VWF bound to the differently coated flow-chambers is displayed on the y-axis, showing an increasing VWF binding with ascending collagen concentrations, whereas the highest amount of VWF bound to the flow-chambers coated with 0.1 mg/mL collagen type III.

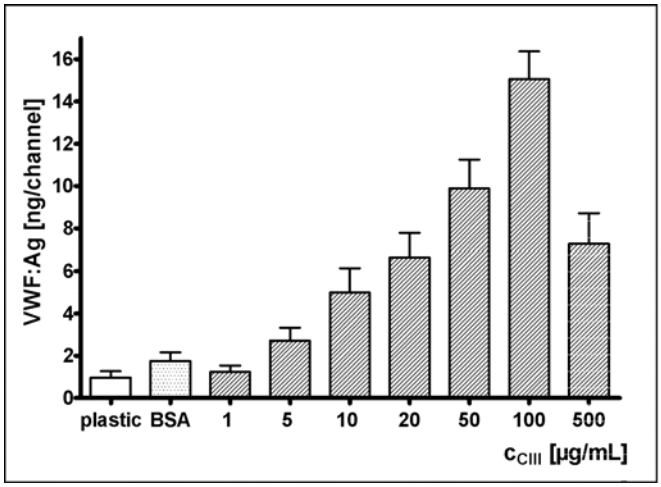

Fig. 10: Evaluation of the suitable collagen coating concentration. The VWF:Ag amount bound to flow-chambers coated with 1, 5, 10, 20, 50, 100 and 500 µg/mL collagen type III under flow at a shear rate of 1,700 s^{-1} was determined. For control, the VWF:Ag values bound to the plastic surface of the flow-chamber or a flow-chamber saturated with 1 % BSA (w/v) were also assigned, showing a background binding of 0.4 to 2.5 ng VWF:Ag per channel in the range of the flow-chambers coated with 1 and 5 µg/mL collagen type III. All other concentrations revealed a binding level above the background value with the highest binding using 100 µg/mL collagen for coating. At 500 µg/mL the binding level decreased again. Data is expressed as mean + SEM; n = 4.

Interestingly, at coating concentrations of 0.5 mg/mL the amount of flow-bound VWF decreased again. Flow-chambers coated with 1 or 5 µg/mL exhibited a VWF binding level close to the background signal of the negative controls. Considering these results and economic aspects, a coating concentration of 0.1 mg/mL collagen was used for all subsequent experiments.

Atomic force microscopy of the collagen surface

For characterisation of the flow-chamber collagen coating, µ-slides VI were coated using a concentration of 0.1 mg/mL of either human pepsin digested collagen type III or equine tendon fibrillar collagen type I. The bottom of the flow-chambers were excised and subjected to AFM. Fig. 11 shows the height images and profiles of the uncoated slide (Fig. **11**A), the collagen type III-coated flow-chamber (Fig. 11B) and the flow-channel coated with fibrillar collagen type I (Fig. 11C). Images were obtained scanning an appropriate area of 1,000 to 5,000 nm, whereas the microscope was operated in a tapping mode using silicone probes at resonance frequencies of 150 - 190 kHz under ambient conditions. Lighter areas are representative for higher structures, whereas dark areas represent low/no topology. In contrast to the uncoated µ-slide with a height profile of about 1.5 nm, the collagen type III-coated chamber bottom exhibited a homogeneous distribution of small collagen fibrils with a height of 3 - 3.5 nm. The collagen fibrils of collagen type I in Fig. 11C depicted a heterogeneous surface with fibres at various height profiles ranging between 19 - 36 nm.

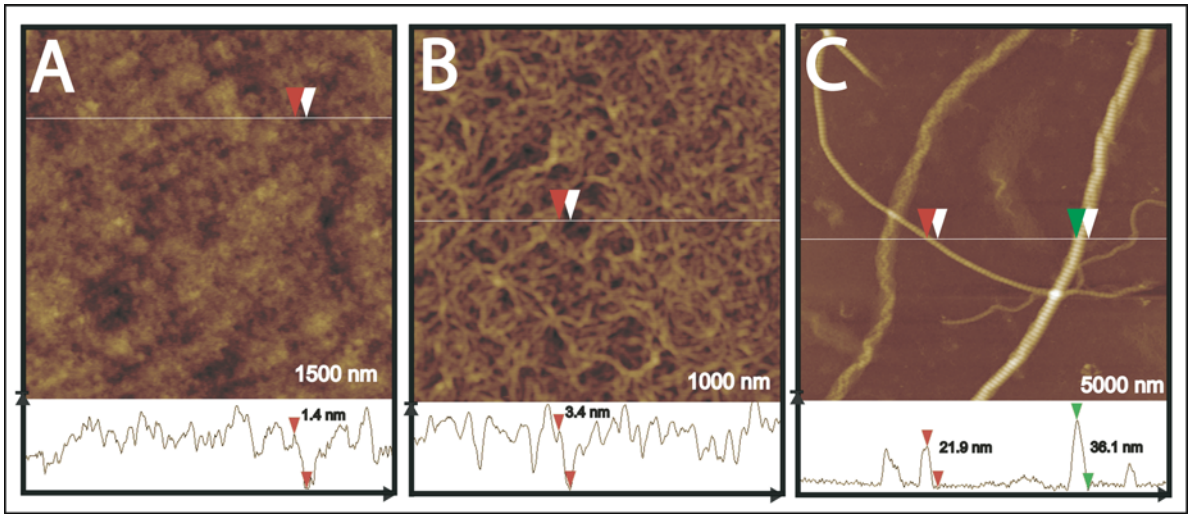

Fig. 11: Characterisation of the collagen-coated flow-chamber surfaces using AFM. The height image at a data scale of 1,500 nm and profile of the cross sectional area of the uncoated µ-slide are illustrated in (A), exhibiting a diffuse pattern with a height of about 1.5 nm. In contrast, AFM images of the collagen type III-coated flow-chamber (B) exhibited a homogenous distribution of small collagen fibrils examining a data scale of 1,000 nm. The height profile for the cross section showed a height of 3 - 3.5 nm. A flow-chamber coated with equine tendon collagen type I scanning an area of 5,000 nm (C), depicted a heterogeneous distribution of collagen fibrils with various height profiles in a range of 20 - 35 nm. Small collagen fibrils covered the space between large fibres, generating a consistently active surface. The microscope was operated in the tapping mode using silicone probes at resonance frequencies of 150 - 190 kHz under ambient conditions.

4.1.4 Time- and shear-dependent adhesion of VWF to collagen

Multimeric profile of VWF binding to collagen at 1,700 s^{-1} shear rate

After evaluation of the appropriate coating conditions, the binding profile of VWF to collagen type III was determined. For this purpose, collagen type III-coated flow-chambers applying a collagen coating concentration of 0.1 mg/mL were perfused with VWF using a physiological VWF:Ag concentration of 1 IU/mL with increasing perfusion times at 1,700 s^{-1} shear rate. VWF was dissolved from the flow-chambers and subjected to VWF multimer analysis using 1.2 % agarose gels. Low-resolution gels of around 1 % agarose are used to resolve the whole multimer pattern, especially the HMW VWF multimers [Budde *et al.*, 2008]. For determination of the VWF sub-band distribution, medium resolution gels with 1.6 % agarose were applied.

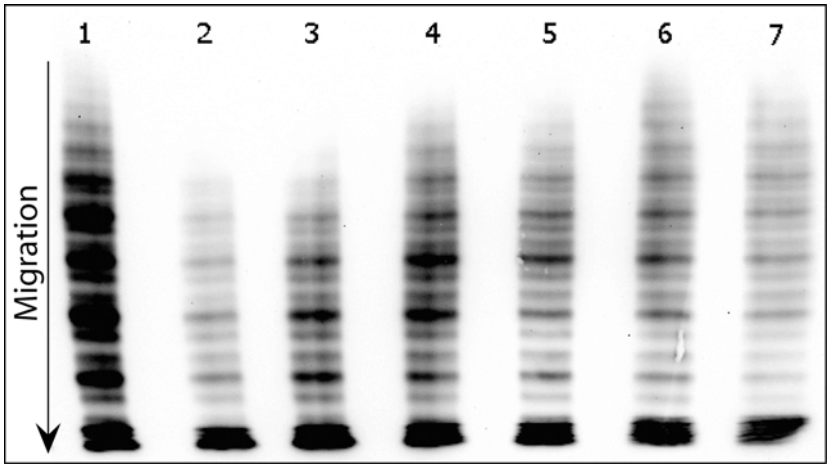

Fig. 12: Time-dependent binding of VWF to collagen type III at 1,700 s^{-1} shear rate. VWF was perfused over a collagen type III-coated flow-chamber for 0.5 (lane 2), 1 (lane 3), 2 (lane 4), 3 (lane 5), 4 (lane 6) and 5 min (lane 7). After dissolution of VWF, the samples were subjected to VWF multimer analysis using 1.2 % agarose gels. Lane 1 represents the VWF multimer pattern of the sample before application to the flow-chamber. The VWF samples perfused for 2 to 5 min (lane 4 to 7) and the sample prior to perfusion (lane 1) exhibited an equal VWF multimer pattern, whereas samples perfused for 0.5 or 1 min showed a decreased portion of the higher molecular weight VWF multimers.

The multimeric profile of time-dependent VWF adhesion to collagen is displayed in Fig. 12 for perfusion times of 0.5, 1, 2, 3, 4 and 5 min at 1,700 s^{-1} shear rate, respectively (Fig. 12; lanes 2 to 7). The multimer pattern of the VWF sample before application to the flow-chamber is displayed in lane 1. Multimer patterns of VWF samples perfused for 0.5 or

1 min showed a relative decrease of the high molecular weight (HMW) VWF multimers, whereas no difference was detected in samples perfused for 2 - 5 min over the collagen surface.

To verify the visual impression, VWF multimer distributions were analysed by densitometric evaluation (Fig. 13), whereas one peak equals to one multimer band of the gel out of Fig. 12. Small multimers are depicted at the right hand side of the x-axis, whereas HMW VWF multimers are displayed on the left hand side. The intensity of the chemiluminescence signal is represented by the y-axis, corresponding to the concentration of the applied VWF sample. Peak shoulders depict faster and slower migrating sub-bands of a VWF multimer, clearly distinguishable only for the smaller VWF multimers.

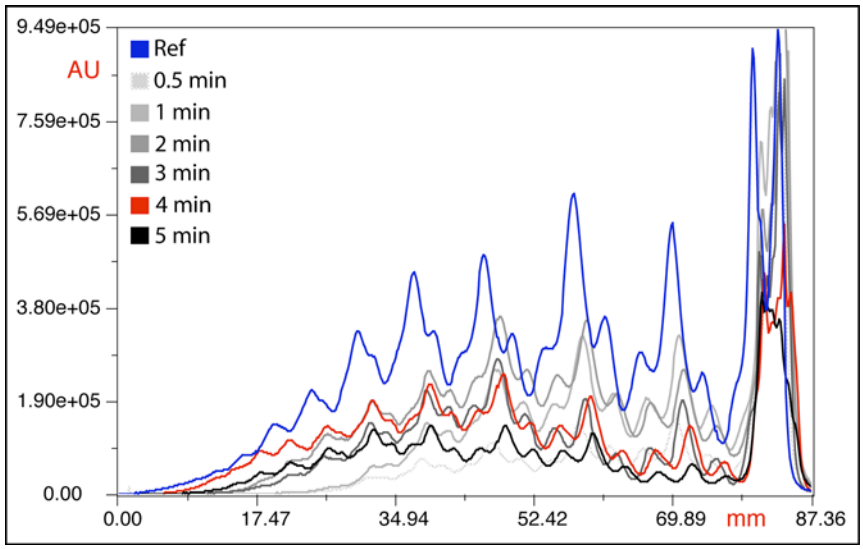

Fig. 13: Densitometric evaluation of VWF multimers bound to collagen type III under flow at different perfusion times. The densitometric values of the VWF multimers out of Fig. 12 are shown, whereas one peak equals to one multimer band of the gel. Small multimers are depicted at the right hand side of the x-axis, whereas HMW VWF multimers are displayed on the left hand side. The intensity of the chemiluminescence signal is represented by the y-axis and expressed as Absorption Units (AU). Peak shoulders depict the faster and slower migrating sub-bands of a VWF multimer. VWF samples were perfused over collagen type III-coated flow-chambers for 0.5, 1, 2, 3, 4 and 5 min at 1,700 s^{-1} shear rate. The densitometic pattern showed a decreased intensity of HWM VWF multimers for the samples perfused over collagen for 0.5 and 1 min (dotted grey and light grey curves), but for longer perfusion times the multimeric distribution approximated the multimeric profile of the VWF sample before application to the flow-chamber. A perfusion time of 4 min was chosen for all subsequent experiments (red curve). Ref: Sample before application to the flow-chamber (blue curve).

The densitometic pattern showed a decreased intensity of HWM VWF multimers for the samples perfused over collagen for 0.5 and 1 min (dotted grey and light grey curves, Fig. 13), but for longer perfusion times the multimeric distribution approximated the multimeric profile of the VWF sample before application to the flow-chamber (blue curve). A perfusion time of 4 min was chosen for all subsequent experiments (red curve, Fig. 13).

To investigate whether the decrease in the higher molecular weight forms of VWF obtained with perfusion times of 0.5 and 1 min was a phenomenon of an impaired binding of HMW VWF multimers to collagen under flow, a dilution series of Wilate® with concentrations ranging from 0.75 to 0.01 IU/mL VWF:Ag was subjected to VWF multimer analysis (Fig. 14). Compared to standard human plasma pool (NP), the VWF multimer pattern of Wilate® exhibited a slight decrease in the portion of HMW VWF multimers with the strongest chemiluminescence signal for VWF multimers 1 - 10. The multimeric pattern of the dilution series revealed that the decrease of HWM as well as IMW VWF multimers out of Wilate® is strongly concentration dependent, and can therefore not be attributed to a diminished binding affinity of higher molecular weight VWF multimers to collagen type III under flow.

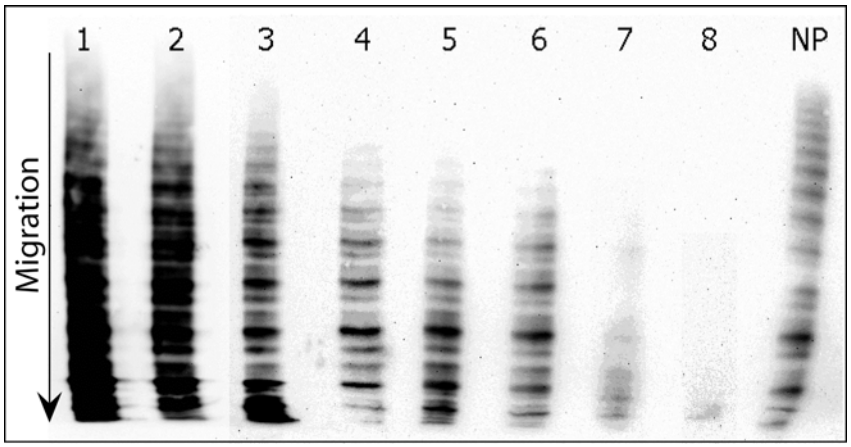

Fig. 14: Multimeric profile of a VWF dilution series. A Wilate® sample with diminishing concentrations of 0.75 (lane 1), 0.5 (lane 2), 0.1 (lane 3), 0,05 (lane 4) 0.04 (lane 5), 0.03 (lane 6), 0.02 (lane 7) and 0.01 IU/mL VWF:Ag (lane 8) was subjected to VWF multimer analysis. With increasing dilution, an initial loss of HMW VWF multimers was determined, followed by the decrease of intermediate molecular weight VWF multimers up to the very low VWF multimers at concentrations of 0.02 and 0.01 IU/mL VWF:Ag (lane 7 and 8, respectively). NP: Standard human plasma.

VWF-binding to collagen with increasing shear rates

For determination of the VWF:Ag amount binding to collagen-coated flow-chambers at low to high shear rates, flow-channels were coated with 0.1 mg/mL collagen type III, and 1 IU/mL VWF:Ag was perfused over the flow-chambers with increasing shear rates of 400, 1,700 and 4,000 s^{-1} for 4 min each, resulting in an increasing amount of VWF:Ag bound to collagen due to the higher quantity of VWF perfused over the flow-chambers with increasing flow rate (Fig. 15). The shear rate is indicated on the x-axis of the graph, whereas the y-axis represents the VWF:Ag amount bound to a flow-chamber. At 4,000 s^{-1} shear rate, corresponding to a flow rate of 24.32 mL/min using the µ-slide VI, the amount of VWF:Ag bound to collagen type III per flow-chamber nearly doubled compared to the amount bound at 400 s^{-1}, corresponding to $1/10^{th}$ of the flow rate at 4,000 s^{-1} shear rate. At a shear rate of 1,700 s^{-1}, approximating a flow rate of 10 mL/min, about 12 ng VWF:Ag bound to a collagen type III-coated flow-chamber. For equine collagen type I, the amount of VWF bound to the flow-chambers at different shear rates was very low, since the affinity of VWF for collagen type I is around 15fold lower than for collagen type III [Li *et al.*, 2002], and the signal was barely distinguishable from the background (data not shown).

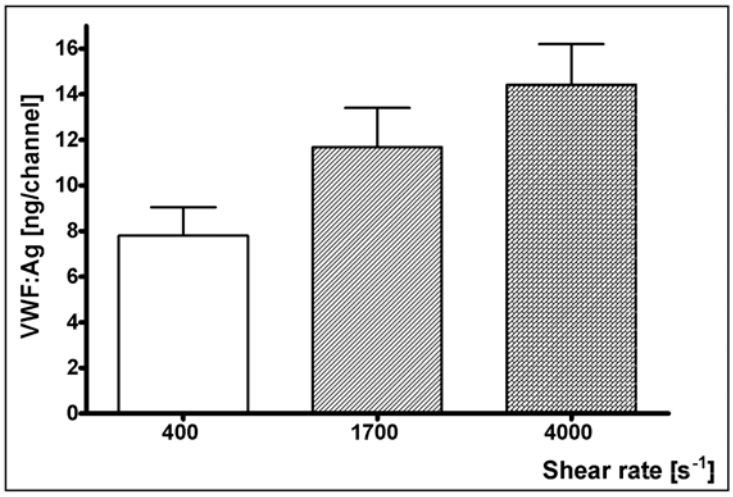

Fig. 15: Amount of VWF:Ag bound to the collagen coated flow-chambers at different shear rates. VWF was perfused over a flow-chamber coated with 0.1 mg/mL collagen type III for 4 min at shear rates of 400, 1,700 and 4,000 s^{-1}. The amount of VWF:Ag increased shear rate dependent, corresponding to the increasing quantity of VWF perfused over a flow-chamber at higher flow rates. Data is expressed as mean + SEM; n = 6.

Evaluating the VWF multimer pattern bound to flow chamber coated with either human pepsin digested collagen type III or equine tendon fibrillar collagen type I at different shear rates, VWF was dissolved from the flow-channels after perfusion at 400 (Fig. 16, lanes 2), 1,700 (lanes 3) or 4,000 s^{-1} shear rate (lanes 4) for 4 min each, and subjected to VWF multimer analysis using 1.6 % agarose gels for high resolution of VWF sub-bands (Fig. 16A and B, respectively). The VWF multimer distribution of the appropriate sample before application to the flow-chamber is displayed in lanes 1; NP indicates standard human plasma pool. The multimeric pattern at all shear rates equalled to the VWF multimer distribution of the reference sample before application to the flow-chamber not only for collagen type III (Fig. 16A), but also for collagen type I (Fig. 16B). No difference in the VWF multimeric pattern was detected applying densitometric analysis (data not shown). Since *in vivo* platelet adhesion is dependent of VWF only at high arterial shear rate above a threshold of 800 - 1,000 s^{-1} [Ruggeri, 2006], no difference in the VWF multimer distribution was detected at higher shear rates of 4,000 s^{-1}, and a shear rate of 1,700 s^{-1} equals to the median physiological shear rate found in human circulation [Tangelder *et al.*, 1988], this shear rate was selected for all subsequent experiments.

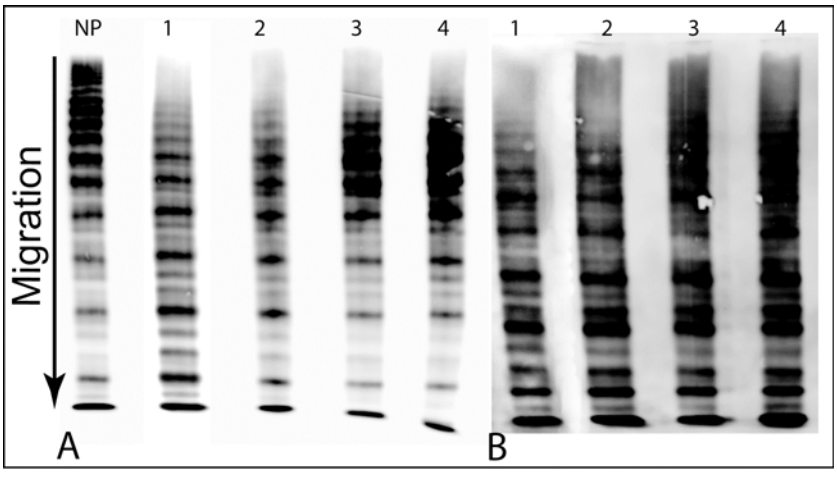

Fig. 16: Multimeric pattern of VWF bound to collagen-coated flow-chambers at different shear rates. VWF multimers bound to human pepsin digested collagen type III (A) and equine tendon fibrillar collagen type I (B) were separated by 1.6 % agarose gel electrophoresis, subsequently blotted, immunostained and the chemiluminescence signal was visualised by image analysis. Multimers attached to the flow-chamber at 400 (lanes 2), 1,700 (lanes 3) or 4,000 s^{-1} shear rate (lanes 4) compared to the appropriate reference sample before application to the flow chamber (lanes 1) are shown. Since the affinity of VWF to collage type I is about 15fold less than for collagen type III, lane 1 in (B) emanates from the same gel but different exposure time than lanes 2 - 4. NP: standard human plasma pool.

4.2 Activity of VWF under flow

4.2.1 Exposition of GPIb binding domains responsible for platelet interaction

Under physiological conditions, plasmatic VWF does not bind to platelets in circulation. The affinity to the platelet GPIb receptor, resulting in platelet tethering, translocation and finally adhesion to areas of injured vessel walls via interactions of several ligands on the platelet surface with basement matrix proteins [rewieved by Ruggeri, 2006], is induced by immobilisation of VWF after binding to exposed structures of the ECM – like collagen I, III or VI – leading to a conformational change of VWF with exposition of the GPIb binding region within the A1 domain of the VWF protein.

Therefore, the exposition of the GPIb binding domain is the critical step with regard to the mediation of platelet adhesion in flowing blood. To investigate this function of VWF, collagen-coated flow-chambers were perfused with 1 IU/mL VWF:Ag at 1,700 s^{-1} shear rate for 4 min. Immunofluorescence staining on a collagen type III-coated flow-chamber using a specific monoclonal antibodie against the VWF-GPIb binding domain (Fig. 17B) and antibodies against the entire VWF molecule (Fig. 17A) in multiple labelling technique revealed almost no background staining when no VWF was applied, whereas the flow-bound VWF on collagen type III provided homogeneous signals for both anti-VWF and anti-VWF-GPIb fluorescence staining (Fig. 17C and D, respectively). The exposed GPIb binding domains responsible for platelet binding were found to be present to a similar extend as bound VWF, and appeared proximal to VWF staining on both collagens.

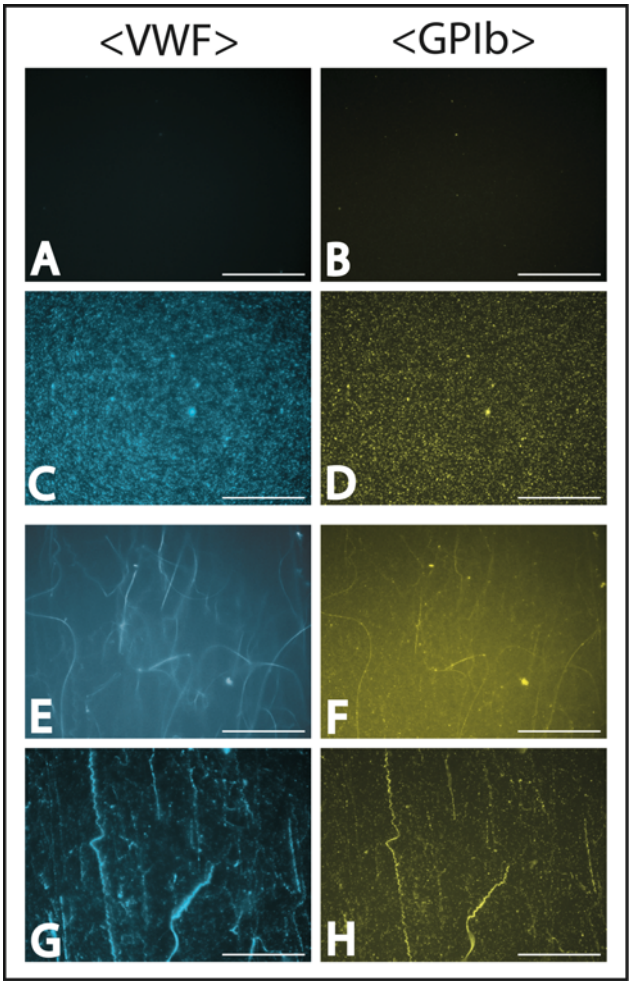

Fig. 17: Fluorescence stained collagen-bound VWF at 1,700 s^{-1} shear rate with exposed immunostained GPIb binding domains. The flow-bound VWF was visualised by multiple labelling immuno-fluorescence using a polyclonal antibody against the whole VWF molecule (left panel) as well as a monoclonal antibody against the GPIb binding domain (right panel). Compared to the background staining when no VWF was present (A, B), VFW bound to collagen type III under flow revealed a homogeneous distribution of VWF with adjacent exposed GPIb binding domains (C, D). On collagen type I the staining in the absence of VWF elicited a high back-ground signal with stronger stained collagen fibrils for both VWF and GPIb (E, F). After perfusion of VWF, the immunofluorescence signal increased especially for the collagen fibres showing VWF molecules with exposed GPIb binding domains (G and H, respectively). Scale bar; 50 µm.

In contrast, the anti-VWF and anti-VWF-GPIb background staining on fibrillar collagen type I was very high (Fig. 17E and F, respectively), even though no VWF was applied to the flow-chamber. Although the signal of stained collagen type I fibrils was very weak, it was not possible to reduce the background signal analogue to collagen type III. After application of VWF under flow, the staining intensity increased especially for the collagen fibrils, but the VWF apparently bound as well to small collagen fibres covering the space between whole fibrils. Similar to collagen type III, the GPIb binding domains were exposed to a similar extend as the flow-bound VWF and appeared close to the immunofluorescence signal of the whole VWF molecules, as expected.

Examining the specificity, interaction between VWF and collagen was blocked using a monoclonal antibody against the A3 domain of VWF (mAb 82D6A3) at a concentration of 2.5 µg/mL (Fig. 18). Collagen-bound VWF under flow was immunostained using a polyclonal anti-human VWF antibody, demonstrating an almost complete inhibition of VWF binding to collagen type III under flow (Fig. 18A), but just a partial inhibition of VWF-binding to equine tendon fibrillar collagen type I (Fig. 18B).

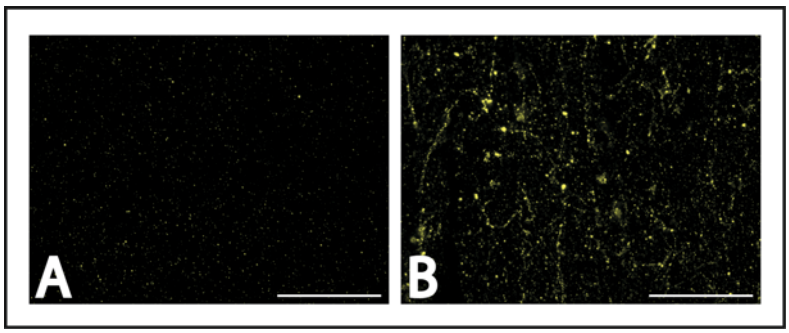

Fig. 18: Immunostaining of collagen-bound VWF at 1,700 s^{-1} shear rate after inhibition of VWF-collagen binding. VWF was pre-incubated with a monoclonal antibody directed against the VWF-A3 domain (mAb 82D6A3) prior to the perfusion experiment in order to inhibit the interaction with collagen. Immunostaining was carried out using a polyclonal anti-human VWF antibody. Binding of VWF to collagen type III under flow was nearly completely abolished (A), whereas the immunostaining on collagen type I revealed only a partial inhibition of VWF-collagen binding (B). Scale bar; 50 µm.

4.2.2 VWF-mediated platelet adhesion on collagen at 1,700 s^{-1} shear rate

To investigate the ability of collagen-bound VWF under flow to mediate platelet adhesion at high shear rate conditions, the area covered by adhered platelets was determined with time lapse microscopy during perfusion of fluorescence-labelled platelets reconstituted with physiological amounts of red blood cells over collagen-coated flow-chambers subsequent to perfusion of VWF using 1 IU/mL VWF:Ag at 1,700 s^{-1} shear rate (Fig. 19).

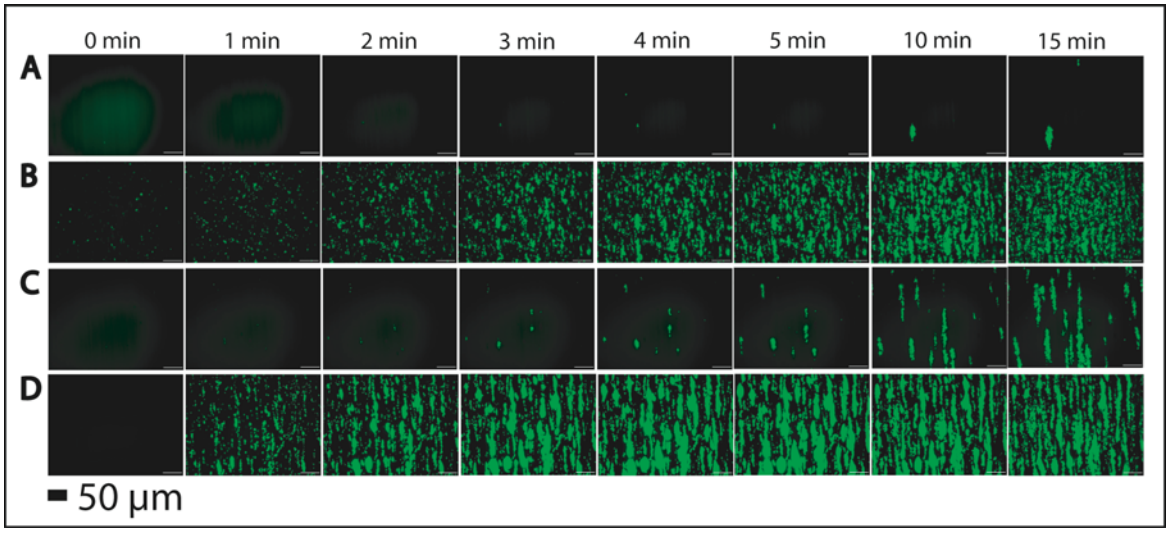

Fig. 19: Attached fluorescence-labelled platelets on collagen-coated flow-chambers at 1,700 s^{-1} shear rate. Images are representative for time lapse microscopy experiments of platelet adhesion after perfusion of 1 IU/mL VWF:Ag (B) compared to the area covered by adhered platelets on collagen type III without substitution of VWF (A). VWF-mediated platelet adhesion under flow was inhibited using a monoclonal antibody against the A3 domain of VWF (mAb 82D6A3, C). Platelet adhesion on collagen type I without addition of VWF is shown in D, revealing a highly thrombogenic surface with adhered platelets along the collagen fibrils and subsequent thrombus formation. Time dependent platelet adhesion up to 15 minutes perfusion time is shown, indicated on top of the graph. Scale bar; 50 µm.

Without substitution of VWF, almost no platelet binding to the collagen type III-coated surface was observed at 1,700 s^{-1} shear rate, monitoring a perfusion time up to 15 minutes (Fig. 19A). With addition of VWF, the surface was considerably more active to mediate platelet adhesion examining a time period of 15 minutes (Fig. 19B). Adhered fluorescence labelled platelets on the surface exhibited a homogeneous distribution with incipient aggregation at prolonged perfusion time.

Investigating the specificity, the interaction of VWF to collagen type III was inhibited using an antibody against the VWF A3 domain (mAb 82D6A3, Fig. 19C). Even though the platelet coverage could not be blocked completely, it was markedly reduces.

In contrast, on collagen type I platelet adhesion took place even in the absence of VWF, exhibiting adhered platelets along collagen fibrils leading to rapid thrombus formation observing a perfusion time of 15 minutes (Fig. 19D), and platelet adhesion on collagen type I could not be blocked by the antibody against the VWF A3 domain (data not shown). Therefore, the applied collagen type I preparation was considered to be not suitable to study the role of VWF in platelet adhesion to collagen.

The percentage of the area covered by adhered platelets was evaluated using computer-based image analysis, showing almost no adhesion on collagen type III when no VWF was subjected to the flow chamber (Fig. 20; rhombs), whereas after pre-perfusion of VWF about 40 % of the area was covered with fluorescence labelled platelets after 5 min perfusion time (Fig. 20; squares), corresponding well to perfusion experiments done with

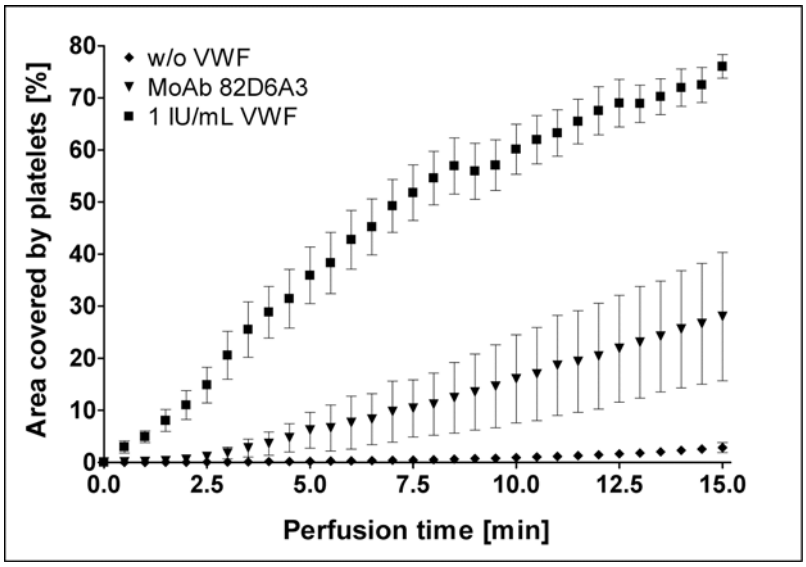

Fig. 20: Percentage of the area covered by adhered platelets on human collagen type III at a shear rate of 1,700 s^{-1}. Platelets were perfused over the channel subsequent to perfusion of 1 IU/mL VWF:Ag (squares, n = 6) compared to the area covered by adhered platelets without substitution of VWF (rhomb, n = 6). Platelet adhesion on collagen type III was inhibited by blocking the VWF-collagen interaction using an antibody against the VWF-A3 domain (MoAb 82D6A3; inversed triangle, n = 2). The area covered by adhered platelets displaying 15 min perfusion time is shown. Data is expressed as mean ± SEM.

whole blood [e.g. Moroi *et al.*, 1996; Lankhof *et al.*, 1997; reviewed by Sakariassen *et al.*, 2004]. Platelet adhesion to collagen type III was specifically blocked using an antibody against the VWF A3 domain (mAb 82D6A3), revealing an inhibition level of around 75 % after 5 minutes platelet perfusion (Fig. 20; inversed triangles). This is in line with the inhibition level shown by Vanhoorelbeke *et al.* [2003], demonstrating between 60 - 85 % inhibition of platelet surface coverage at 1,300 and 2,600 s^{-1} shear rate, respectively.

4.3 Definition of the established *in vitro* flow-chamber system

4.3.1 Parameters of the flow-chamber experimental setup

The established *in vitro* flow-chamber model was designed for the evaluation of both important VWF functions, (i) the binding of VWF to collagen under flow with exhibition of the GPIb binding domain crucial for the interaction to platelets, and (ii) the ability of VWF to mediate platelet adhesion under defined flow conditions in real time. Therefore, the introduced flow-chamber system is a two-step model investigating both VWF functions separately. The criteria for the experimental setup of the flow-chamber system were defined according to examination of all aspects contributing to the variability of the model and are summarised in Table 3. A schematic diagram is displayed in Fig. 21. The flow-chamber is coated with a collagen concentration of 0.1 mg/mL, followed by perfusion of physiological concentrations of 1 IU/mL VWF:Ag to determine VWF-collagen binding under flow. VWF multimer analysis can be conducted after perfusion for the evaluation of the contribution of the multimeric profile, or VWF bound to collagen can be quantified via VWF:Ag determination. Examining VWF-mediated platelet adhesion, physiological concentrations of 2.5×10^8 platelets/mL, mixed with washed red blood cells to obtain a haematocrit of around 33 %, are perfused over the channel, and platelet adhesion is determined either in real time using time-lapse microscopy, or after five minutes for end point determination of platelet adhesion. The defined criteria for the flow-chamber are closely related to *in vivo* conditions of haemostasis, providing a promising tool for standardised assessment of VWF function under physiological flow conditions.

Table 3: Parameters for the experimental setup of the established flow-chamber system.

Coating density	0.1 mg/mL collagen type III
Shear rate	1,700 s^{-1} equates to 10.3 mL/min (µ-slide VI) equates to 16.4 dyn/cm^2 (aqueous solution)
Concentration of VWF	1 IU/mL VWF:Ag
VWF perfusion time	4 min
Platelet concentration	2.5 x 10^8 platelets/mL
Concentration of red blood cells	33 % haematocrit
Perfusion time for endpoint determination of platelet adhesion	5 min

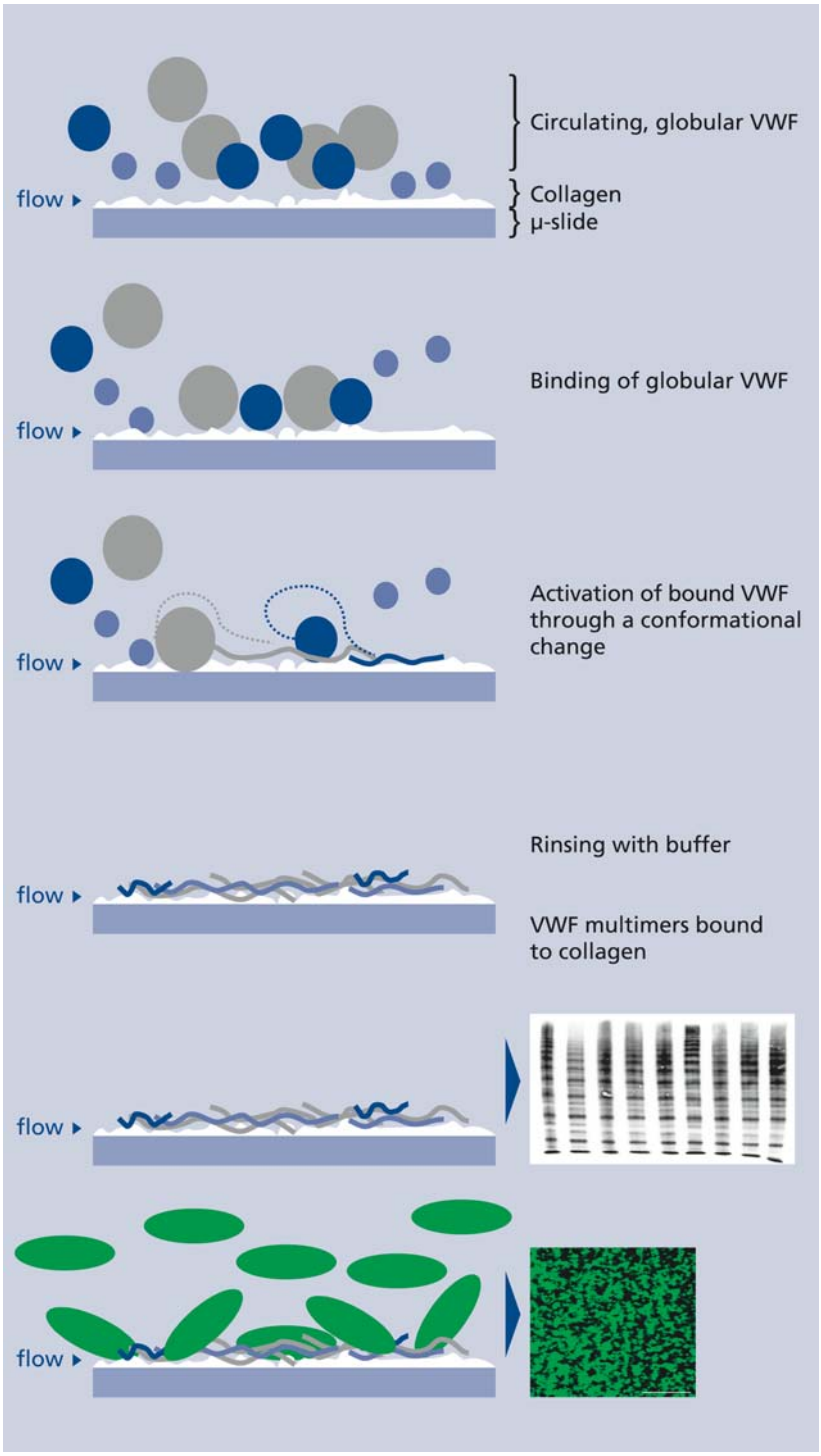

Fig. 21: Schematic diagram of the experimental setup. The perfusion chamber is coated with collagen, followed by perfusion of VWF enabling binding to collagen under flow. The collagen-bound VWF is either dissolved for VWF multimer analysis, or fluorescence labelled platelets are perfused over the flow-chamber to determine the VWF-mediated platelet adhesion under physiological flow conditions via the percentage of the area covered by adhered platelets using software-based image analysis. The graph was prepared in cooperation with V. Besier, concept design.

4.4 Implementation of the flow-chamber system

4.4.1 Mediation of platelet adhesion by different VWF-containing concentrates

Treatment with VWF-containing concentrates is pivotal for patients suffering from VWD type 3. Various VWF-containing concentrates are commercially available, providing different qualities and quantities of VWF. At present, the quality of VWF-containing concentrates is evaluated by static VWF assays, e.g. VWF:RCo, VWF:CB and VWF:Ag, neglecting the importance of the physical properties of blood flow on haemostasis. Methods for assessing VWF-mediated platelet adhesion under flow conditions are advantageous compared to artificial activity assays, because they approximate more closely the situation of platelet adhesion *in vivo*. Therefore, the flow-chamber model was used to investigate VWF-mediated platelet adhesion to collagen type III provided by five commercially available VWF-containing concentrates, two batches each, at a mean physiological shear rate of 1,700 s^{-1}.

Multimer pattern of VWF-containing concentrates

The multimeric composition of the VWF provided by five commercially available VWF-containing concentrates resulted in a heterogeneous distribution: Whereas the VWF multimeric profiles of concentrate A and D were comparable to the multimeric distribution of plasmatic VWF (NP) using low resolution agarose gels of 1.2 %, Wilate® and concentrates B and C revealed a relative loss of the portion of HMW VWF multimers (Fig. 22). This was visible examining the chemiluminescence signals on the nitrocellulose membranes, and was confirmed for both batches by densitometric evaluation of the VWF multimer pattern of the low resolution gels, which is depicted in Fig. 22B and D, respectively.

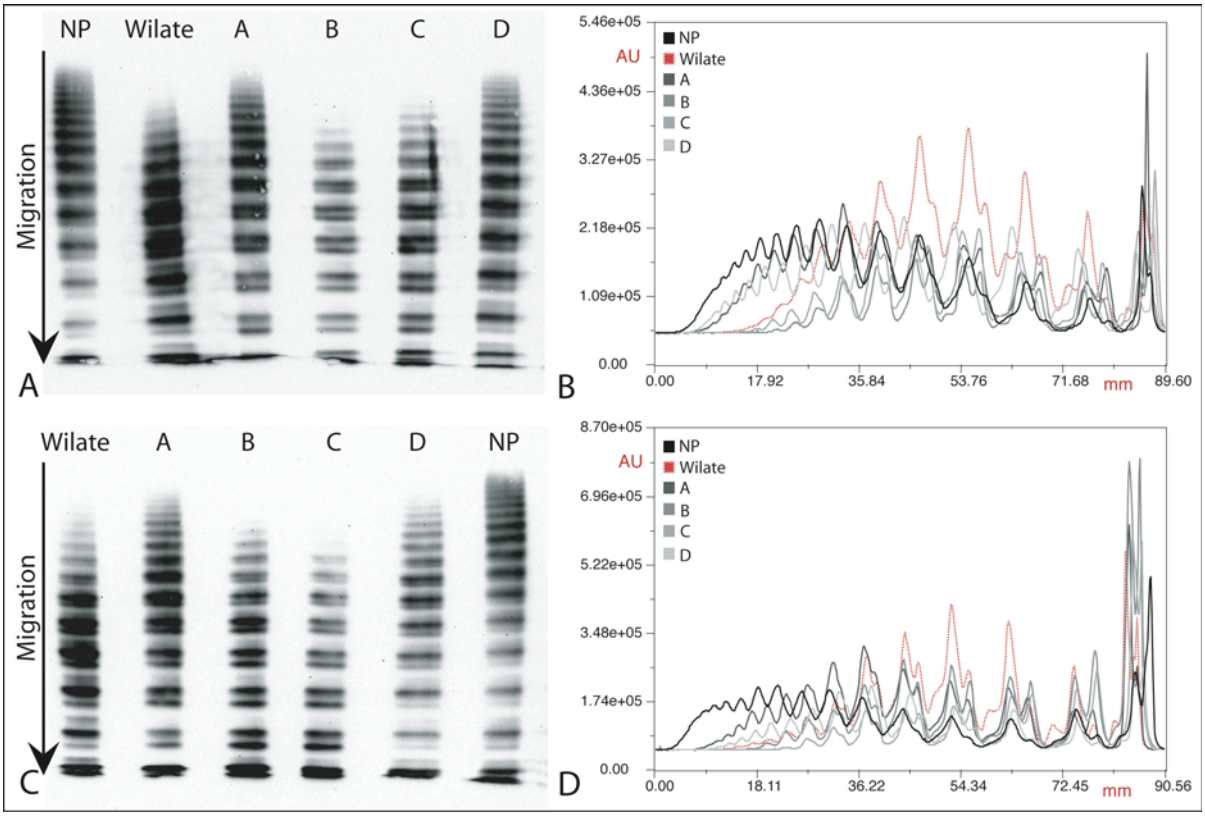

Fig. 22: VWF multimeric pattern of different commercially available VWF-containing concentrates using low resolution gels. Two batches of each Wilate® and four other concentrates A - D were subjected to VWF mutlimer analysis using low resolution 1.2 % agarose gels (A, C), blotted to nitrocellulose membranes and the chemiluminescence signals were detected using a polyclonal HRP-conjugated anti-VWF antibody. Both batches of concentrate A and D exhibited a multimer distribution similar to standard human plasma (NP), whereas Wilate® and concentrates B and C showed a decreased content of HMW VWF multimers. Graphs B and D represent the densitometric evaluation of the VWF multimer pattern depicted in A and C, respectively. Every peak equals to one VWF multimer band on the 1.2 % agarose gels. The intensity of the chemiluminescence signal is illustrated on the y-axis as absorption units (AU), whereas the x-axis indicates the migration distance of a given multimer. Small multimers are depicted on the right hand side, and HWM VWF multimers on the left hand side of the graphs. Both batches of Wilate® as well as concentrate B and C showed a relative decrease in the portion of HMW VWF multimers compared to standard human plasma (NP, black line).

Examining the VWF sub-band distribution using 1.6 % high resolution agarose gels, only Wilate® and concentrate D provided a plasma VWF-like triplet pattern, whereas concentrates A - C contained a pronounced proteolytic faster migrating triplet band with virtually absent slower migrating triplet bands (Fig. 23), also visible on the basis of the three clearly distinguishable shoulders compared to standard human plasma (NP, black line) of one multimer peak for Wilate® and concentrate D in the densitometric profile (Fig. 23B, D). Both batches of concentrates A - C exhibited clearly pronounced faster migrating satellite bands resulting in bifurcated peaks of single multimers (Fig. 23B, D; dark grey to light grey lines).

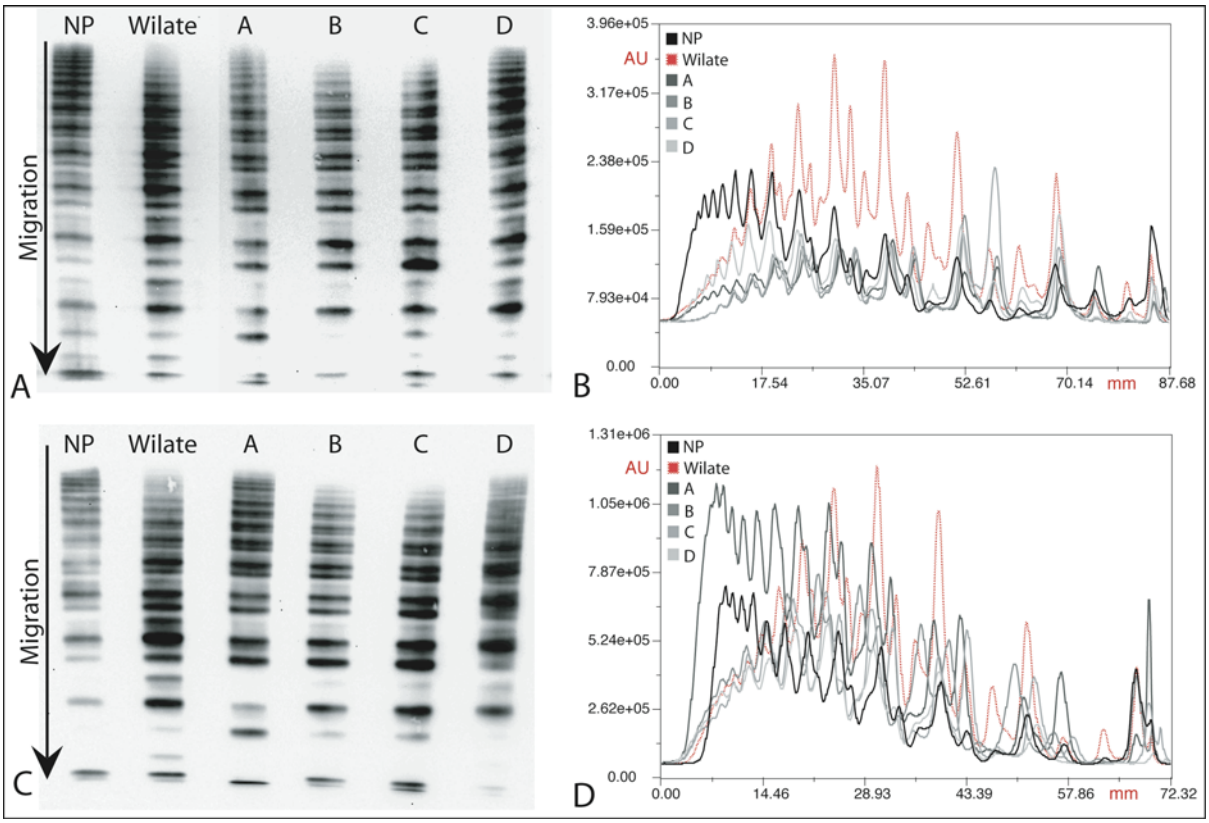

Fig. 23: VWF sub-band distribution of various concentrates using high resolution gels. Using 1.6 % agarose for the investigation of the VWF triplet distribution of the concentrates, only Wilate® and concentrate D provided a plasma VWF-like triplet pattern, whereas both batches of concentrates A - C contained a pronounced proteolytic faster migrating triplet band with virtually absent slower migrating triplet bands. Graphs B and D represent the densitometric evaluation of the VWF multimer pattern depicted in A and C, resulting from VWF multimer analysis of two batches of five VWF-containing concentrates. Every peak equals to one VWF multimer band on 1.6 % agarose gels. For explanation of the graph refer to Fig. 22. Plasma VWF-like sub-band distribution (NP, black line) was confirmed for Wilate® and concentrate D, visible on the basis of the three clearly distinguishable shoulders of one multimer peak. Concentrates A - C exhibited clearly pronounced faster migrating satellite bands resulting in bifurcated peaks of single multimers (B and D, dark grey to light grey lines).

Mediation of platelet adhesion under flow using VWF-containing concentrates

Investigating the function of the VWF-containing concentrates to mediate platelet adhesion, 1 IU/mL VWF:Ag of each concentrate was applied to collagen type III-coated flow-chambers at 1,700 s^{-1} shear rate for 4 min. Experiments were performed in duplicate, a collagen type III-coated flow-cell without VWF served as control for the activation level of the platelet preparation. Both batches were analysed with two different platelet preparations. Fluorescence labelled platelets were perfused over the surface at 1,700 s^{-1} shear rate for 5 min, and the area covered by adhered platelets was determined in end point evaluation. For each flow-chamber, 24 images were randomly chosen along the centre of the flow-cell to exclude boundary effects of platelet adhesion, and analysed using computer-based software analysis. Results of the comparative analysis of the five concentrates are displayed in Fig. 24, whereas the area covered by adhered platelets is represented through the y-axis of the graphs. The x-axis is labelled with the five concentrates investigated; batch 1 is displayed in Fig. 24A, batch 2 in Fig. 24B. Control of the activation level of the platelet preparation resulted in a platelet coverage below 1 % for batch 1, and below 4 % for batch 2. Since the pre-activation level for batch 2 was slightly higher, a higher overall platelet adhesion was observed for these batches. But the area covered by adhered platelets after five minutes platelet perfusion showed the same tendency compared to batch 1 of the concentrates. Interestingly, the results revealed a significantly higher platelet adhesion for both batches of Wilate® tested, although this concentrate showed a relative decrease of HMW VWF multimers.

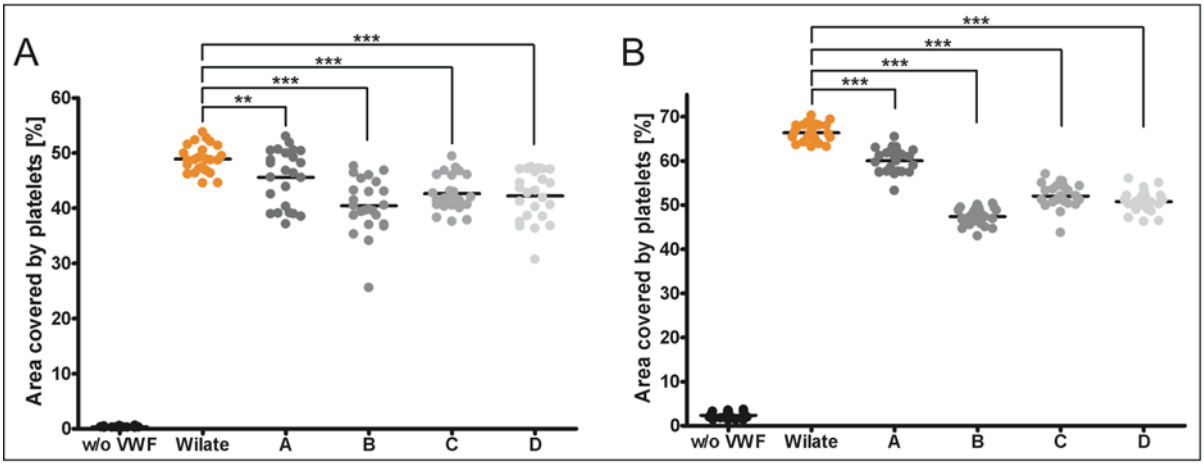

Fig. 24: VWF-mediated platelet adhesion after five minutes perfusion time at 1,700 s^{-1} shear rate. Vertical scatter plots of two batches A and B of five commercially available VWF-containing concentrates are shown. Statistical evaluation exhibited a significantly higher platelet coverage for Wilate® for both batches evaluated compared to concentrates A - D. The area covered by adhered platelets was analysed after 5 min platelet perfusion at 1,700 s^{-1} shear rate subsequent to perfusion of 1 IU/mL VWF:Ag each over a collagen type III-coated flow-chamber. A collagen-coated flow-chamber without perfusion of VWF served as control for the quality of the platelet preparation, exhibiting platelet coverage below 1 % for batch 1 (A) and below 4 % for batch 2 (B). Due to a higher pre-activation level of the platelet preparations, the absolute area covered by adhered platelets is higher for batch 2 (B). VWF-mediated platelet adhesion using the five different concentrates resulted in areas covered by adhered platelets between 30-70 % depending on the used concentrate and platelet preparation. Images were analysed for the percentage of platelet surface coverage using software-based images analysis. Data result from n = 4 for each batch, evaluating 24 randomly chosen images over the length of a flow-channel for each experiment. Black horizontal bars indicate the mean values. ** $p = 0.0057$, *** $p < 0.0001$.

4.4.2 Correlation between VWF multimer size and function

Fractionation of VWF multimers

VWF multimers were fractionated according to their molecular weight via FPLC using a SEC column. After each SEC run, fractions were collected according to FPLC ultraviolet (UV) detector unit signal. A characteristic chromatogram profile is shown in Fig. **25**, indicating collected 5 ml fractions on top of the graph. The duration of the SEC run in hours is depicted on the x-axis. The left y-axis represents the absorbance at 280 nm wavelength, whereas the conductivity is illustrated on the right y-axis. The dark grey line represents the protein elution profile on top of the graph; the light grey line below symbolises the elution of conducting particles. Collected fractions were analysed for multimeric composition by agarose gel electrophoresis, followed by Western blot and chemiluminescence imaging. HMW VWF multimers eluted first, followed by elution of smaller multimers, whereas multimers of lowest molecular weight eluted henceforward fraction 13 (data not shown).

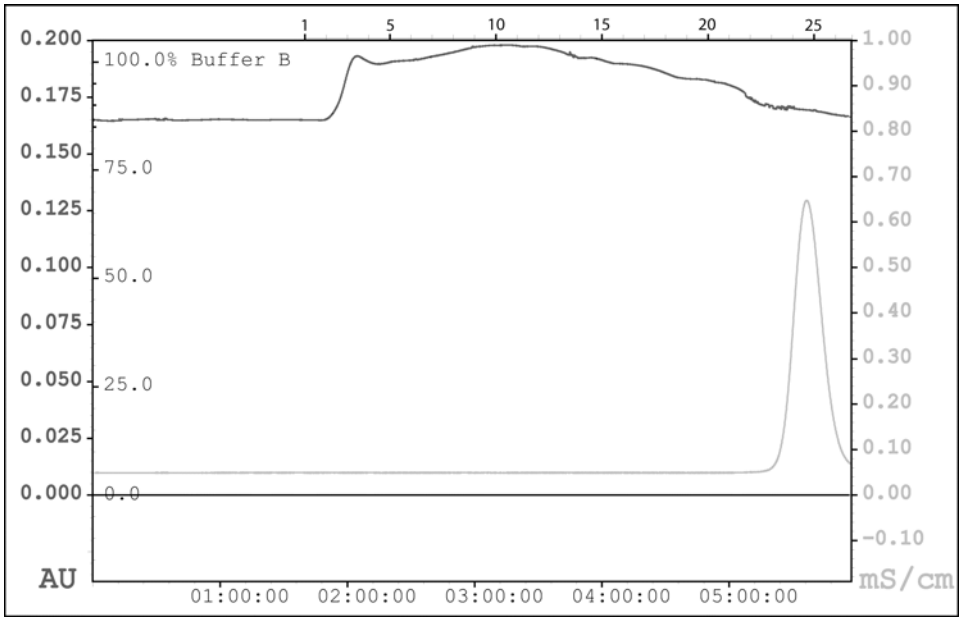

Fig. 25: SEC chromatogram of VWF separation. The graph illustrates the separation of 300 IU VWF:Ag pdVWF preparation at a flow rate of 0.5 ml/min using a sepharose 2B column. The left y-axis indicates the absorbance at 280 nm wavelengths, and the conductivity is displayed on the right y-axis. The duration of the separation run is illustrated at the x-axis. The protein elution profile is represented by the dark grey curve on top, whereas the light grey line beneath symbolises the elution of conducting particles (salt); numbers on top of the diagram indicate the 5 ml fractions collected.

Appropriate fractions of several SEC runs were pooled according to multimer size, and additionally, a mixture of equal proportions of low- (LMW), intermediate- (IMW) and high molecular weight (HMW) VWF multimers, specified as 'Mix', was prepared. The multimeric profiles of these fractions are demonstrated in Fig. 26A. The LMW VWF fraction exhibited the highest amount of VWF dimers and trimers, whereas other multimer sizes are present in much lower concentration: according to densitometric evaluation values (Fig. 26B) 2- and 3mers together made up over 60 % of the whole multimeric profile (green curve). The IMW VWF fraction contained predominantly 4-, 5- and 6mers representing the majority of all multimer sizes (70 %, light grey curve). The HMW fraction consisted predominantly of 5 - 8mers (around 65 %, black curve). The profile of the Mix fraction exhibited nearly consistent distribution of all VWF multimers (blue curve).

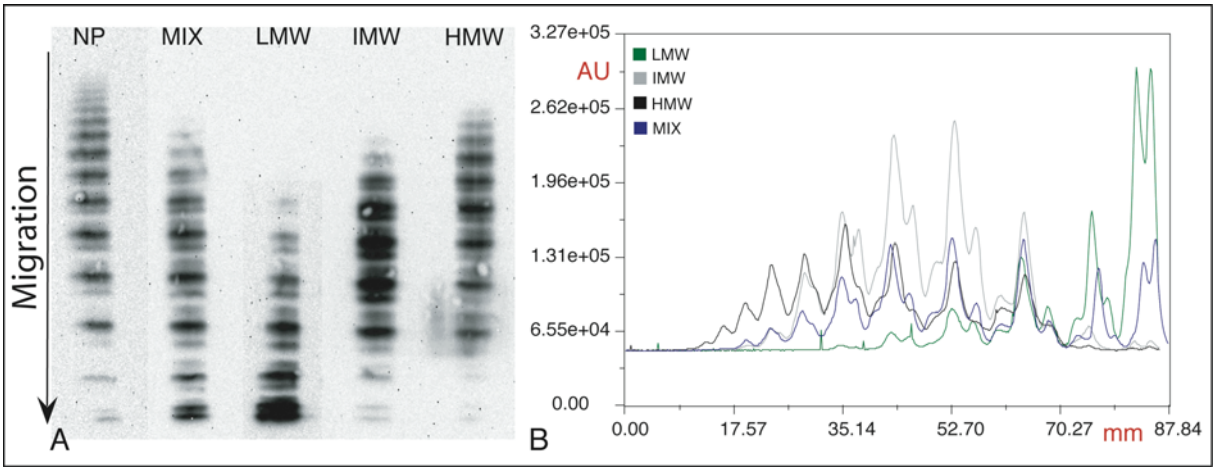

Fig. 26: VWF multimer analysis of pooled fractions using 1.2 % agarose gel electrophoresis. SEC fractions were pooled according to VWF multimer size to obtain samples of low molecular weight (LMW, 1 - 5mer), intermediate molecular weight (IMW, 3 - 9mer) and high molecular weight (HMW, 3 - 12mer). A mixture of all samples was used as control (MIX). NP indicates standard human plasma. The pattern of the VWF multimer distribution is displayed in (A), and the densitometric evaluation is shown in (B). The VWF dimer is represented by the first bifurcated peak on the right hand side of (B), and HWM VWF multimers are depicted on the left hand side of the graph. The y-axis indicates the intensity of the chemiluminescence signal. LMW VWF multimers are displayed in green exhibiting a predominant presence of VWF multimers 2 - 3, the IMW VWF multimer sample contained predominantly VWF multimers 4 - 6 (light grey), whereas the HMW fraction was mainly composed of VWF multimers 5 - 8 (black curve). The profile of the MIX sample exhibited a nearly consistent distribution of all VWF multimers (blue curve).

VWF-mediated platelet adhesion under physiological flow conditions

VWF fractions with different VWF multimeric structure were prepared to investigate the influence of multimerisation on the function of VWF under physiological flow conditions. Samples of LMW, IMW and HMW VWF multimers were perfused over collagen type III-coated flow-chambers at a shear rate of 1,700 s^{-1} for 4 min, followed by perfusion of fluorescence labelled platelets containing physiological amounts of red blood cells for 5 min at the same shear rate. After fixation, the area covered by adhered platelets was determined by computer-based image analysis, whereas 24 images were evaluated per flow-channel. Representative images are displayed in Fig. 27. Platelet adhesion mediated by LMW (Fig. **27**C), IMW (Fig. 27D), HMW (Fig. 27E), or a mixture of all VWF multimers after SEC (Fig. **27**F) are shown, compared to the area covered by fluorescence labelled platelets without VWF (Fig. 27A) or after pre-perfusion of 1 IU/mL VWF:Ag Wilate® (Fig. 27B).

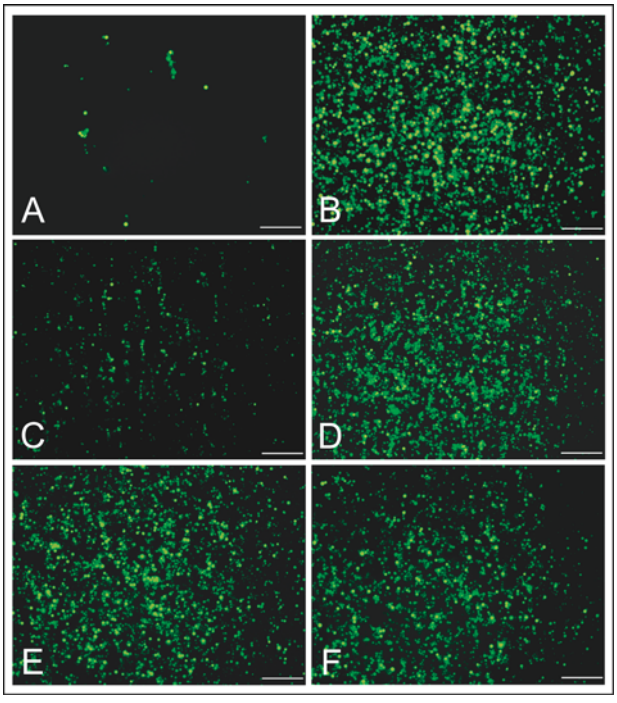

Fig. 27: Platelet adhesion under physiological flow conditions mediated by VWF of different multimeric composition. Preparations of 1 IU/mL VWF:Ag of LMW (C), IMW (D), and HMW VWF multimers (E) were perfused over collagen type III-coated flow-chambers followed by perfusion of fluorescence labelled platelets at 1,700 s^{-1} shear rate. A mixture of all multimers served as control (F), as well as a flow-chamber without pre-perfusion of VWF (A) to assure the quality of the platelet preparation, and a Wilate® sample without treatment for positive control (B). Images are representative for the area covered by adhered platelets after 5 min perfusion time. Flow direction; top to bottom. Scale bar; 50 µm.

To determine whether the platelet adhesion mediated by VWF preparations of varying multimer distribution was significantly different, statistical analysis was performed using the student's t-test to compare the single values resulting from two independent experiments conducted with two different platelet preparations, each performed in duplicate. After 5 min platelet perfusion, 24 images were taken along the centre of the flow-chamber. Comparing the percentage of the area covered by adhered platelets using preparations of LMW (inversed triangles), IMW (rhombs) and HMW VWF multimers (triangles, Fig. 28), no statistical significant difference was found between IMW and HMW samples, but the platelet adhesion was significantly lower using LMW VWF multimers, composted mainly of VWF dimers and trimers.

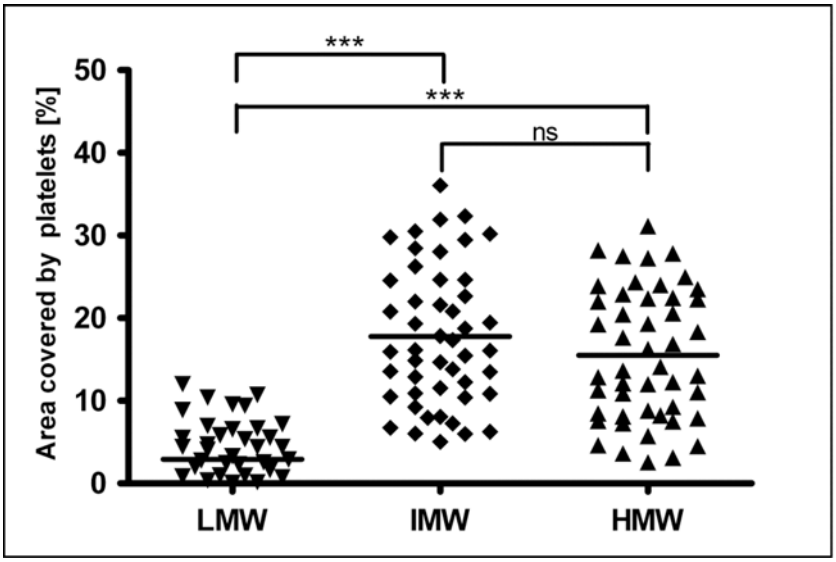

Fig. 28: Statistical evaluation of the area covered by adhered platelets mediated by VWF of different multimeric composition. After perfusion of platelets for 5 min at 1,700 s^{-1} shear rate subsequent to pre-perfusion of LMW (inversed triangle), IMW (rhomb) or HMW VWF multimers (triangle), 24 images were taken over the centre of the flow-chamber. The percentage of the area covered by adhered platelets (y-axis) was determined using software-based image analysis, and data is representative of experiments conducted with two different platelet preparations, each performed in duplicate. Black horizontal bars indicate mean values. Ns: not significant ($p = 0.1752$); *** $p < 0.0001$.

Collagen binding kinetics of VWF preparations of varying multimeric composition

The function of VWF is often determined using static collagen binding ELISAs. These assays are designed to be sensitive against HMW VWF multimers, developed as a diagnostic tool to discriminate patients suffering from VWD type 2 subtypes. Since the process of haemostasis is highly dependent on the physical properties of blood flow, the ability of VWF samples composed of different multimeric distribution to bind to human pepsin digested collagen type III under flow was determined using SPR (Fig. 29). VWF preparations containing LMW (Fig. 29A), IMW (Fig. 29B) and HMW VWF multimers (Fig. **29**C) as well as a sample composed of all VWF multimers (Fig. 29D) were perfused over a CM5 chip surface coated with human pepsin digested collagen type III at continuous flow of 20 µL/min, corresponding to a flow rate of 1,650 s^{-1}. The amount of collagen immobilised on the chip surface was 674 RU for analysis of HWM and Mix sample binding, whereas for the IMW and LMW fractions 1,184 RU collagen were immobilised. Increasing concentrations, ranging from around 10 - 900 nM for the HMW, IMW and LMW fraction and 1 - 80 nM for the Mix sample, were injected for 3 min each with repeated surface regeneration. The maximal binding (R_{max}) of all samples ranged from 10 - 22 RU (data not shown).

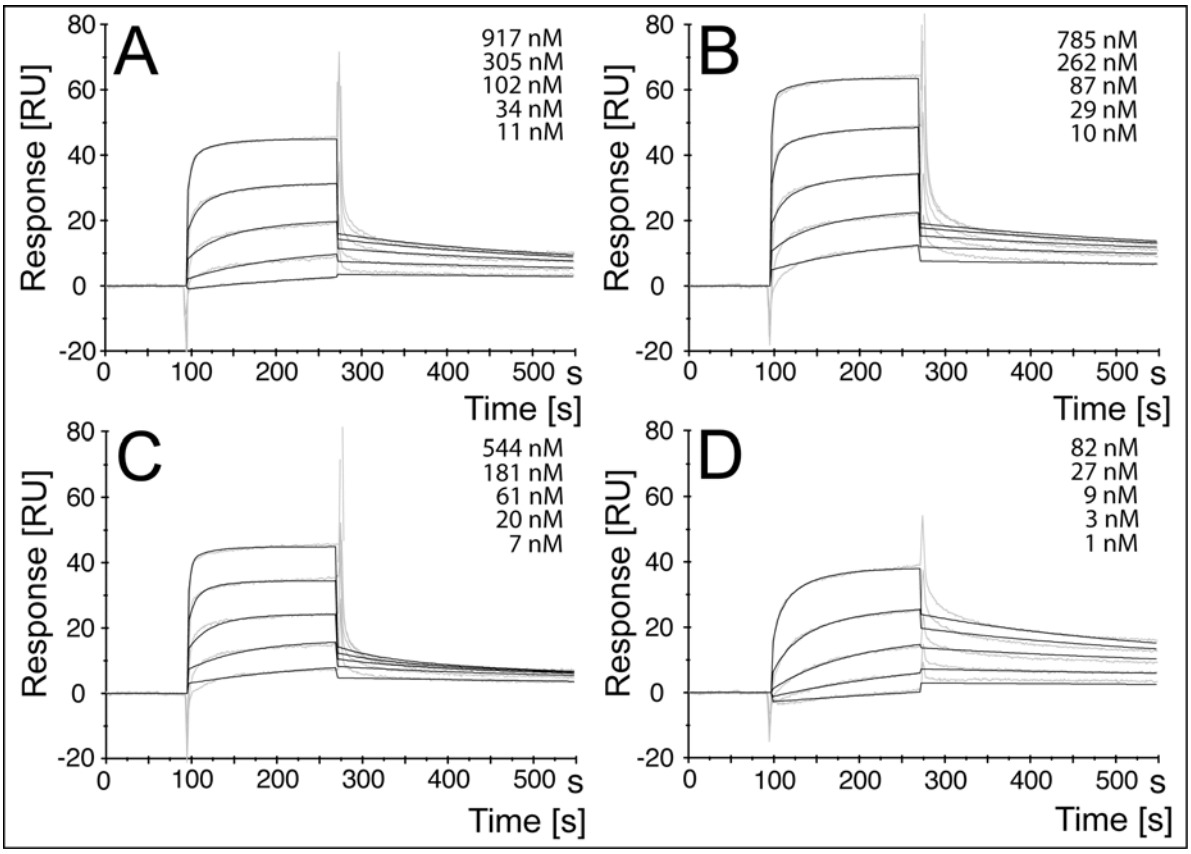

Fig. 29: Collagen binding curves of VWF preparations with varying multimeric distribution using SPR. Response units (RU) of different VWF concentrations are plotted as a function of time. Each grey curve corresponds to a dilution step in a concentration range between 7 to 917 nM of LMW (A), IMW (B), HMW VWF multimers (C), and a mixture of all VWF multimers with concentrations of 1 - 82 nM (D; bottom to top). The specific concentrations for each sample are indicated on the upper right hand side of the graphs. Black curves indicate the mathematical alignment using the model for bivalent analyte. Samples were injected with increasing concentrations, whereas a positive slope of the grey curve indicates the association of VWF to collagen until equilibrium applying higher concentrations, followed by a negative slope indicating dissociation of VWF from collagen.

After subtraction of the reference cell signal, binding curves were analysed using software-based mathematical correlations. VWF to collagen type III-binding was observed in each sample. Mathematical simulation of 1:1 (Langmuir) binding as well as for bivalent analyte was fitted into each binding profile. Cumulated differences between measured binding and the mathematical model are expressed as the chi-square distribution (χ^2). For the shown binding profile, χ^2 was below 2 for all samples, indicating a very good approximation to the obtained binding curve.

The kinetic data and dissociation equilibrium constant of the VWF-collagen type III binding curves are summarised in Table 4, obtained using the mathematical model of 1:1 interaction, and Table 5 applying the model for bivalent analyte, whereas both correlations based on the molecular weight of the VWF monomer of 270 kDa.

Table 4: Kinetic binding data of VWF preparations to collagen: 1:1 (Langmuir) binding model. χ^2: approximation between obtained binding curves and mathematical model; k_a: association rate constant; k_d: dissociation rate constant; K_D: equilibrium dissociation rate constant.

	k_a [1/Ms]	k_d [1/s]	K_D [M]	χ^2
LMW	1.49 E+05	1.69 E-03	1.13 E-08	0.692
IMW	3.89 E+05	8.28 E-04	2.13 E-09	1.413
HMW	6.24 E+05	1.69 E-03	2.71 E-09	0.562
MIX	8.13 E+05	1.36 E-03	1.68 E-09	1.928

The χ^2-values using the 1:1 molecular interaction model were below 2, indicating virtually coincidence between the obtained binding curves and the applied mathematical model. Association rate constants from 1.5×10^5 1/Ms for the LMW fraction to 6.2×10^5 1/Ms for the HMW fraction, and highest for the Mix fraction with 8.1×10^5 1/Ms were obtained, but all values were found to be in the same range. In contrast, k_d values differed slightly with the lowest value for the IMW VWF fraction with 8.3×10^{-4} 1/s, suggesting a slightly higher affinity for this fraction. Concerning the K_D-value, the LMW fraction exhibited the highest value with 11.3 nM, indicating a decreased overall affinity compared to all other fractions exhibiting K_D-values in the range of 1.7 - 2.7 nM.

Table 5: Kinetic data of VWF preparations binding to collagen: Bivalent analyte model. χ^2: approximation between obtained binding curves and mathematical model; k_a: association rate constant; k_d: dissociation rate constant; K_D: equilibrium dissociation rate constant.

	k_a1 [1/Ms]	k_d1 [1/s]	K_D1 [M]	k_a2 [1/Ms]	k_d2 [1/s]	K_D2 [M]	χ^2
LMW	7.17 E+04	2.58 E-03	3.60 E-08	3.33 E+05	3.14 E-02	9.40 E-05	0,287
IMW	1.98 E+05	1.47 E-03	7.47 E-09	5.93 E+05	2.96 E-02	5.00 E-05	0,552
HMW	1.70 E+05	8.29 E-03	4.87 E-08	9.09 E+05	2.48 E-02	2.73 E-05	0,405
MIX	3.57 E+05	2.39 E-03	6.69 E-09	9.17 E+05	2.78 E+01	3.03 E-02	0,758

Applying the mathematical model for bivalent analyte, association rate constants (k_a1) for the first binding of the analyte from around 7.17 x 10^4 1/Ms for the LMW fraction to 2 - 3 x 10^5 1/Ms for all other fractions were obtained, indicating a faster association rate for VWF multimers larger than four. Dissociation rate constants (k_d1) ranged from 2 - 8 x 10^{-3} 1/s, indicating a faster dissociation rate for the HMW sample. Examining the second binding of the analyte, association and dissociation rate constants were comparable except for the dissociation rate constant of the sample containing all VWF multimers, showing a k_d2-value of around 2.8 1/s. Generally, very low K_D1-values were observed for all VWF preparations, ranging from 36 nM for the LMW fraction to around 7 nM for the IMW fraction and the sample containing all VWF multimers. Surprisingly, the K_D1-value for the HMW fraction was comparable to the LMW fraction with around 49 nM due to a faster dissiciation rate of this sample, indicating lower overall affinity.

Examining the second interaction using the mathematical model of bivalent analyte, k_a2-values ranging from 3 - 9 x 10^5 1/Ms and k_d2-values around 3 x 10^{-2} 1/s were obtained, except for the Mix sample containing all VWF multimers with a k_d2-value of about 3 1/s. This resulted in a remarkably higher K_D2-value for this sample of 3 x 10^{-2} M, compared to the values of the other samples ranging from 3 - 9 x 10^{-5} M, indicating lower affinity for the samples containing all VWF multimers, which might be attributed to the lower concentration range used for SPR experiments. Overall, the second interaction exhibited a markedly decreased affinity compared to the first interaction with very high affinities for VWF binding to collagen type III.

5 Discussion and prospects

Platelet adhesion at sites of exposed ECM components in vessel walls at physiological high arterial shear rates is mediated by VWF, leading to platelet tethering, translocation and finally adhesion to injured subendothel. A variety of flow-chamber models to study *in vivo* haemostasis have been developed since 1972, employing mostly annular perfusion chambers and parallel-plate perfusion chambers. Flow-chamber models represent a powerful tool to emphasise the shear rate dependency of thrombotic and physiological haemostatic mechanisms as well as the efficacy of drugs [Baumgartner & Haudenschild, 1972; Baumgartner, 1973; Sakariassen *et al.*, 1983; Moroi *et al.*, 1996; Bonnefoy *et al.*, 2003]. Measurement of VWF-mediated platelet adhesion under flow conditions is advantageous compared to the currently used VWF activity assays, e.g. VWF:RCo, VWF:CB and FVIII:C, because they approximate more closely the situation of *in vivo* platelet adhesion. Although flow-chamber models are continually improved, there are still no standardised *in vitro* flow-devices available, which satisfactory give reliable, sensitive and validated results, also with regard to a potential benefit in VWD diagnosis [Zwaginga *et al.*, 2006].

Therefore, this thesis focus on the establishment of an *in vitro* flow-chamber model designed to study the function of VWF under physiological blood flow conditions, using commercially available flow-devices allowing direct visualisation and quantification of VWF-mediated platelet adhesion in real time.

5.1 Characterisation of the established *in vitro* flow-chamber system

In order to characterise a flow-chamber system, numerous VWF-containing sample was required. It was not possible to use the international standard for VWF/FVIII concentrates, because it is available only in limited amounts, and purified plasma-derived VWF is very cost-intensive. Therefore, the commercially available VWF/FVIII preparation (Wilate®) was used for the establishment of the *in vitro* flow-chamber system, which was extensively characterised by Stadler *et al.* [2006]. The concentrate was designed for patients suffering from VWD and haemophilia A, providing a physiological ratio of VWF to FVIII close to that found in healthy individuals, and exhibits a VWF multimeric pattern comparable to standard human plasma with a relatively lower portion of the highest VWF multimers, but a

physiological distribution of VWF sub-bands. DLS measurements revealed a pure preparation with presence of only one particle with a hydrodynamic radius of about 36 nm after filtration, corresponding to electron microscopy results suggesting the typical VWF multimeric forms present as loosely tangled coil with an overall size of 100 - 300 nm [Fowler *et al.*, 1985] as well as findings using light and small angle neutron scattering, suggesting an ellipsoid structure of VWF in solution with a radius of gyration of 75 and 30 nm for the VWF multimer and protomer, respectively [Singh *et al.*, 2006]. SDS-PAGE under reducing conditions and Western blot analysis revealed a pure preparation with the presence of a main protein band at around 200 kDa, and a fainter band at 450 kDa, both detected by a polyclonal anti-human VWF antibody, indicating the presence of the VWF monomer and small portions of the VWF dimer after reduction.

5.1.1 Considerations of the choice of collagen

About 40 % of of the vessel walls' total protein content is represented by collagens, of which type I, III and VI are considered to be the most active ones in terms of haemostasis [Saelman *et al.*, 1993; Sixma *et al.*, 1995]. Interactions between fibrillar collagens type I, III and VWF are attributed to an induced-fit mechanism involving negatively charged residues of the A3 domain of VWF and positively charged residues on collagen [Huizinga *et al.*, 1997]. In contrast, binding of VWF to non-fibrillar collagen type VI has been attributed to involve the VWF A1 domain [Denis *et al.*, 1993], even though the A1 domain was shown to substitute for the A3 domain in platelet recruitment to fibrillar collagen under flow if the A3 domain is lacking [Bonnefoy *et al.*, 2006]. Thus, careful consideration of the choice of collagen and characterisation of the coated surface are critical for the establishment of a reproducible VWF flow assay.

For development of the presented flow-chamber model, two commercially available types of collagen crucial for thrombus formation were tested with regard to feasibility, surface characteristics after coating, and mediation of platelet adhesion: (i) limited pepsin digested collagen type III from human placental villi, predominantly composed of shortened triple-helical α-chains, and (ii) equine tendon acid soluble fibrillar collagen type I. The choice for these two types of collagens were attributed to their widely use in assays for VWD diagnosis, namely the VWF:CB. In static VWF:CB assays, these two types of collagen exhibit different

VWF binding characteristics: the human collagen type III is equally able to bind all VWF multimers, whereas equine tendon collagen type I exhibits a higher sensitivity to the HMW VWF multimers, allowing discrimination of VWD subtypes with relatively loss of the largest VWF multimers. This distinction led to the recommendation for the use of equine tendon collagen type I for static VWF:CB assays in terms of VWD diagnosis [Favaloro, 2000]. The use of equine tendon collagen type I is certainly beneficial in diagnostics, but conclusions drawn using non-human collagen to study *in vivo* haemostasis must be interpreted with caution regarding the physiology.

Characterising the collagen coating, AFM measurements revealed a homogeneous distribution of small collagen fibrils in the flow-channel coated with collagen type III, whereas a heterogeneous distribution of collagen I fibres of various sizes was observed, indicating the presence of a barely reproducible surface not ideally suited to study real time platelet adhesion. But since this type of collagen is widely used not only in VWD diagnosis, but also in flow-chamber models investigating VWF-mediated platelet adhesion [Reininger *et al.*, 2006], the properties of equine tendon collagen type I to study the function of VWF under flow were further examined.

The binding of VWF to subendothelial collagen is the first and crucial step of *in vivo* haemostasis under high arterial shear rate conditions, whereas type III collagen is the main component of connective tissue in non-capillary blood vessels. Since a correlation between VWF multimer size and affinity to fibrillar collagen under static conditions was shown using crossed immunoelectrophoresis [Santoro, 1983], the multimeric pattern of VWF bound to collagen under flow was investigated. Interestingly, all VWF multimers bound to both collagens at low shear rates of 400 s^{-1} as well as high shear rates of 4,000 s^{-1}. In contrast to static VWF collagen I binding assays, which are sensitive against the multimer distribution of the VWF sample [Favaloro 2000], VWF bound to collagen type I with increasing shear rates showed no alteration in its multimeric profile when compared to the sample before application to the flow-chamber. Multimers bound to collagen type III with increasing shear rates exhibited a somewhat stronger chemiluminescence signal in the portion of the HMW VWF multimers. However, perfusion experiments with VWF over a flow-chamber coated with collagen type III at a constant shear rate of 1,700 s^{-1} with increasing perfusion times of 0.5 to 5 min did not show an initial binding of HMW VWF multimers. Additionally, dilution series of the used sample in VWF MMA revealed a concentration dependent loss of the portion of

HMW VWF multimers, which also hampers the attribution to a diminished or enhanced binding affinity of discrete VWF multimers to collagen under flow. Hence, it is difficult to draw conclusions on the affinity of individual VWF multimers to collagen under flow just from perfusion experiments and analysis of the multimeric profile, because of the limitations of VWF MMA with respect to produce ideally suited gels for quantitative evaluation [Budde, 2006 (2)].

The overall amount of VWF bound to collagen type III under flow was much higher than for collagen type I, indicating a higher affinity of VWF to collagen type III, which is in accordance with data presented by others [Sixma *et al.*, 1995; Li *et al.*, 2002; Moroi & Jung, 2007]. The greatly lower affinity of VWF to equine tendon collagen type I also impedes the interpretation of the VWF:CB used in VWD diagnosis, recommending the application of a mixture of collagen type I – for sensitivity against the HMW VWF multimers – and collagen type III to enhance the optical end-color development of the ELISA method [Favaloro, 2007]. Taken together, these findings suggest that collagen type III is the main binding partner for VWF *in vivo*, and platelet adhesion to injured endothelium is mainly dependent on the interaction between subendothelial collagen type III and VWF, whereas collagen type I plays only in minor role in VWF-mediated platelet adhesion.

Consequentially, the use of collagens optimised for determination of VWD subtypes does not necessarily reflect the *in vivo* function of VWF, suggesting to develop VWF collagen-binding assays specifically designed for the use either in VWD diagnostics or determination of VWF activity.

5.1.2 Functional epitope for platelet recruitment

Immunostaining of collagen-bound VWF after perfusion at 1,700 s^{-1} shear rate with a polyclonal anti-VWF antibody revealed homogeneous distribution of VWF on collagen type III, whereas on fibrillar collagen type I VWF adhered preferentially to long collagen fibers. Applying multiple labeling immunofluorescence technique, the GPIb binding domains provided by the collagen-bound VWF under flow, responsible for interaction with platelets, were detected. Since the VWF bound to both collagens at a shear rate of 1,700 s^{-1}, the fluores-

cence staining of the GPIb binding domain using a specific monoclonal antibody most likely reflects the capability of the adhered VWF to mediate platelet adhesion under flow conditions.

The utilised anti-VWF-GPIb antibody (clone RFF-VIII:R/1) has been shown to reflect VWF-GPIb binding activity [Goodall *et al.*, 1985; Chand *et al.*, 1986; Murdock *et al.*, 1997], but conflicting data using this antibody suggest rather a correlation with VWF:Ag than with VWF function [Fischer *et al.*, 1998 (1)]. However, it is most likely that in both studies the monoclonal antibody reflects the presence of potential GPIb binding epitopes.

The specificity of VWF-collagen binding was verified using the well-characterised mAb 82D6A3, which binds to the VWF-A3 domain and inhibits VWF-binding to collagen under flow [Wu *et al.*, 2002; Vanhoorelbeke *et al.* 2003]. Almost complete inhibition of VWF binding to collagen type III under flow was obtained. In contrast, background staining of the collagen I-coated flow-chamber was very high, and VWF-binding to fibrillar collagen type I was only partially blocked by the inhibitory antibody, suggesting that the collagen type I preparation used in this study contained trace amounts of collagen-associated VWF. This has been shown previously for two other commercially available equine tendon collagens type I by Bernardo *et al.* [2004], and underlines the importance to thoroughly characterise collagen preparations intended for use in flow-chamber assays. For future studies, each collagen preparation will be examined with respect to its purity prior to perfusion experiments.

5.1.3 VWF-mediated platelet adhesion under flow

The ability of collagen-bound VWF with respect to the mediation of platelet adhesion at high shear rates was also determined in a two-step model: (i) perfusion of VWF over a collagen type III-coated flow-chamber, and (ii) perfusion of fluorescence labelled platelets over the generated surface followed in real time, applying a shear rate of 1,700 s^{-1}. Using isolated platelets and washed red blood cells without additional anticoagulants, only negligible platelet adhesion to collagen type III was observed when no VWF was present. When VWF was flow-bound to collagen type III prior to platelet perfusion, an area covered by adhered platelets of about 36 % after 5 min perfusion time was achieved, corresponding well to the platelet surface coverage observed by others using full blood [Moroi *et al.*, 1996; Wu *et al.*, 2002; Vanhoorelbeke *et al.*, 2003; Bernardo *et al.*, 2004]. Although time dependent platelet

adhesion mediated by collagen-bound VWF under flow up to 15 min was determined, investigation of platelet adhesion for five minutes perfusion time – covering the physiologically relevant time frame for primary haemostasis [Watson & Greaves, 2008] – seems sufficient. Extended flow-based platelet adhesion experiments rather reflect the functionality of the applied platelet- than the tested VWF preparation, as fully attached functional platelets are activated and release endogenous thrombogenic substances, which will recruit further platelets from perfusate to build larger aggregates [Hoylaerts, 1997; Ruggeri, 2004].

In contrast to collagen type III, platelet adhesion to immobilised fibrillar collagen type I under high flow occurred without addition of exogenous VWF. This result is in agreement with the control experiments using the inhibitory antibody mAb 82D6A3, whereby only a partial inhibition of VWF-binding to collagen under flow was accomplished. Interestingly, Bernardo *et al.* [2004] found trace amounts of VWF in two commercially available collagen type I preparations from equine tendon, resulting in platelet adhesion without substitution of exogenous VWF. Moreover, large batch-to-batch variations for this particular collagen and contamination with collagen type III and VWF [Favaloro, 2007; Sakariassen, pers. comm.] as well as the heterogeneous mixture of collagen type I fibrils, impede comparative and reproducible analyses. The varying quality and composition of commercially available collagen preparations may be overcome by the use of recombinant human collagens and/or synthetic collagen peptides, which as well will facilitate the standardisation of thrombogenic surfaces in the future [Lisman *et al.*, 2006; Raynal *et al.*, 2006; Cejas *et al.*, 2008; Farndale *et al.*, 2008]. However, a potential influence of the fibrillar collagen structure on the mediation of platelet adhesion under flow must be considered and will be evaluated in future studies.

In conclusion, the established *in vitro* flow-chamber model allows the evaluation of both important VWF functions, VWF-collagen interaction and VWF-mediated platelet adhesion under defined flow conditions in real time. All VWF multimers, from LMW up to HMW, are able to bind to both collagens type I and III even at high shear rates of 4,000 s^{-1}. VWF bound to collagen at 1,700 s^{-1} shear rate exposes GPIb binding domains required for platelet recruitment, whereas the binding epitopes are present to a similar extend co-localised with the fluorescence signal of the polyclonal anti-VWF antibody. Collagen type III is most applicable with only marginal platelet adhesion without exogenous VWF, whereas collagen type I already triggers platelet adhesion without substitution of VWF, and is, therefore, not suitable to study VWF-mediated platelet adhesion in the established flow-chamber system.

5.2 Comparison of VWF-containing concentrates

Since the first description of VWD in 1926 through Erik A. von Willebrand, basic understanding of the disease and its management significantly improved over the last decades, and treatment becomes more specific due to more precise discrimination between VWD subtypes. The most frequent inherited bleeding disorder, resulting in a quantitative (type 1 and 3) or qualitative (type 2) VWF deficiency, exhibits a broad range of malfunctioned coagulation with mild bleeding tendency up to life threatening haemorrhages [Cox Gill, 2004; Schneppenheim, 2005]. The primary treatment goal for VWD patients comprises the normalisation of VWF activity in plasma as well as FVIII replacement in case of severe VWD [Budde *et al.*, 2006]. Desmopressin (DDAVP) is the treatment of choice in type 1 VWD, releasing endothelial VWF with correction of VWF and FVIII plasma levels [Mannucci, 2001]. But adverse events or major surgery, patients suffering from VWD type 2 with qualitative abnormal VWF as well as type 3 patients demand substitution therapy with VWF-containing concentrates [Pasi *et al.*, 2004; Ingerslev *et al.*, 2004; Federici, 2005]. Several plasma derived VWF/FVIII concentrates, initially developed for the treatment of haemophilia A patients [Federici, 2005], are approved for the treatment of VWD, providing efficacy in medical practise albeit the variety in their biochemical profile and content of HMW VWF multimers [Mannuccio *et al.*, 1994; Budde *et al.*, 2006 (1)].

To assess the function of VWF provided by commercially available VWF-containing concentrates fulfilling the criteria for the treatment of VWD [Mazurier, 2006], two batches each of five concentrates were tested with regard to the mediation of platelet adhesion using the established flow-chamber system. With respect to VWF, the concentrates differed in the VWF multimeric content as well as their VWF triplet structure, most likely due to a varying degree of proteolytic breakdown during manufacturing and virus inactivation [Budde *et al.*, 2006 (1)].

Applying physiological concentrations of 1 IU/mL VWF:Ag, all tested concentrates were able to mediate a level of stable platelet adhesion comparable to results published by others using whole blood perfusion [Moroi *et al.*, 1996; Lankhof *et al.*, 1997; Vanhoorelbeke *et al.*, 2003; reviewed by Sakariassen *et al.*, 2004]. Interestingly, both batches of Wilate® tested revealed a significantly higher platelet adhesion to collagen type III, albeit this concentrate exhibited a relative loss of HMW VWF multimers, and concentrates showing a loss of

large VWF multimers are considered to be less suitable for VWD treatment [Budde & Drewke, 1994]. Products A - C present an enhanced faster migrating VWF triplet band, indicating proteolytic breakdown during purification process. Product B and C additionally showed loss of HMW VWF multimers. Only product D exhibited a plasma-like VWF triplet structure as well as the presence of HMW VWF multimers, but mediated comparable platelet adhesion to concentrates B and C.

The functional integrity of VWF is strongly dependent on its conformation, which is sensitive to adhesive surfaces and shear forces. It is very likely that the manufacturing and virus inactivation process influences the quality and functionality of VWF. Since the experimental setup was designed to allow the determination of VWF-mediated platelet adhesion solely dependent on collagen-bound VWF under flow, presumably the VWF of the tested concentrates comprise functional variations except from different VWF multimer and triplet patterns. Harsh conditions during purification and formulation might cause conformational transitions of the globular VWF protein; centrifugation steps may extend VWF to a linear conformation, allowing susceptibility for proteolytic cleavage, and recent studies suggest also mechanical destruction of HMW VWF multimers [Michiels *et al.*, 2001]. High salt concentrations are also known to induce ADAMTS-13 cleavage of VWF in the absence of shear forces *in vitro* [Furlan & Lämmle, 2002]. Together with impurities in the tested concentrates – especially the content of proteases like ADAMTS-13 – these factors might influence the integrity and functionality of the VWF protein, and are likely responsible for the loss of HMW VWF multimers [Mannuccio *et al.*, 1994]. However, more precise statements are only possible after thorough investigation of the manufacturing process of the concentrates, inspection of concomitant proteins with particular attention to the content of ADAMTS-13 cleavage protease, and examination of a possible impact of VWF triplet structure on VWF function.

5.3 Correlation between VWF multimer size and function

It is widely assumed, that the largest VWF multimers reveal a higher activity in terms of haemostasis. This theory is deduced from several observations: (i) the selective absence of HMW and IMW VWF multimers in VWD type 2A cause bleeding, (ii) defects in VWF proteolysis by ADAMTS-13 with accumulation of very HMW forms of VWF in

circulation result in thrombotic thrombocytopenic purpura (TTP) with spontaneous platelet aggregation and thrombi formation, and (iii) static VWF activity assays – like VWF:RCo, RIPA or VWF:CB – are sensitive against HMW VWF multimers. However, very few experimental data is available on the impact of VWF multimer size, and no data exist showing a clear correlation between a defined multimer size and VWF function. Whereas some research groups attributed a higher functionality to the HMW VWF multimers [Santoro, 1983; Fischer *et al.*, 1998 (1); Favaloro, 2000; Neugebauer *et al.*, 2002; Turecek *et al.*, 2002], conflicting results indicate no functional correlation with respect to VWF multimer size [Sixma *et al.*, 1984; Sakariassen *et al.*, 1986; Meyer *et al.*, 1991].

To examine a possible correlation between VWF multimer size and function under flow, VWF was fractionated via SEC to obtain LMW (mainly 2 - 3mers), IMW (predominantly 4 - 6mers) and HMW VWF multimer samples (primarily 5 - 8mers). Albeit it is not possible to obtain 'pure' preparation of single multimers via SEC, this method was chosen to avoid additional separation of VWF subbands occurring during heparin affinity chromatography [Fischer *et al.*, 1999], or chemical treatment required for susceptibility for ADAMTS-13 cleavage *in vitro* [McMullen *et al.*, 1991; Furlan & Lämmle, 2002] and reduction using dithiothreitol (DTT) [Ohmori *et al.*, 1982], which presumably influence the nativity of the VWF protein accompanied by loss of function.

5.3.1 Flow-chamber assays

To evaluate the ability of VWF preparations with different multimer size to mediate platelet adhesion under flow, samples containing LMW, IMW and HMW VWF multimers were perfused over collagen type III-coated flow-chambers at 1,700 s^{-1} shear rate, corresponding to a shear stress of 16.4 dyn/cm^2 in the established flow-system. Subsequently, fluorescence labelled platelets mixed with red blood cells to a haematocrit of 33 % were perfused over the surface at the same shear rate for 5 min, resulting in around 50 dyn/cm^2 shear stress considering the dynamical viscosity of blood with 3 - 4 x 10^{-3} Pas. Statistical analysis after determination of the area covered by adhered platelets revealed that the fractions containing IMW and HMW VWF multimers were equally active to mediate platelet adhesion, whereas the LMW fraction exhibited a statistically significant decreased platelet surface coverage compared to the IMW and HMW preparations, suggesting a lower activity

for VWF multimers smaller than four. However, the overall area covered by adhered platelets was reduced compared to the sample before SEC. This is likely attributed to a loss of VWF activity during fractionation procedure and storage, supported also by a lower platelet adhesion level found for the Mix-sample of fractions after SEC containing all VWF multimers, compared to the sample before SEC fractionation. These results are in accordance with flow experiments describing a comparable activity for multimeric VWF, but a 50 % reduction in case of recombinant dimeric VWF, when applied in equal concentrations [Wu *et al.*, 1996]. Furthermore, this study revealed that VWF dimers were also equally functional when applied at higher concentrations. The results presented here and outcomes of studies done by others suggest that all VWF multimers contribute to VWF-mediated platelet adhesion under flow. Very low molecular weight VWF multimers might exhibit a reduced activity compared to multimers larger than four, but are possibly equally active when applied in higher concentrations. In this regard the capacity of VWF self-adhesion might also be an interesting aspect.

However, determination of ‘VWF concentration’ has to be carefully considered when interpreting results obtained by flow experiments. It is speculative but possible that the VWF:Ag ELISA utilising the polyclonal anti-VWF antibody does not solely reflect the presence of VWF, but might also underestimate samples containing intact HMW VWF multimers because of globular conformation and inaccessibility of antigenic determinants. This in turn challenges the obtained diminished ability of LMW multimers smaller than four in relation to a possible higher response in VWF:Ag determination.

Overall, investigation of samples containing various VWF multimer distribution revealed that HMW and IMW VWF multimers were equally active in mediating platelet adhesion on collagen type III, whereas multimers containing predominantly 2 - 3mers are less active to mediate platelet adhesion when applying an equal concentration of 1 IU/mL VWF:Ag. In contrast, VWF activity assays under static conditions indicate a far more critical role of VWF multimer size with respect to VWF function. This underlines the importance of conducting flow-based assays to determine VWF *in vivo* function, which might not be correctly reflected by static VWF activity assays performed in VWD diagnosis.

5.3.2 SPR-based collagen binding studies

SPR-based binding studies allow the determination of not only affinity (K_D), but also kinetics, such as k_a and k_d. Measurements of the binding affinity under flow conditions also assures shear, reflecting more closely the *in vivo* situation in flowing blood, even though blood cells are not present during the experimental procedure. SPR binding studies were performed using immobilised pepsin digested collagen type III and perfusion of different VWF preparations at 20 µL/min, corresponding to a shear rate of 1,650 s^{-1} in the Biacore 2000 instrument. The manufacturer provides a most serviceable website to introduce the instrument, experimental design, analyses and interpretation of the results [http://www.sprpages.nl].

For kinetic measurements of ligand-analyte interactions, low-density surface coverage of the ligand is recommended. This minimises the so-called mass transport effect, which limits the binding kinetic of the analyte, and consequently results in incorrect binding parameters. The chosen ligand densities resulted in R_{max} of 10 - 22 RU, slightly below the recommended experimental conditions of 50 - 100 RU. Mass transfer experiments have not been performed, as it is known that very low ligand density as chosen for the experiments minimise mass transport effects, and therefore can be neglected [Biacore, 2006]. The control of the correlation between experimental data and mathematical model of the VWF collagen interaction yielded low χ^2-values indicating good congruence and appropriate experimental conditions.

Comparison of k_a, k_d, and K_D-values between samples with various multimer sizes after SEC and a Wilate® sample as control was done applying the 1:1 (Langmuir) binding model, or the mathematical model for bivalent analyte. Kinetic data obtained from the measurement using the 1:1 interaction indicated relatively fast complex binding with a celerity of 1.5×10^5 complexes/Ms for the LMW fraction, and around 6×10^5 1/Ms for the HMW fraction (typical range $1 \times 10^3 - 5 \times 10^7$ 1/Ms), whereas the Mix sample showed the fastest k_a with about 8×10^5 1/Ms. The complexes were quite stable with k_d-values of around 1.5×10^{-3} 1/s for the LMW, HMW and Mix fraction (typical range 1×10^{-1}- 5×10^{-6} 1/s), whereas the control- as well as the IMW sample exhibited slightly higher stability with around 5 - 8×10^{-4} complex decays per second. Previous SRP studies reported k_a-values of around 3×10^5 1/Ms and k_d-values between 3 - 5×10^{-4} 1/s [Li *et al.*, 2002; Bonnefoy *et al*,

2006] for the same interaction, whereas these studies were performed with flow rates of 10 and 30 µl/min, respectively.

Calculated equilibrium dissociation constants using the 1:1 binding model were very low, ranging from 11.3 nM for the LMW fraction to 2 - 3 nM for all other samples indicating high affinity. These values correspond well to previous SRP binding studies reporting K_D-values of 1 - 3 nM for the binding of VWF to collagen type III [Van der Plas *et al.*, 2000; Li *et al.*, 2002; Romijn *et al.*, 2003; Bonnefoy *et al.*, 2006]. The higher K_D-value for the LMW fraction suggests a somewhat lower collagen binding affinity of VWF multimers smaller than four, also corresponding to results seen in the flow-chamber system exhibiting a diminished platelet adhesion using this sample.

Binding curves were analysed with the mathematical model for bivalent analyte resulting in a much better correlation. Obtained association and dissociation rate constants were higher for the first interaction resulting in K_D1-values between 12.1 - 48.7 nM for the Wilate® sample and LMW and HMW fractions, respectively, whereas the values of around 7 nM were obtained for the IMW and Mix samples, indicating higher affinity. For the second interaction, equilibrium dissociation rate constants of 2.5×10^{-4} M for the Wilate® sample and between $3 - 9.5 \times 10^{-5}$ M for the SEC fractions were calculated, whereas the K_D2-value for the Mix fraction was only 3×10^{-2} M. These results indicate affinities in the range of cell adhesion molecules or major histocampatibility complex (MHC) - T-cell interactions for the second binding of the analyte.

Comparing association and dissociation rates of LMW, IMW and HMW VWF multimer fractions among each other, both mathematical models result in the same tendency: with a decrease in VWF molecular mass the association rate decreased, whereas the difference between LMW and IMW was not very distinct, but HMW showed much higher k_a-values than LMW and IMW VWF multimers. Regarding the dissociation rates, the lowest value (slowest dissociation) was represented by the IMW VWF multimer fraction. The HMW VWF multimer fraction showed the highest k_d-value. These results suggest that the HMW VWF multimers are binding very fast to collagen type III, but build unstable complexes. The IMW multimers and LMW bind comparable fast to collagen, but with much lower affinity than the HMW VWF multimers, however, forming more stable complexes.

Albeit analysis of VWF-collagen binding kinetics under flow using SPR is very attractive, several aspects must be taken into account interpreting results obtained using these mathematical models. First of all, consideration of the interacting partners' MW is essential for SPR-based determination of binding parameters. In SPR, the measurements depend on changes in the refractive index on the surface of the sensor chip upon binding, and the signal response is proportional to the surface mass. Therefore, binding of larger multimers most probably causes a higher change in the refractive index than binding of smaller VWF multimers.

Furthermore, the measurement region using SPR comprises a range of 300 nm from the sensor surface. Considering the thickness of the dextran matrix with about 100 nm, and a collagen type III layer exhibiting an overall size of below 5 nm referring to the AFM measurements of the coated flow-chamber, and a globular size of VWF between 200 - 300 nm, binding of very HMW VWF multimers might result in a less intense signal than smaller multimers, because according to their size they possibly are out of the evanescent wave region. This is not likely for the samples used in this SPR experiments, but should be taken into account for samples containing ultra-large VWF multimers, e.g. platelet- or recombinant VWF, or VWF isolated from patients with TTP.

In addition, evaluation of the binding curves using the model based on a 1:1 interaction, binding of VWF multimers of different molecular weight – exhibiting a different number of collagen binding sites in one molecule – does not correspond to the prerequisites of the evaluation model, since the software calculates the binding parameters based on the molar concentration of the injected analyte. For this reason, all studies investigating VWF-collagen interaction used the MW of the VWF monomer for calculation of the binding parameters. However, it is not known, whether all collagen-binding sites are available in VWF multimers of different MW, or whether all collagen-binding sites exhibit the same affinity towards collagen. Theoretically, calculation of the VWF concentration using the calculated average molecular mass of multimers present in the SEC fractions instead of the MW of the VWF monomer referring to densitometric quantification would result in a 5-fold lower concentration of the LMW sample, 8-fold lower concentration of IMW sample and 12-fold lower concentration of HMW sample. This would yield higher association rates, and – since dissociation rate does not depend on analyte concentration and the dissociation affinity

constant is a ratio of k_a to k_d – the K_D-values would be appropriately lower, indicating stronger affinity.

Analysis of the data using the mathematical model for bivalent analyte resulted in a better correlation between obtained data and mathematical simulation, but does not necessarily mimic the *in vivo* situation more closely, because presumably vessel wall collagen as well as the multimeric VWF exhibits multivalent binding properties. Interestingly, examining the obtained binding curves especially for high VWF concentrations, association curves exhibited a small bend after reaching nearly equilibrium binding. This effect is probably attributed to VWF self-association. Interaction between VWF was described for higher concentrations of VWF (above 50 µg/mL corresponding to 5 IU/mL) perfused over a VWF-coated slide at high shear rates, leading to the formation of a filamentous network [Barg *et al.*, 2007; Schneider *et al.*, 2007]. Considering these results, the application of the mathematical model for the bivalent analyte possibly reflects (i) high affinity interaction between VWF and collagen, and (ii) weaker self-association of VWF perfused over the chip surface with high concentrations up to around 10 IU/mL. However, it cannot be excluded that the curve bends might reflect the unfolding of collagen-bound VWF with allocation of further binding sites for collagen binding.

Moreover, the source and quality of the immobilised collagen type III may result in different binding constants, and it is also possible that the determination of the VWF concentration using the VWF:Ag ELISA does produce results dependent on the VWF multimeric distribution of an analysed sample. Overall, measuring the affinity between collagen type III and VWF under flow using SPR allows relative comparison of VWF samples, but interpretation of the absolute affinity and kinetic data has to consider the multimeric distribution of the analysed sample as well as the complexity of the multivalent protein-protein interaction.

6 Summary

The von Willebrand factor (VWF) is the critical determinant of thrombus formation in flowing blood. The multimeric glycoprotein present in human plasma as a series of multimers, containing a variable number of subunits with sizes of 500 to >10,000 kDa, is required for platelet recruitment to injured vessel walls at physiological high arterial shear rates. Binding of VWF to exposed structures of the subendothelium results in platelet tethering, activation and finally adhesion. Furthermore, VWF functions as a carrier for coagulation factor VIII (FVIII) protecting it from rapid proteolytic inactivation. VWF deficiency results in the most common inherited bleeding disorder, the von Willebrand disease (VWD). VWD patients suffer from mild to severe bleeding, and – depending on the severity of haemorrhages – require normalisation of plasma VWF and FVIII levels via VWF/FVIII concentrates.

Currently, VWF activity assays are performed under static or low shear rate conditions, albeit *in vivo* VWF exhibits its function primarily above a critical shear rate of >1,000 s^{-1}. The presented work describes the establishment of an *in vitro* flow-chamber system to investigate VWF-mediated platelet adhesion under defined shear rate conditions present in circulation. The device is extensively characterised with respect to coating, choice of collagen, VWF-collagen binding and exposition of binding domains responsible for platelet interaction, as well as mediation of platelet recruitment under flow, whereas the established model allows the investigation of platelet adhesion solely depending on the presence of VWF.

Results suggest the contribution of all VWF multimers to platelet adhesion on collagen due to binding of low- as well as high molecular weight VWF multimers at all shear rates investigated. Platelet binding domains co-localised to the VWF molecule were exposed to a similar extent. Implementation of the flow-chamber model to compare five commercially available VWF-containing concentrates showed effective platelet recruitment for all concentrates tested, but revealed significant differences in the degree of platelet adhesion, which did not correlate with the VWF multimer distribution of the applied sample.

Fractionation of VWF into different sized multimers and investigation of collagen-binding kinetics using surface plasmon resonance as well as their ability to mediate platelet

adhesion under flow revealed a dimished capability for multimers below four, but a comparable activity of intermediate- and high molecular weight multimers.

In conclusion, the established flow-chamber system provides a promising tool for the investigation of VWF function under defined shear rate conditions. Subsequent studies investigating the impact of VWF triplet structure as well as the implementation of the system to study VWD variants will show the contribution of the developed flow device to a possible use in classification of VWD and quality control of VWF-containing concentrates.

7 Zusammenfassung

Der von Willebrand-Faktor (vWF) ist ein Plasmaglykoprotein, das essentiell an der Blutgerinnung beteiligt ist, und im Blutplasma in globulärer Konformation aus unterschiedlich großen Multimeren mit Molekulargewichten zwischen 500 und >10.000 kDa zirkuliert. Neben der Initiation der primären Hämostase bei arteriellen Scherraten durch Bindung an exponierte Strukturen des Gefäßendothels, schützt er den Blutgerinnungsfaktor VIII (FVIII) durch Komplexbildung vor Inaktivierung und Abbau. Liegt eine Gefäßverletzung vor, bindet der vWF an subendotheliale Matrixproteine, wodurch die Affinität zwischen Thrombozyten und vWF induziert wird. Dies führt über die Bindung an Oberflächenrezeptoren der Thrombozyten zur Plättchenadhäsion. Mangel an vWF bzw. eine fehlerhafte Synthese des Proteins verursachen die häufigste erblichen Blutungskrankheit, das von Willebrand-Syndrom (vWS). Schwere Formen der Krankheit müssen durch Substitutionstherapie mit VWF/FVIII-Kombinationspräparaten behandelt werden.

Derzeit wird die Aktivität des vWFs durch Tests unter statischen Bedingungen bzw. bei sehr geringen Scherraten bestimmt, wobei die Funktionsfähigkeit des vWFs *in vivo* erst bei Scherraten >1.000 s^{-1} essenziell ist. Um die vWF-vermittelte Thrombozytenadhäsion unter definierten Strömungsbedingungen zu untersuchen, wurde ein *in vitro* Flusskammersystem entwickelt. Eine ausführliche Charakterisierung erfolgte im Hinblick auf Beschichtung, Wahl des Kollagens, vWF-Kollagen-Bindung und Verfügbarkeit der für die Rezeptorbindung zu Thrombozyten verantwortlichen Bindungsdomänen. Das etablierte Modell ermöglicht die Untersuchung der Thrombozytenadhäsion ausschließlich in Abhängigkeit des vWFs, wobei der zeitliche Verlauf direkt unter dem Mikroskop verfolgt werden kann.

Die Ergebnisse deuten darauf hin, dass alle vWF-Multimere an der Vermittlung der Thrombozytenadhäsion beteiligt sind. Der Einsatz des entwickelten Flusskamermodells für den Vergleich von fünf VWF/FVIII-Präparaten zeigte für alle Produkte eine effektive Thrombozytenadhäsion bei hohen Scherraten, wobei der Grad der Adhäsion stark variierte. Die beobachteten Unterschiede korrellierten dabei allerdings nicht mit der vWF-Multimerenverteilung der Präparate. Eine Trennung in Fraktionen mit unterschiedlich großen Multimeren zeigte, dass vWF-Fraktionen mit Multimeren kleiner vier im Vergleich zu Franktionen, die mittlere und hohe vWF-Multimere enthielten, eine verminderte Kollagen-

Bindung in der Oberflächenplasmonresonanz sowie eine geringere Thrombozytenadhäsion unter hohen Flussraten aufwiesen.

Das etablierte Flusskammermodell stellt ein viel versprechendes Instrument zur Analyse der vWF-Funktion unter definierten Scherraten dar. Weiterführende Untersuchungen zum Einfluss der vWF-Triplettstruktur auf die Funktion des Proteins sowie der Einsatz für Studien an vWS-Subtypen werden zeigen, ob das entwickelte System einen Beitrag zur vWS-Diagnostik und Qualitätskontrolle von vWF/FVIII-Präparaten leisten kann.

8 Bibliography

Arya M, Anvari B, Romo G, Cruz M, Dong J, McIntre L, Moake J, López J. Ultralarge multimers of von Willebrand factor form spontaneous high strength bonds with the platelet glycoprotein Ib-IX complex: studies using optical tweezers. *Blood.* 2002; **99:** 3971-3977

Barg A, Ossig R, Goerge T, Schneider MF, Schillers H, Oberleithner H, Schneider SW. Soluble plasma-derived von Willebrand factor assembles to a haemostatically active filamentous network. *Thromb Haemost.* 2007; **97:** 514-526

Baumgartner HR, Haudenschild C. Adhesion of platelets to subendothelium. *Ann NY Acad Sci*. 1972; **201**: 22-36

Baumgartner HR. The role of blood flow in platelet adhesion, fibrin deposition, and formation of mural thrombi. *Microvasc Res.* 1973; **5:** 167-179

Baumgartner HR, Muggli R, Tschopp TB, Turitto VT. Platelet adhesion, release and aggregation in flowing blood: effects of surface properties and platelet function. *Thromb Haemost.* 1976; **35:** 124-138

Bernardo A, Bergeron AL, Sun CW, Guchhait P, Cruz MA, López JA, Dong JF. Von Willebrand factor present in fibrillar collagen enhances platelet adhesion to collagen and collagen-induced platelet aggregation. *J Thromb Haemost.* 2004; **2:** 660-669

Bonnefoy A, Yamamoto H, Thys C, Kito M, Vermylen J, Hoylaerts MF. Shielding the front-strand beta 3 of the von Willebrand factor A1 domain inhibits its binding to platelet glycoprotein Ibα. *Blood.* 2003; **10:** 1375-1383

Bonnefoy A, Romijn RA, Vandervoort PA, VAN Rompaey I, Vermylen J, Hoylaerts MF. Von Willebrand factor A1 domain can adequately substitute for A3 domain in recruitment of flowing platelets to collagen. *J Thromb Haemost.* 2006; **4:** 2151-2161

Bradford MM. A rapid and sensitive method for the quantification of microgram quantities of protein utilizing the principle of protein-dye binding. *Anal Biochem.* 1976; **72:** 341-347

Brown JE, Bosak JO. An ELISA test for the binding of von Willebrand antigen to collagen. *Thromb Res.* 1986; **43:** 303–311

Brown SA, Collins PW, Bowen DJ. Heterogeneous detection of A-antigen on von Willebrand factor derived from platelets, endothelial cells and plasma. *Thromb Haemost.* 2002; **87:** 990-996.

Budde U, Schneppenheim R, Plendl H, Ruggeri ZM, Zimmerman TS. Luminographic detection of von Willebrand factor multimers in agarose gels and on nitrocellulose membranes. *Thromb Haemost.* 1990; **63:** 312-315

Budde U, Scharf RE, Franke P, Hartmann-Budde K, Dent J, Ruggeri ZM. Elevated platelet count as a cause of abnormal von Willebrand factor multimer distribution in plasma. *Blood.* 1993; **82:** 1749-1757

Budde U, Drewke E. Von Willebrand factor multimers in virus-inactivated plasmas and FVIII concentrates. *Beitr Infusionsther Transfusionsmed.* 1994; **32:** 408-414

Budde U, Drewke E, Mainusch K, Schneppenheim R. Laboratory diagnosis of congenital von Willebrand disease. *Semin Thromb Hemost.* 2002; **28:** 173-190

Budde U, Metzner HJ, Müller HG. Comparative analysis and classification of von Willebrand factor/factor VIII concentrates: impact on treatment of patients with von Willebrand disease. *Semin Thromb Hemost.* 2006; **32:** 626-635 (1)

Budde U, Pieconka A, Will K, Schneppenheim R. Laboratory testing for von Willebrand disease: contribution of multimer analysis to diagnosis and classification. *Semin Thromb Hemost.* 2006; **32:** 514-521 (2)

Budde U. Diagnosis of von Willebrand disease subtypes: implications for treatment. *Haemophilia.* 2008; **14 Suppl 5:** 27-38

Carew JA, Browning PJ, Lynch DC. Sulfation of von Willebrand factor. *Blood.* 1990; **76:** 2530-2539

Cejas MA, Kinney WA, Chen C, Vinter JG, Almond HR Jr, Balss KM, Maryanoff CA, Schmidt U, Breslav M, Mahan A, Lacy E, Maryanoff BE. Thrombogenic collagen-mimetic peptides: self-assembly of triple helix-based fibrils driven by hydrophobic interactions. *Proc Natl Acad Sci.* 2008; **105:** 8513-8518

Chand S, McCraw A, Hutton R, Tuddenham EG, Goodall AH. A two-site, monoclonal antibody-based immunoassay for von Willebrand factor – demonstration that VWF function resides in a conformational epitope. *Thromb Haemost.* 1986; **55:** 318-324

Cox Gill J. Diagnosis and treatment of von Willebrand disease. *Hematol Oncol Clin N Am.* 2004; **18**: 1277-1299

Dasgupta S, Repesse J, Bayry J, Navarrete A, Wootla B, Delignat S, Irinopoulou T, Kamate C, Saint-Remy J, Jacquemin M, Lenting P, Borel-Derlon A, Kaveri S, Lacroix-Desmazes S. VWF protects FVIII from endocytosis by dendritic cells and subsequent presentation to immune effectors. *Blood.* 2007; **109:** 610-612

Denis C, Baruch D, Kielty CM, Ajzenberg N, Christophe O, Meyer D. Localization of von Willebrand factor binding domains to endothelial extracellular matrix and to type VI collagen. *Arterioscler Thromb.* 1993; **13:** 398-406

Denis CV, Christophe OD, Oortwijn BD, Lenting PJ. Clearance of von Willebrand factor. *Thromb Haemost.* 2008; **99:** 271-278

Dent JA, Galbusera M, Ruggeri ZM. Heterogeneity of plasma von Willebrand factor multimers resulting from proteolysis of the constituent subunit. *J Clin Invest.* 1991; **88:** 774-782

Dong JF, Moake JL, Nolasco L, Bernardo A, Arceneaux W, Shrimpton CN, Schade AJ, McIntire LV, Fujikawa K, López JA. ADAMTS-13 rapidly cleaves newly secreted ultralarge von Willebrand factor multimers on the endothelial surface under flowing conditions. *Blood.* 2002; **100:** 4033-4039

Dong J-F. Cleavage of ultra-large von Willebrand factor by ADAMTS-13 under flow conditions. *J Thromb Haemost*. 2005; **3:** 1710-1716

Ellies LG, Ditto D, Levy GG, Wahrenbrock M, Ginsburg D, Varki A, Le DT, Marth JD. Sialyltransferase ST3Gal-IV operates as a dominant modifier of hemostasis by concealing asialoglycoprotein receptor ligands. *Proc Natl Acad Sci USA.* 2002; **99:** 10042-10047

Fang H, Wang L, Wang H. The protein structure and effect of factor VIII. *Thromb Res.* 2007; **119:** 1-13

Farndale RW, Lisman T, Bihan D, Hamaia S, Smerling CS, Pugh N, Konitsiotis A, Leitinger B, de Groot PG, Jarvis GE, Raynal N. Cell-collagen interactions: the use of peptide toolkits to investigate collagen-receptor interactions. *Biochem Soc Trans.* 2008; **36:** 241-250

Favaloro E. Collagen binding assay for von Willebrand factor (VWF:CBA): Detection of von Willebrands disease (VWD), and discrimination of VWD subtypes, depends on collagen source. *Thromb Haemost.* 2000; **83:** 127–135

Favaloro EJ. An update on the von Willebrand factor collagen binding assay: 21 years of age and beyond adolescence but not yet a mature adult. *Semin Thromb Hemost.* 2007; **33:** 727-744

Federici AB. Management of von Willebrand disease with factor VIII/von Willebrand factor concentrates: results from current studies and surveys. *Blood Coagul Fibrinolysis.* 2005; **16 Suppl 1:** S17-21

Fischer BE, Thomas KB, Dorner F. Von Willebrand factor: measuring its antigen or function? Correlation between the level of antigen, activity, and multimer size using various detection systems. *Thromb Res.* 1998; **91:** 39-43 (1)

Fischer BE, Thomas KB, Schlokat U, Dorner F. Triplet structure of human von Willebrand factor. *Biochem J.* 1998; **331:** 483-488 (2)

Fischer BE, Thomas KB, Schlokat U, Dorner F. Selectivity of von Willebrand factor triplet bands towards heparin binding supports structural model. *Eur J Haematol.* 1999; **62:** 169-173

Fowler EW, Fretto LJ, Hamilton KK, Erickson HP, McKee PA. Substructure of human von Willebrand factor. *J Clin Invest.* 1985; **76:** 1491-1500

Furlan M, Robles R, Affolter D, Meyer D, Baillod P, Lämmle B. Triplet structure of von Willebrand factor reflects proteolytic degradation of high molecular weight multimers. *Proc Natl Acad Sci USA.* 1993; **90:** 7503-7507

Furlan M, Lämmle B. Assays of von Willebrand factor-cleaving protease: a test for diagnosis of familial and acquired thrombotic thrombocytopenic purpura. *Semin Thromb Hemost.* 2002; **28:** 167-172

Godall AH, Jarvis J, Chand S, Rawlings E, O'Brien DP, McGraw A, Hutton R, Tuddenham EGD. An immunoradiometric assay for human factor VIII/von Willebrand factor (VIII:vWF) using a monoclonal antibody that defines a functional epitope. *B J Haemat.* 1985; **59:** 565-577

Goto S, Salomon DR, Ikeda Y, Ruggeri ZM. Characterization of the unique mechanism mediating the shear-dependent binding of soluble von Willebrand factor to platelets. *J Biol Chem.* 1995; **270:** 23352-23361

Gutierrez E, Petrich BG, Shattil SJ, Ginsberg MH, Groisman A, Kasirer-Friede A. Microfluidic devices for studies of shear-dependent platelet adhesion. *Lab Chip.* 2008; **8:** 1486-1495

Howard MA, Firkin BG. Ristocetin – a new tool in the investigation of platelet aggregation. *Thromb Diath Haemorrh.* 1971; **26:** 362-369

Hoylaerts MF. Platelet-vessel wall interactions in thrombosis and restenosis role of von Willebrand factor. *Verh K Acad Geneeskd Belg.* 1997; **59:** 161-183

Ingerslev J, Hvitfeldt Poulsen L, Sorensen B. Current treatment of von Willebrand's disease. *Haemostaseol.* 2004; **24**: 56-64

Inoue O, Suzuki-Inoue K, Ozaki Y. Redundant mechanism of platelet adhesion to laminin and collagen under flow: involvement of von Willebrand factor and glycoprotein Ib-IX-V. *J Biol Chem.* 2008; **283:** 16279-16282

Jenkins PV, O'Donnell JS. ABO blood group determines plasma von Willebrand factor levels: a biologic function after all? *Transfusion.* 2006; **46:** 1836-1844

Jönsson U, Fägerstam L, Ivarsson B, Johnsson B, Karlsson R, Lundh K, Löfås S, Persson B, Roos H, Rönnberg I, Sjölander S, Stenberg E, Ståhlberg R, Urbaniczky C, Östlin H, Malmquist M. Real-time biospecific interaction analysis using surface plasmon resonance and a sensor chip technology. *Biotechniques.* 1991; **11:** 620-627

Kang I, Raghavachari M, Hofmann CM, Marchant RE. Surface-dependent expression in the platelet GPIb binding domain within human von Willebrand factor studied by atomic force microscopy. *Thromb Res.* 2007; **6:** 731-740

Karlsson R, Michaelsson A, Mattsson L. Kinetic analysis of monoclonal antibody-antigen interactions with a new biosensor based analytical system. *J Immunol Methods.* 1991; **145:** 229-240

Karlsson R. Real-time competitive kinetic analysis of interactions between low-molecular-weight ligands in solution and surface-immobilized receptors. *Anal Biochem.* 1994; **221:** 142-151

Kaufman RJ. Post-translational modifications required for coagulation factor secretion and function. *Thromb Haemost.* 1998; **79:** 1068-1079

Kehrel B. Platelet-collagen interactions. *Semin Thromb Hemost.* 1995; **21:** 123-129

Kessler CM. Diagnosis and treatment of von Willebrand disease: new perspectives and nuances. *Haemophilia*. 2007; **13:** 3-14

Lacroix-Desmazes S, Repessé Y, Kaveri SV, Dasgupta S. The role of VWF in the immunogenicity of FVIII. *Thromb Res.* 2008; **122 Suppl 2:** S3-6

Lankhof H, Damas C, Schiphorst ME, Schiphorst ME, IJsseldijk MJ, Bracke M, Sixma JJ, Vink T, de Groot PG. Functional studies on platelet adhesion with recombinant von Willebrand factor type 2B mutants R543Q and R543W under conditions of flow. *Blood.* 1997; **89:** 2766-2772

Lenting PJ, Van Schooten CJ, Denis CV. Clearance mechanisms of von Willebrand factor and factor VIII. *J Thromb Haemost.* 2007; **5:** 1353-1360

Leytin V, Mody M, Semple JW, Garvey B, Freedman J. Flow Cytometric Parameters for characterizing platelet activation by measuring P-Selectin (CD62P) expression: theoretical consideration and evaluation in thrombin-treated platelet populations. *Biochem Biophys Res Commun.* 2000; **269:** 85-90.

Leytin V, Allen DJ, Mody M, Rand ML, Hannach B, Garvey B, Freedman J. A rabbit model for monitoring in vivo viability of human platelet concentrates using flow cytometry. *Transfusion.* 2002; **42:** 711-718.

Li F, Moake JL, McIntire LV. Characterization of von Willebrand factor interaction with collagens in real time using surface plasmon resonance. *Ann Biomed Eng.* 2002; **30:** 1107-1116

Lillicrap D. Von Willebrand disease – Phenotype versus genotype: Deficiency versus disease. *Thromb Res.* 2007; **120:** S11-16

Lisman T, Raynal N, Groeneveld D, Maddox B, Peachey AR, Huizinga EG, De Groot PG, Farndale RW. A single high-affinity binding site for von Willebrand factor in collagen III, identified using synthetic triple-helical peptides. *Blood.* 2006; **108:** 3753-3756

Lisman T, Farndale RW, De Groot PG. A mechanism to safeguard platelet adhesion under high-shear flow: von Willebrand factor-glycoprotein Ib and integrin alpha2beta1-collagen interactions make complementary, collagen-type-specific contributions to adhesion: a rebuttal. *J Thromb Haemost.* 2007; **5:** 1338-1339

Mannucci PM. How I treat patients with von Willebrand disease. *Blood.* 2001; **97**:1915-1919

Mannuccio PM, Lattuada A, Ruggeri ZM. Proteolysis of von Willebrand factor in therapeutic plasma concentrates. *Blood.* 1994; **83:** 3018-3027

Marti T, Rösselet SJ, Titani K, Walsh KA. Identification of disulfide-bridged substructures within human von Willebrand factor. *Biochemistry.* 1987; **26:** 8099-8109

Matsui T, Titani K, Mizuochi T. Structures of the asparagine-linked oligosaccharide chains of human von Willebrand factor. Occurrence of blood group A, B, and H(O) structures. *J Biol Chem.* 1992; **267:** 8723-8731

Matsui T, Fujimura Y, Nishida S, Titani K. Human plasma alpha 2-macroglobulin and von Willebrand factor possess covalently linked ABO(H) blood group antigens in subjects with corresponding ABO phenotype. *Blood.* 1993; **82:** 663-668

Matsui T, Shimoyama T, Matsumoto M, Fujimura Y, Takemoto Y, Sako M, Hamako J, Titani K. ABO blood group antigens on human plasma von Willebrand factor after ABO-mismatched bone marrow transplantation. *Blood.* 1999; **94:** 2895-2900

Matsushita T, Dong Z, Sadler JE. Von Willebrand's factor and von Willebrand's disease. *Curr Opin Hematol.* 1994; **1:** 362-368

Mazurier C. Composition, quality control, and labelling of plasma-derived products for the treatment of von Willebrand disease. *Semin Thromb Hemost* 2006; **32**: 529-536

McMullen BA, Fujikawa K, Davie EW. Location of the disulfide bonds in human plasma prekallikrein: the presence of four novel apple domains in the amino-terminal portion of the molecule. *Biochemistry.* 1991; **30:** 2050-2056

Meyer D, Piétu G, Fressinaud E, Girma JP. Von Willebrand factor: structure and function. *Mayo Clin Proc.* 1991; **66:** 516-523

Michiels JJ, Budde U, van der Planken M, van Vliet HH, Schroyens W, Berneman Z. Acquired von Willebrand syndromes: clinical features, aetiology, pathophysiology, classification and management. *Best Pract Res Clin Haematol.* 2001; **14:** 401-436

Michiels JJ, Berneman Z, Gadisseur A, van der Planken M, Schroyens W, van de Velde A, van Vliet H. Classification and characterization of hereditary types 2A, 2B, 2C, 2D, 2E, 2M, 2N, and 2U (unclassifiable) von Willebrand disease. *Clin Appl Thromb Hemost.* 2006; **12:** 397-420

Millar CM, Brown SA. Oligosaccharide structures of von Willebrand factor and their potential role in von Willebrand disease. *Blood.* 2006; **20:** 83-92

Morell AG, Gregoriadis G, Scheinberg IH, Hickman J, Ashwell G. The role of sialic acid in determining the survival of glycoproteins in the circulation. *J Biol Chem.* 1971; **246:** 1461-1467

Moroi M, Jung SM, Shinmyozu K, Tomiyama Y, Ordinas A, Diaz-Ricart M. Analysis of platelet adhesion to a collagen-coated surface under flow conditions: the involvement of glycoprotein VI in the platelet adhesion. *Blood.* 1996; **88:** 2081-2092

Moroi M, Jung SM, Nomura S, Sekiguchi S, Ordinas A, Diaz-Ricart M. Analysis of the involvement of the von Willebrand factor-glycoprotein Ib interaction in platelet adhesion to a collagen-coated surface under flow conditions. *Blood.* 1997; **90:** 4413-4424

Moroi M, Jung S. A mechanism to safeguard platelet adhesion under high shear flow: von Willebrand factor–glycoprotein Ib and integrin α2β1–collagen interactions make complementary, collagen-type-specific contributions to adhesion. *J Thromb Haemost.* 2007; **5:** 797-803

Moroi M, Jung SM. A mechanism to safeguard platelet adhesion under high-shear flow: von Willebrand factor-glycoprotein Ib and integrin α2β1-collagen interactions make complementary, collagen-type-specific contributions to adhesion: reply to a rebuttal. *J Thromb Haemost.* 2007; **5:** 1340-1342

Murdock PJ, Woodhams BJ, Matthews KB, Pasi KJ, Goodall AH. Von Willebrand factor activity detected in a monoclonal antibody-bases ELISA: an alternative to the ristocetin cofactor platelet agglutination assay for diagnostic use. *Thromb Haemost.* 1997; **78:** 1272-1277

Neugebauer BM, Goy C, Budek I, Seitz R. Comparison of two von Willebrand factor collagen-binding assays with different binding affinities for low, medium, and high multimers of von Willebrand factor. *Semin Thromb Hemost.* 2002; **28:** 139-148

O'Donnell J, Laffan MA. The relationship between ABO histo-blood group, factor VIII and von Willebrand factor. *Transfus Med.* 2001; **11:** 343-351

Ohmori K, Fretto LJ, Harrison RL, Switzer ME, Erickson HP, McKee PA. Electron microscopy of human factor VIII/Von Willebrand glycoprotein: effect of reducing reagents on structure and function. *J Cell Biol.* 1982; **95:** 632-640

Pareti FI, Niiya K, McPherson JM, Ruggeri ZM. Isolation and characterization of two domains of human von Willebrand factor that interact with fibrillar collagen types I and III. *J Biol Chem.* 1987; **262:** 13835-13841

Pasi KJ, Collins PW, Keeling DM, Brown SA, Cumming AM, Dolan GC, Hay CR, Hill FG, Laffan M, Peake IR. Management of von Willebrand disease: a guideline from the UK Haemophilia Centre Doctor's Organisation. *Haemophilia.* 2004; **10**: 218-231

Peake I, Goodeve A. Type 1 von Willebrand disease. *J Thromb Haemost.* 2007; **5 Suppl 1:** 7-11

Raynal N, Hamaia SW, Siljander PR-M, Maddox B, Peachey AR, Fernandez R, Foley LJ, Slatter DA, Jarvis GE, Farndale RW. Use of synthetic peptides to locate novel integrin $\alpha_2\beta_1$-binding motifs in human collagen III. *J Biol Chem.* 2006; **281:** 3821-3831

Read MS, Smith SV, Lamb MA, Brinkhous KM. Role of botrocetin in platelet agglutination: formation of an activated complex of botrocetin and von Willebrand factor. *Blood.* 1989; **74:** 1031-1035

Refaai MA, Van Cott EM, Lukoszyk M, Hughes J, Eby CS. Loss of factor VIII and von Willebrand factor activities during cold storage of whole blood is reversed by rewarming. *Lab Hematol.* 2006; **12:** 99-102

Reininger AJ, Heijnen HF, Schumann H, Specht HM, Schramm W, Ruggeri ZM. Mechanism of platelet adhesion to von Willebrand factor and microparticle formation under high shear stress. *Blood.* 2006; **107:** 3537-3545

Remijn JA, Wu YP, Ijsseldijk MJ, Zwaginga JJ, Sixma JJ, de Groot PG. Absence of fibrinogen in afibrinogenemia results in large but loosely packed thrombi under flow conditions. *Thromb Haemost.* 2001; **85:** 736-742

Reverter JC, Escolar G, Sanz C, Cases A, Villamor N, Niewenhuis HK, Lopes J, Ordinas A. Platelet activation during hemodialysis measured through exposure of p-selectin: Analysis by flow cytometry and ultrastructural techniques. *J Lab Clin Med.* 1994; **124:** 79–85

Romijn RA, Westein E, Bouma B, Schiphorst ME, Sixma JJ, Lenting PJ, Huizinga EG. Mapping the collagen-binding site in the von Willebrand factor-A3 domain. *J Biol Chem.* 2003; **278:** 15035-15039

Roth GJ, Titani K, Hoyer LW, Hickey MJ. Localization of binding sites within human von Willebrand factor for monomeric type III collagen. *Biochemistry.* 1986; **25:** 8357-61

Ruggeri ZM, Ware J. Von Willebrand factor. *FASEB J.* 1993; **7:** 308-316

Ruggeri ZM. Platelets in atherothrombosis. *Nat Med*. 2002; **8:** 1227-1234

Ruggeri ZM. Platelet and von Willebrand factor interactions at the vessel wall. *Hamostaseologie.* 2004; **24:** 1-11

Ruggeri ZM. Platelet interactions with the vessel wall components during thrombogenesis. *Blood Cells Mol Dis.* 2006; **36:** 145-147

Ruggeri ZM. Von Willebrand factor: Looking back and looking forward. *Thromb Haemost.* 2007; **98:** 55-62

Sadler JE. Von Willebrand factor. *J Biol Chem.* 1991; **266:** 22777-22780

Sadler JE. A revised classification of von Willebrand disease. *Thromb Haemost.* 1994; **71**: 520-525

Sadler JE. Biochemistry and genetics of von Willebrand factor. *Annu Rev Biochem.* 1998; **67:** 395-424

Sadler JE, Budde U, Eikenboom JC, Favaloro EJ, Hill FG, Holmberg L, Ingerslev J, Lee CA, Lillicrap D, Mannucci PM, Mazurier C, Meyer D, Nichols WL, Nishino M, Peake IR, Rodeghiero F, Schneppenheim R, Ruggeri ZM, Srivastava A, Montgomery RR, Federici AB; Working Party on von Willebrand Disease Classification. Update on the pathophysiology and classification of von Willebrand disease: a report of the sub-committee on von Willebrand factor. *J Thromb Haemost.* 2006; **4:** 2103-2114

Sadler JE. Von Willebrand factor, ADAMTS13, and thrombotic thrombocytopenic purpura. *Blood.* 2008; **112:** 11-18

Saelman EU, Nieuwenhuis HK, Hese KM, de Groot PG, Heijnen HF, Sage EH, Williams S, McKeown L, Gralnick HR, Sixma JJ. Platelet adhesion to collagen types I through VIII under conditions of stasis and flow is mediated by GPIα (α2β1-integrin). *Blood.* 1993; **83:** 1244-1250

Saenko E, Kannicht C, Loster K, Sarafanov A, Khrenov A, Kouiavskaia D, Shima M, Ananyeva N, Schwinn H, Gruber G, Josic D. Development and applications of surface plasmon resonance-based von Willebrand factor - collagen binding assay. *Anal Biochem.* 2002; **302:** 252-262

Sakariassen KS, Aarts PA, de Groot PG, Houdijk WP, Sixma JJ. A perfusion chamber developed to investigate platelet interaction in flowing blood with human vessel wall cells, their extracellular matrix, and purified components. *J Lab Clin Med.* 1983; **102:** 522-535

Sakariassen KS, Fressinaud E, Girma JP, Baumgartner HR, Meyer D. Mediation of platelet adhesion to fibrillar collagen in flowing blood by a proteolytic fragment of human von Willebrand factor. *Blood.* 1986; **67:** 1515-1518

Sakariassen KS, Turitto VT, Baumgartner HR. Recollections of the development of flow devices for studying mechanisms of hemostasis and thrombosis in flowing whole blood. *J Thromb Haemost.* 2004; **2:** 1681-1690

Samor B, Michalski JC, Mazurier C, Goudemand M, De Waard P, Vliegenthart JF, Strecker G, Montreuil J. Primary structure of the major O-glycosidically linked carbohydrate unit of human von Willebrand factor. *Glycoconj J.* 1989; **6:** 263-270

Santoro SA. Preferential binding of high molecular weight forms of von Willebrand factor to fibrillar collagen. *Biochim Biophys Acta.* 1983; **756:** 123-126

Savage B, Saldivar E, Ruggeri ZM. Initiation of platelet adhesion by arrest onto fibrinogen or translocation on von Willebrand factor. *Cell.* 1996; **84:** 289-297

Savage B, Almus-Jacobs F, Ruggeri ZM. Specific synergy of multiple substrate-receptor interactions in platelet thrombus formation under flow. *Cell.* 1998; **94:** 657-666

Savage B, Ginsberg MH, Ruggeri ZM. Influence of fibrillar collagen structure on the mechanisms of platelet thrombus formation under flow. *Blood.* 1999; **94:** 2704-2715

Savage B, Sixma JJ, Ruggeri ZM. Functional self-association of von Willebrand factor during platelet adhesion under flow. *Proc Natl Acad Sci USA.* 2002; **99:** 425-430

Schneider SW, Nuschele S, Wixforth A, Gorzelanny C, Alexander-Katz A, Netz RR, Schneider MF. Shear-induced unfolding triggers adhesion of von Willebrand factor fibers. *Proc Natl Acad Sci USA.* 2007; **104:** 7899-7903

Schneppenheim R, Budde U. Phenotypic and genotypic diagnosis of von Willebrand disease: a 2004 update. *Semin Hematol.* 2005; **42:** 15-28

Schneppenheim R. The evolving classification of von Willebrand disease. *Blood Coagul Fibrinolysis.* 2005; **Suppl 1:** S3-10

Siedlecki CA, Lestini BJ, Kottke-Marchant KK, Eppell SJ, Wilson DL, Marchant RE. Shear dependent changes in the three-dimensional structure of human von Willebrand factor. *Blood.* 1996; **88:** 2939-2950

Singh I, Shankaran H, Beauharnois ME, Xiao Z, Alexandridis P, Neelamegham S. Solution structure of human von Willebrand factor studied using small angle neutron scattering. *J Biol Chem.* 2006; **281:** 38266-38275

Sixma JJ, Sakariassen KS, Beeser-Visser NH, Ottenhof-Rovers M, Bolhuis PA. Adhesion of platelets to human artery subendothelium: effect of factor VIII-von Willebrand factor of various multimeric composition. *Blood.* 1984; **63:** 128-139

Sixma JJ, van Zanten GH, Saelman EUM, Verkleij M, Lankhof H, Nieuwenhuis HK, De Groot PG. Platelet adhesion to collagen. *Thromb Haemost*. 1995; **74:** 454-459

Slayter H, Loscalzo J, Bockenstedt P, Handin RI. Native conformation of human von Willebrand protein. Analysis by electron microscopy and quasi - elastic light scattering. *J Biol Chem.* 1985; **260:** 8559-8563

Sodetz JM, Paulson JC, McKee PA. Carbohydrate composition and identification of blood group A, B, and H oligosaccharide structures on human Factor VIII/von Willebrand factor. *J Biol Chem.* 1979; **254:** 10754-10760

Spiegel PC, Murphy P, Stoddard BL. Surface-exposed hemophilic mutations across the FVIII C2 domain have variable effects on stability and binding activities. *J Biol Chem.* 2004; **279:** 53691–53698.

Stadler M, Gruber G, Kannicht C, Biesert L, Radomski KU, Suhartono H, Pock K, Neisser-Svae A, Weinberger J, Römisch J, Svae T-E. Characterisation of a novel high-purity, double virus inactivated von Willebrand factor and factor VIII concentrate (Wilate®). *Biologicals.* 2006; **34:** 281-288

Stroev PV, Hoskins PR, Easson WJ. Distribution of wall shear rate throughout the arterial tree: A case study. *Atherosclerosis.* 2007; **191:** 276-280

Suda Y, Arano A, Fukui Y, Koshida S, Wakao M, Nishimura T, Kusumoto S, Sobel M. Immobilization and clustering of structurally defined oligosaccharides for sugar chips: an improved method for surface plasmon resonance analysis of protein-carbohydrate interactions. *Bioconjug Chem.* 2006; **17:** 1125-1135

Tangelder GJ, Slaaf DW, Arts T, Reneman RS. Wall shear rate in arterioles in vivo: least estimates from platelet velocity profiles. *Am J Physiol.* 1988; **254:** H1059-1064.

Titani K, Kumar S, Takio K, Ericsson LH, Wade RD, Ashida K, Walsh KA, Chopek MW, Sadler JE, Fujikawa K. Amino acid sequence of human von Willebrand factor. *Biochemistry.* 1986; **25:** 3171-3184

Turecek PL, Siekmann J, Schwarz HP. Comparative study on collagen-binding enzyme-linked immunosorbent assay and ristocetin cofactor activity assays for detection of functional activity of von Willebrand factor. *Semin Thromb Hemost.* 2002; **28:** 149-160

Van der Plas RM, Gomes L, Marquart JA, Vink T, Meijers JC, de Groot PG, Sixma JJ, Huizinga EG. Binding of von Willebrand factor to collagen type III: role of specific amino acids in the collagen binding domain of vWF and effects of neighboring domains. *Thromb Haemost.* 2000; **84:** 1005-1011

Van Schooten CJ, Denis CV, Lisman T, Eikenboom JC, Leebeek FW, Goudemand J, Fressinaud E, van den Berg HM, de Groot PG, Lenting PJ. Variations in glycosylation of von Willebrand factor with O-linked sialylated T antigen are associated with its plasma levels. *Blood.* 2007; **109:** 2430-2437

Vanhoorelbeke K, Depraetere H, Romijin RAP, Huizinga EG, De Maeyer M, Deckmyn H. A consensus tetrapeptide selected by phage display adopts the conformation of a dominant discontinuous epitope af a monoclonal anti-VWF antibody that inhibits the von Willebrand factor-collagen interaction. *J Biol Chem.* 2003; **278:** 37815-37821

Vlot AJ, Koppelman SJ, Bouma BN, Sixma JJ. Factor VIII and von Willebrand factor. *Thromb Haemost.* 1998; **79:** 456-465

Vollmar B, Slotta JE, Nickels RM, Wenzel E, Menger MD. Comparative analysis of platelet isolation techniques for the in vivo study of the microcirculation. *Microcirculation.* 2003; **10:** 143-152

Von Willebrand EA. Über hereditäre Pseudohämophilie. *Acta Medica Scandinavica.* 1926; **76:** 521-549

Von Willebrand EA, Jürgens R. Über ein neues vererbbares Blutungsübel: die konstitutionelle Thrombopathie. *Dtsch Arch Klin Med.* 1933; **175:** 453-483

Wagner DD, Mayadas T, Marder VJ. Initial glycosylation and acidic pH in the Golgi apparatus are required for multimerization of von Willebrand factor. *J Cell Biol.* 1986; **102:** 1320-1324

Wagner DD, Saffaripour S, Bonfanti R, Sadler JE, Cramer EM, Chapman B, Mayadas TN. Induction of specific storage organelles by von Willebrand factor propolypeptide. *Cell.* 1991; **64:** 403-413.

Wakao M, Saito A, Ohishi K, Kishimoto Y, Nishimura T, Sobel M, Suda Y. Sugar Chips immobilized with synthetic sulfated disaccharides of heparin/heparan sulfate partial structure. *Bioorg Med Chem Lett.* 2008; **18:** 2499-24504

Walkowiak B, Kesy A, Michalec L. Microplate reader – a convenient tool in studies of blood coagulation. *Thromb Res.* 1997; **87:** 95-103

Watson HG, Greaves M. Can we predict bleeding? *Semin Thromb Hemost.* 2008; **34:** 97-103

Weiss HJ. Abnormalities of factor VIII and platelet aggregation – use of ristocetin in diagnosing the von Willebrand syndrome. *Blood.* 1975; **45:** 403-412

Weiss HJ, Turitto VT, Baumgartner HR. Effect of shear rate on platelet interaction with subendothelium in citrated and native blood. I. Shear rate-dependent decrease of adhesion in von Willebrand's disease and the Bernard-Soulier syndrome. *J Lab Clin Med.* 1978; **92:** 750-764

Wu D, Vanhoorelbeke K, Cauwenberghs N, Meiring M, Depraetere H, Kotze HF, Deckmyn H. Inhibition of the von Willebrand (VWF)-collagen interaction by an antihuman VWF monoclonal antibody results in abolition of in vivo arterial platelet thrombus formation in baboons. *Blood*. 2002; **99:** 3623-3628

Wu YP, van Breugel HH, Lankhof H, Wise RJ, Handin RI, de Groot PG, Sixma JJ. Platelet adhesion to multimeric and dimeric von Willebrand factor and to collagen type III preincubated with von Willebrand factor. *Arterioscler Thromb Vasc Biol.* 1996; **16:** 611-620

Zwaginga JJ, Nash G, King MR, Heemskerk JW, Frojmovic M, Hoylaerts MF, Sakariassen KS; Biorheology Subcommittee of the SSC of the ISTH. Flow-based assays for global assessment of hemostasis. Part 1: Biorheologic considerations. *J Thromb Haemost.* 2006; **4:** 2486-2487; full paper: *J Thromb Haemost*. doi: 10.1111/j.1538-7836.2006.02177.x

Zwaginga JJ, Sakariassen KS, King MR, Diacovo TG, Grabowski EF, Nash G, Hoylaerts M, Heemskerk JW. Can blood flow assays help to identify clinically relevant differences in von Willebrand factor functionality in von Willebrand disease types 1-3? *J Thromb Haemost.* 2007; **5:** 2547-2549.

8.1 Books

Colman RW, Hirsh J, Marder VJ, Clowes AW, George JN: Hemostasis and Thrombosis – Basic principles & clinical practice. 4th ed., Lippincott Williams & Wilkins 2001, ISBN 0-7817-1455-9, Chapter 14: Structure and function of von Willebrand factor. Montgomery RR, p253.

Biacore 2006. Kinetic and affinity analysis with Biacore – Level 1. Biacore AB Uppsala, Sweden.

9 List of abbreviations

AFM	Atomic force microscopy
BSA	Bovine serum albumin
CMFDA	5-chloromethylfluorescein diacetate
DLS	Dynamic light scattering
DTT	Dithiothreitol
EDC	1-ethyl-3-(3-dimethyl-aminopropyl) carbodiimide
EDTA	Ethylenediaminetetraacetic acid
ELISA	Enzyme-linked immunosorbent assay
FACS	Fluorescence activated cell sorting
FITC	Fluorescein isothiocyanate
FPLC	Fast protein liquid chromatography
FVIII	Coagulation factor VIII
FVIII:C	FVIII coagulant activity
GAM	Goat anti-mouse
GAR	Goat anti-rabbit
GP	Glycoprotein
HCl	Hydrochloric acid
HEPES	N-[2-hydroxyethyl)-piperazine-N'-[2-ethanesulfonic acid]
HMW	High molecular weight (predominantly VWF MM 5 - 8)
HRP	Horseradish peroxidase
HSA	Human serum albumin
IMW	Intermediate molecular weight (predominantly VWF MM 4 - 6)
ISTH	International Society on Thrombosis and Haemostasis
IU	International unit
k_a	Association rate constant
k_d	Dissociation rate constant
K_D	Dissociation equilibrium constant
kDa	Kilo Dalton
LMW	Low molecular weight (predominantly VWF MM 2 - 3)
mAb	Monoclonal antibody

MM	Multimer
MTP	Microtitre plate
MW	Molecular weight
NaAc	Sodium acetate
NHS	N-hydroxy succinimide
NIBSC	National Institute for Biological Standards and Control
o/n	Over night
OPD	*O*-phtaldialdehyde
PBS	Phosphate-buffered saline
pd	Plasma derived
PFA	Paraformaldehyde
RIPA	Ristocetin induced platelet aggregation
RT	Room temperature
SDS	Sodium dodecyl sulfate
SDS-PAGE	SDS-Polyacrylamide gel electrophoresis
SEC	Size exclusion chromatography
SEM	Standard error of mean
SPR	Surface plasmon resonance
SSC	Scientific and Standardization Committee
TBS	Tris-buffered saline
Tris	2-Amino-2-(hydroxymethyl)-propane-1.3-diol
TTP	Thrombotic thrombocytopenic purpura
Tween-20	Polyoxyethylene sorbitan monolaurate
UDP-Gal	Uridin-5’-diphospho-galactose
VWF	Von Willebrand factor
VWF MMA	Von Willebrand factor multimer analysis
VWF:Ag	VWF antigen
VWF:CB	VWF collagen binding activity
VWF:RCo	VWF Ristocetin cofactor activity

10 List of publications

10.1 Publications

Fuchs B, Budde U, Schulz A, Kessler CM, Fisseau C, Kannicht C. Flow-based measurements of von Willebrand factor (VWF) function: Binding to collagen and platelet adhesion under physiological shear rate. *Thromb Res., under revision*

Graessmann M, Berg B, Fuchs B, Klein A, Graessmann A. Chemotherapy resistance of mouse WAP-SVT/t breast cancer cells is mediated by osteopontin, inhibiting apoptosis downstream of caspase-3. *Oncogene.* 2007; **26:** 2840-50

10.2 Books

Walker JM and Raplex R. Molecular Biomethods Handbook. 2nd edition, Humana Press, Totowa 2008, US ISBN 078-1-60327-370-1, Chapter 28, pp. 427-49: Post-translational modificiations of proteins. Christoph Kannicht and Birte Fuchs, upon invitation

10.3 Poster presentations

Fuchs B, Budde U, Fisseau C, Schulz A, Kannicht C. (2009) Measurement of von Willebrand factor (VWF) function under physiological flow conditions. 53. Jahrestagung der Gesellschaft für Thrombose- und Hämostaseforschung e.V. (GTH), February 4-7, Vienna, Austria

Fuchs B, Trawnicek L, Fisseau C, Kannicht C. (2009) Von Willebrand factor (VWF) function under physiological flow conditions: Comparison of five VWF/FVIII concentrates in an *in vitro* flow-chamber model. 53. Jahrestagung der Gesellschaft für Thrombose- und Hämostaseforschung e.V. (GTH), February 4-7, Vienna, Austria

Fuchs B, Budde U, Schulz A, Fisseau C, Kannicht C. (2008) Von Willebrand factor (VWF) binding to collages I and III and mediation of platelet adhesion under physiological flow conditions. Hemophilia World Congress, July 1-5, Istanbul, Turkey

Fuchs B, Budde U, Schulz A, Fisseau C, Kannicht C. (2008) Investigating von Willebrand factor (VWF) function under flow: Binding to collagen and platelet adhesion in an *in vitro* flow-chamber model. 52. Jahrestagung der Gesellschaft für Thrombose und Hämostaseforschung e.V. (GTH), February 20-23, Wiesbaden, Germany

Fuchs B, Fisseau C, Schwartz BA, Kessler CM, Kannicht C. (2007) Von Willebrand factor (VWF) function under physiological flow conditions. Investigation of VWF/Factor VIII (FVIII) concentrates – does multimer size really matter? 49th American Society of Hematology (ASH) Annual Meeting, December 8-11, Atlanta, US

Fuchs B, Fisseau C, Kannicht C. (2007) Von Willebrand factor (VWF)-binding to collagen III under physiological flow conditions and VWF-mediated platelet binding. XXIst Congress of the International Society on Thrombosis and Haemostasis (ISTH). July 6-12, Geneva, Switzerland

Fuchs B, Fisseau C, Schwartz B, Kannicht C. (2007) Von Willebrand factor (VWF) under physiological flow conditions: Role of VWF multimer size on binding to collagen III. National Hemophilia Foundation's (NHF) Annual "Washington Days", March 7-9, Washington, US

Fuchs B, Fisseau C, Kannicht C. (2007) Von Willebrand factor (VWF)-mediated platelet binding to collagen III under physiological flow conditions. 51. Jahrestagung der Gesellschaft für Thrombose- und Hämostaseforschung e.V. (GTH), February 21-24, Dresden, Germany